

OLIO
A 7
-6
ER 72/73 -26

LIBRARIES
COLORADO STATE UNIVERSITY
FORT COLLINS, COLORADO

EXPERIMENTAL BEHAVIOR OF
WOOD FLOORING SYSTEMS

Bryan G. Penner
M. E. Criswell
J. Bodig
J. R. Goodman
M. D. Vanderbilt



Structural Research Report No. 7
Civil Engineering Department
Colorado State University
Fort Collins, Colorado 80521

December, 1972

EXPERIMENTAL BEHAVIOR OF
WOOD FLOORING SYSTEMS

Bryan G. Penner

M. E. Criswell

J. Bodig

J. R. Goodman

M. D. Vanderbilt



Structural Research Report No. 7
Civil Engineering Department
Colorado State University
Fort Collins, Colorado 80521

December, 1972

ABSTRACT

EXPERIMENTAL BEHAVIOR OF WOOD FLOORING SYSTEMS

The main objective of the overall project which included this study is to develop a mathematical model of wood joist floor systems which incorporates the T-beam action between the joists and plywood sheathing and the effect of inter-layer slip. Results of tests of wood flooring systems which were constructed and load tested to verify the deflections computed from the mathematical models are presented. Mathematical variations within these floors included joist size and species, plywood species and thickness, and type of nails. Test results showed that concentrated loads of up to eight times that considered allowable by conventional design could be carried before failure of the first joist. It was also found that an average of 300 percent more load could be supported without exceeding deflection limitations assumed in conventional methods of analysis.

This report contains a description of the construction and load-testing of wood flooring systems and T-beams. The T-beams were built to study the effects that a plywood flange attached to the joists had on the strength and stiffness of the floor system. The strains within the plywood flange were measured at several load increments by strain gage transducers attached to the plywood decking. An effective flange width can then be assumed from these strains measured within the plywood flange. Joist deflections were also recorded for various load increments and positions. By comparing T-beam joist deflections with and without the plywood flange attached for one T-beam, a 34 percent

increase in stiffness could be attributed directly to the composite
T-beam action of the plywood (for the range of variables considered).

Bryan Grant Penner
Civil Engineering Department
Colorado State University
Fort Collins, Colorado 80521
December 1972

TABLE OF CONTENTS

<u>Chapter</u>		<u>Page</u>
	ABSTRACT.	iii
	LIST OF TABLES.	vii
	LIST OF FIGURES	viii
1	INTRODUCTION.	1
	1.1 Objective.	1
	1.2 Scope.	1
	1.3 Acknowledgments.	2
	1.4 Literature Review.	3
2	DESCRIPTION OF TEST SPECIMEN.	7
	2.1 Introductory Remarks	7
	2.2 Material	8
	2.3 Property Tests	10
	(a) Performed by the Wood Science Laboratory.	10
	(b) Tests Performed During Construction	14
	2.4 Construction of Test Specimen.	14
	(a) Support Structure	14
	(b) Floors.	15
	(c) T-beams	17
	2.5 Description of Individual Specimens.	18
	(a) Floors.	18
	(b) T-beams	20
3	TESTING PROCEDURE	23
	3.1 Introductory Remarks	23
	3.2 Testing Arrangements	23
	3.3 Application of Load.	24
	3.4 Deflection Measurements.	26
	(a) Mechanical Detection.	26
	(b) Electrical Measurement of Deflection.	27
	(c) Optical Detection	27
	3.5 Strain Indication.	28
4	SPECIMEN BEHAVIOR	30
	4.1 Introductory Remarks	30
	4.2 Elastic Deflections.	30
	(a) Deflection Diagrams	30
	(b) Empirical Load Sharing.	32
	4.3 Mode of Failure.	35
	(a) Deflected Surfaces at Overloads	35
	(b) Description of Inelastic Behavior up to Initial Joist Failure	36
	(c) Description of Final Floor Failure.	38
5	STRENGTH ANALYSIS	41
	5.1 Introductory Remarks	41
	5.2 Analysis	42
	(a) Flexural Strength of Loaded Joist	42
	(b) Membrane Action with Nail-Slip and Pullout	47

TABLE OF CONTENTS - (Continued)

<u>Chapter</u>		<u>Page</u>
6	SUMMARY AND CONCLUSIONS.	50
	6.1 Summary of the Testing Program.	50
	6.2 Conclusions	51
	REFERENCES	53
	FIGURES.	55
	APPENDIX A. DESCRIPTION OF THE TESTING FRAME.	98
	APPENDIX A. Figures	105

LIST OF TABLES

<u>Table</u>		<u>Page</u>
2.1	Individual floor specimens	19
2.2	Individual T-beam specimens	21
4.1	Load-sharing coefficients	34
5.1	Experimental Load Comparisons	43
5.2	T-beam stiffness.	46

LIST OF FIGURES

<u>Figure</u>		<u>Page</u>
2.1	Top view of continuous deflection testing machine for joists.	55
2.2	Apparatus used in determining plywood modulus of elasticity values.	56
2.3	Testing configuration used to obtain nail-slip curves.	56
2.4	Typical nail-slip curve between joist and plywood	57
2.5	Typical beam test performed during construction, used to determine the joist modulus of elasticity	58
2.6	Cut-away view showing floor construction and floor support	59
2.7	Floor numbers for joists and plywood.	60
2.8	Floor No. F4-12E16-1 mounted on the testing frame	61
2.9	T-beam testing configuration.	62
3.1	Load distributing bridge used in T-beam testing.	63
3.2	Deflection dial indicators supported under the floor joists.	64
3.3	Deflection dial indicators supported under the T-beam joists	64
3.4	A deflection dial indicator and LVDT positioned under a floor joist.	65
3.5	X-Y plotters used to draw the continuous load versus deflection curves	66
3.6	Attachment of engineering scales to floor joists.	67
3.7	Strain gauge clips placed across a T-beam flange.	67
3.8	Individual strain gauge clip attached to the plywood decking	68
3.9	Switch and balance unit along with a strain indicator used to measure strains	68

LIST OF FIGURES - (Continued)

<u>Figure</u>		<u>Page</u>
4.1	Illustration of Maxwell's Reciprocal Theorem on floor F4-12E16-1 with 1000 pounds applied.	69
4.2	Continuous load versus deflection curve for load applied at 0707 on floor F1-6E16-1.	70
4.3	Continuous load versus deflection curve for load applied at 0707 on floor F2-8D16-1.	71
4.4	Continuous load versus deflection curve for load applied at 0707 on floor F3-8D16-1.	72
4.5	Continuous load versus deflection curve for load applied at 0707 on floor F4-12E16-1	73
4.6	Deflected shape of an example floor, F4-12E16-1, with load applied of 3500 pounds at position 0707	74
4.7	Deflected shape of floor F16E16-1 with 1000 pounds applied at position 0707	75
4.8	Deflected shape of floor F2-8D16-1 with 1000 pounds applied at position 0707	76
4.9	Deflected shape of floor F3-8D16-1 with 1000 pounds applied at position 0707	77
4.10	Deflected shape of floor F4-12E16-1 with 2500 pounds applied at position 0707	78
4.11	Joist midspan deflections of floor F1-6E16-1 with load applied at 0707.	79
4.12	Joist midspan deflections of floor F2-8D16-1 with load applied at 0707.	80
4.13	Joist midspan deflections of floor F3-8D16-1 with load applied at 0707.	81
4.14	Joist midspan deflections of floor F4-12E16-1 with load applied at 0707.	82
4.15	Joist midspan deflections of floor F1-6E16-1 with load applied until joist failure.	83

LIST OF FIGURES - (Continued)

<u>Figure</u>		<u>Page</u>
4.16	Joist midspan deflection of floor F2-8D16-1 with load applied until joist failure.	84
4.17	Joist midspan deflections of floor F3-8D16-1 with load applied until joist failure.	85
4.18	Joist midspan deflections of floor F4-12E16-1 with load applied until joist failure.	86
4.19	Deflected shape of floor F4-12E16-1 with with load applied at 0707.	87
4.20	Deflected shape of floor F4-12E16-1 with 5000 and 5500 pounds applied at position 0707.	88
4.21	Deflected shape of floor F4-12E16-1 with 6000 and 7000 pounds applied at position 0707.	89
4.22	Typical load-deflection curve plotted until joist failure, F4-12E16-1 loaded at position 0911. . .	90
4.23	Typical joist failure including cracking around knots and along the grain angle, and cross grain tension cracking	91
4.24	Joist failure due to a horizontal shear crack at joist mid-depth	91
4.25	Plywood failure with punching through of the loading pad at position 0707 on the floor.	92
4.26	Typical load-deflection curve plotted until punching through of the plywood, floor F4-12E16-1 loaded at position 0707	93
4.27	Plywood failure with punching through of the loading pad at a joint, position 0704 on the floor	94
4.28	Typical load-deflection curve plotted until punching through of the plywood, floor F3-8D16-1 loaded at position 0704.	95
5.1	Load distribution from the loaded point to neighboring joists.	96
5.2	Load distribution along the loaded joist due to plywood bending and the forces within the nail fasteners.	96

LIST OF FIGURES - (Continued)

<u>Figure</u>		<u>Page</u>
5.3	Compression and tension regions of the plywood with a load applied at the center of a plywood sheet.	97
5.4	Compression and tension regions of the plywood with a load applied at a plywood joint	97
APPENDIX FIGURES:		
A.1	Concrete support structure with sill plates and deflection dial support.	105
A.2	Specimen testing configuration	106
A.3	Positive reinforcement for the sixteen foot beam.	107
A.4	Stirrup reinforcement for the sixteen foot beams	108
A.5	Negative reinforcement for the sixteen foot beam	109
A.6	Positive reinforcement for the twelve foot span	110
A.7	Stirrup reinforcement for the twelve foot span	111
A.8	Negative reinforcement for the twelve foot span	112
A.9	Anchorage reinforcement.	113
A.10	Meshing of reinforcement at a corner column.	114
A.11	Reinforcement used in columns.	115
A.12	Actuator used in applying a concentrated load to a test specimen.	116
A.13	Front view of steel testing frame.	117
A.14	Side view of steel testing frame	118
A.15	Trolley setup used to move the actuator and the movable beam	119
A.16	MTS control console no. 850 used in applying a concentrated load to a test specimen	120

CHAPTER 1

INTRODUCTION

1.1 Objective

Research in the area of wood flooring systems has shown that conventional design methods, which are based almost entirely on the design of individual joists, do not adequately consider the behavior of the entire floor as a unit. Floor behavior supporting a concentrated or uniform load is a function of the plywood modulus of elasticity both parallel and perpendicular to the face grain, joist modulus of elasticity, gaps between plywood sheets and number of sheathing layers. Also included is the stiffness of joist and plywood fasteners (nails and glue), size, grade and species of both plywood and joists and all the parameters which effect the wood properties. Load-sharing by neighboring joists and T-beam action developed when the plywood decking is attached to the joists are the major factors which contribute added strength and stiffness. The overall objective of the research program, of which this study is a part, is to develop mathematical models which incorporate these two factors and yield a better design technique. The objective of this study was to construct and load-test floor specimens to provide data necessary for the verification of these mathematical models. Two T-beams were also constructed and load-tested to determine the extent of T-beam action developed in the plywood flange.

1.2 Scope

This investigation included the construction and load-testing of four wood floors and two T-beam specimens. The testing was limited to applying a single concentrated load through a 4 inch by 4 inch steel

pad at several locations on each specimen or a pair of pads on the T-beams. Extensive data on the deflections of the joists in the loaded floors and T-beams were collected. Continuous load versus deflection curves were drawn for the loaded point and other selected points using two LVDTs mounted beneath the specimen and one LVDT contained within the actuator. Material variations of joist size and species, plywood thickness and species, and nail type were used between the four floors and two T-beams constructed. Additional material combinations will be used in the floors constructed within the continuation of this project.

Wood flooring systems have been the subject of many previous investigations. Several of these are briefly discussed in the literature review contained in this chapter. A complete description of the material used in this study, the construction methods, and the individual floor properties are given in Chapter 2. The procedures involved in loading the floors and T-beams, recording the deflections, and measuring strains along the plywood flange are discussed in Chapter 3. Chapter 4 contains a description of the behavior of wood flooring systems loaded to joist failure and continuing to complete failure when the load punches through the plywood decking. The increased strength and stiffness of the floor due to load-sharing and T-beam action is analyzed in Chapter 5. A summary of the report and the resulting conclusions are given in Chapter 6. Appendix A contains a description of the testing frame and its capacity.

1.3 Acknowledgments

This report is a thesis presented in partial fulfillment of the requirements for the degree of Master of Science in Civil Engineering,

at Colorado State University. Its preparation was under the direction of Professors M. D. Vanderbilt, M. E. Criswell, and J. R. Goodman of the Civil Engineering Department and Professor J. Bodig of the Forest and Wood Science Department. The study reported is a part of a project entitled "A Rational Analysis and Design Procedure for Wood Joist Floor Systems" funded by the National Science Foundation. Support of this author's graduate education was provided by a fellowship from the National Defense Education Act.

A grateful acknowledgement must be given to all the companies supplying the lumber used in the study. These contributors include Weyerhaeuser Company, who supplied all the Douglas fir joists and plywood; Montezuma Plywood Company who provided the Engelmann spruce plywood; and Colorado Forest Products Inc., Kaibab Industries Inc., Cook Lumber Company, and San Juan Lumber Company who supplied the Englemann spruce joists.

Thanks also are due to Meng-Fang Ko, Gordon Penfold, and A. W. Schollett, fellow graduate students and friends, for their assistance in floor construction and collection of testing data.

Finally, a special thanks to my wife, Naomi, for her continual help in drafting this research report.

1.4 Literature Review

In this section a review of several experimental studies related to wood flooring systems are presented. Additional comments concerning some of these studies are given in later sections.

Amana and Booth (1)* investigated the use of stressed-skin components in prefabricated building units. In their study, the problem

* Numbers in parentheses refer to entries in the reference list.

of the effective flange (effective breadth) width of the plywood is described. They also recognized the importance of slip between plywood and joist and conducted nail-slip tests to determine its effect. Tests of five specimens, four of the T-beam configuration and one stressed skin panel, are described in their report. Strain readings were recorded across the flange along with load versus deflection curves of the joists. These results were shown to have good correlation with a proposed theory which was incorporated into a computer program.

Forty-four wood-joist floors were built and load-tested in a study reported by Polensek, Atherton, Corder, and Jenkins (19). These floors were loaded with both concentrated and uniform loads. One of the objectives of this study was to develop a better floor design technique than the simple beam analysis with no T-beam action. T-beam efficiency factors were introduced for use in design of floors to account for the interaction of the joists and the nailed plywood decking. Empirical load-sharing between the joists was also studied and is discussed in Section 4.2. Added stiffness of the floors due to the finish flooring was studied and stiffness increase coefficients were determined.

Hurst (11) investigated the effect that other portions of house construction have on floor stiffness. During this study the wood floors were subjected to a uniform load at 14 different stages of the total house construction. The midspan deflections were continuously recorded during each test. Using conventional techniques the computed bending stress in the joists due to the applied load was 900 psi. A full scale three bedroom home was used in these tests. The test results indicated increased resistance to floor deflection and vibrations due to partitions, continuity of joists from blocking, and finish flooring. Hurst recommends

that this added stiffness of the floors be included to design calculations to reduce cost and material.

The static and dynamic performance of minimum wood joist floor construction was studied by the National Association of Home Builders (14). Four two-span floors were built using 2 x 8 joists on 16 inch centers and clear spans of 13 feet. Joist mid-span deflections were recorded for an initial uniform load of 50 psf and then the floor was cyclically loaded between 0 and 20 psf. After 250 cycles of uniformly applied load at 20 psf, joist mid-span deflections were again recorded for a uniform load of 50 psf. The objective of the study was to determine the effect of repeated loadings on both static and dynamic load properties of wood flooring systems. The total floor stiffness was measured as the ratio of the joist deflection to the joist span under a 50 psf uniform load. By comparing the floor stiffness values of before and after the cyclic loadings it was found that the stiffness essentially remained constant after the initial loading. Based on the average stiffness of the joists used in the floors constructed, the measured stiffness of the floor system was found to be 35 percent higher than that predicted by conventional design procedures. This increase was attributed to a significant amount of continuity over the center support (nailed lapped joist plus plywood decking) plus the contribution of the T-beam action of the nailed plywood.

A Forest Products Laboratory publication of October 1970 (21) included descriptions of present research and expected future publications by this organization on all facets of wood construction. Composite construction and T-beam action in wood flooring systems where the plywood is glued and nailed to the joists is discussed.

A study has been completed by Polensek (18) in which the effects of gluing and nailing plywood to joists was examined. In this study the stiffness and strength of two floors, one nailed and the other nailed and glued, were compared. Polensek concluded that gluing the plywood subfloor to the joists produced a stronger and stiffer floor than nailing, but only when the floor was tested with a uniformly distributed load. The distribution of a concentrated load in the direction perpendicular to the joist span was found to be equal for the glued and the nailed floors. However, the glued floors appeared to be more acceptable from the viewpoint of human response to vibrations than its nailed-only counterpart.

CHAPTER 2

DESCRIPTION OF TEST SPECIMEN

2.1 Introductory Remarks

Four floors were constructed and load-tested to failure to determine deflections and behavior, including conditions at ultimate load. Material variations for each floor including wood species, joist size, and plywood thickness are discussed in Section 2.2. Several computer programs were written by other members of the project to predict the deflected shape of loaded floor and T-beams (12,20). The input data required by these programs includes the modulus of elasticity of the joists and plywood and nail-slip constants. The tests performed to determine these properties are briefly described in Section 2.3. The general construction procedure followed in building the floor specimen is discussed in Section 2.4(a).

A primary purpose for constructing and testing these floors was to provide experimental data for use in verifying the mathematical model for the floor system. For purposes of analysis the floor is divided into strips going in the two principal directions. This procedure is called the crossing beam technique. One joist with its plywood flange forms the beam in one direction. Interlayer slip and effective flange width must be considered in simulating the behavior of the joist beam strip. To verify the computed deflected shape, two T-beams were constructed and tested. The general construction procedure used in constructing the T-beams is described in Section 2.4(b).

The material components of each floor or T-beam differed considerably and these variations are described in Section 2.5. An identifying mark was assigned to each specimen which also identified the value of

center of the two inch bearing, the clear span of these floors was twelve feet.

The joists were supplied by five lumber companies. All the Douglas fir lumber was supplied by Weyerhaeuser Company of Tacoma, Washington. The Engelmann spruce was provided by four suppliers: Colorado Forest Products Inc. of Dolores, Colorado; Kaibab Industries Inc. of Eagle, Colorado; Cook Lumber Company Inc. of Fort Collins, Colorado; and San Juan Lumber Company Inc. of Pagosa Springs, Colorado.

Two grades of lumber were used in building the test specimen. Number three grade was used in all four floors. Select structural grade was used in building two T-beams.

Two species of plywood were used in constructing the test specimen. The Weyerhaeuser Company supplied all the Douglas fir plywood used in testing. All the Engelmann spruce plywood was supplied by Montezuma Plywood Company of Cortez, Colorado.

The Douglas fir plywood came in 4' x 8' sheets and was either 3/4 or 5/8 inches thick. The 3/4 inch plywood was tongue and groove along the eight foot side and the 5/8 inch was of a straight side cut. The grade of the Douglas fir was a standard CD plywood with interior grade glue.

The Engelmann spruce plywood was either 5/8 in. or 1/2 in. thick. The grade of the Engelmann spruce was the standard CD plywood with exterior glue. The 1/2 inch thick plywood sheets were a full four foot by eight foot. The 5/8 inch plywood was tongue and groove cut from a

four by eight sheet and yielding in-place dimensions of three feet eleven one-half inches by eight feet.

Nail properties are very important in determining the stiffness of each floor or T-beam. Both cement-coated and common nails were used. The first two floors were constructed using cement coated nails and the last two floors contained common nails. These two types of nails have different load-slip or stiffness constants, which are discussed later.

Eight penny nails were used to fasten the plywood to the joists. The nail spacing used varied from floor to floor. Sixteen penny nails were used to toenail the joist to the still plate and to nail the header joist to the individual joists.

The cement-coated eight penny nails used in the first two floors and all the six and sixteen penny common nails were manufactured by CF&I Steel Corporation. The six penny common nails will be used to fasten particle board to the plywood underneath as a third layer in future flooring systems. The last two floors contained eight penny common nails manufactured by U.S. Steel Corporation.

2.3 Property Tests

(a) Performed by the Wood Science Laboratory

The modulus of elasticity (MOE) values along the longitudinal axis of each joist were determined by nondestructive tests conducted by the Wood Science Laboratory of Colorado State University. These tests provided an average MOE for each foot along the length of the joists. The MOE values were calculated using a computer program and the deflection data gathered with the test setup shown in Fig. 2.1.

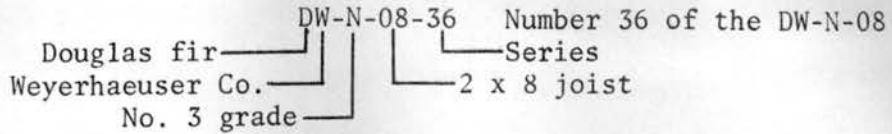
The testing procedure entailed applying a constant load on the widest dimension of a plank simply supported over a three-foot span. As the lumber is driven through the testing apparatus, a Linear Variable Differential Transformer (LVDT) indicates deflections at the loaded point. By knowing the plank dimensions, applied load and resulting deflection, the MOE along each section tested is obtained. In these tests, the load is applied to the lumber in a plank orientation. However, in the floor or T-beam tests, the lumber is used in a joist orientation. Through several studies it has been substantiated that a relatively good correlation (correlation coefficients from 0.62 to 0.85) exists between plank and joist MOE values (16). Work by O'Halloran (16) documents this procedure and provides test results to substantiate the plank and joist correlation.

After the determination of these properties, each joist was given a descriptive number consisting of three letters and four numbers. The first letter indicates the species: D for Douglas fir or E for Engelmann spruce. The second letter represents the company supplying the lumber as follows:

C = Colorado Forest Products Inc.
F = Cook Lumber Company Inc.
K = Kaibab Industries Inc.
S = San Juan Lumber Company Inc.
W = Weyerhaeuser Company

The last letter indicates the lumber grade: N for number three and S for select structural. Two numbers designating the joist size are next. A nominal 2 x 6 joist has been designated by a 06, 2 x 8 by a 08, and 2 x 12 by a 12. The last two numbers indicate the sequence number.

For example:



The joist identification number was always placed on the end of the joist serving as an origin for identification of the measured MOE values.

The MOE values for all the plywood and particle board used in building the test specimen were also measured. MOE values were determined for both the long and short directions. These tests were also conducted at the Wood Science Laboratory using the apparatus shown in Fig. 2.2.

In determining the plywood MOE values, the plywood is assumed to act as a wide beam. The testing apparatus supports the plywood at one end and at approximately the center. A steel bar of suitable weight is placed along the free end to produce a line load. Deflection of this loaded end is determined as the average deflection value from three LVDT transducers each placed to measure the deflection of 1/3 the plywood width. This procedure is duplicated with the plywood rotated 180 degrees. The plywood was then turned over and the two tests repeated. This gave four test results for each direction. These four values are averaged to obtain the static MOE value. The same procedure is used to determine the MOE for the face grain both perpendicular and parallel to the span. McClain (13) describes this testing procedure in more detail.

A numbering system was also used to identify the plywood. This system was similar to that used for the joists and consists of two letters and four numbers. The first letter indicates the species:

floor. The necessary tests were performed by the Wood Science Laboratory with the testing setup shown in Fig. 2.3. In this setup, load is applied to the joist and the two side pieces of plywood are supported. A plot is then made of applied load versus the deflection of the joist. A typical nail-slip curve is shown in Fig. 2.4. The required nail-slip constants are the slopes determined from these curves. This testing procedure along with results are described by Patterson (17).

(b) Tests Performed During Construction

A simple beam test using a concentrated 250 pound load at mid-span as shown in Fig. 2.5 was conducted on each joist to determine the average edgewise MOE values. A MOE value was then computed from the normal beam deflection equation, $\Delta = PL^3/48EI$, using measured joist dimensions and observed centerline deflections. The beam deflection tests were performed with all the joists standing and nailed to the header joist.

2.4 Construction of Test Specimen

(a) Support Structure

A means of supporting the test specimens at a height allowing access to the bottom of the specimen had to be provided before construction could be done on the floors or T-beams. A reinforced concrete frame consisting of beams and six-foot high columns was constructed to support the test specimens. Appendix A.1 contains further details on this frame. To insure a uniform supporting surface for the joist, a sill plate was grouted in place on two opposite sides of the supporting frame as shown in Fig. 2.6. The sixteen-foot long sill plates were 2 x 6 Engelmann spruce lumber. White hydrocal was used to grout the sill plates. Each sill plate was attached to the concrete by two

standard coil inserts and four heavy lifting inserts. As the hydrocal hardened, the sill plates were leveled by tightening the bolt inserts.

(b) Floors

The first step in the floor construction was the selection of joists. Two methods were used to select the joists and their order in the floor. One method was to use the top thirteen joists from the lumber stack and a random placement of the joists within the floor. A second method was to use the average MOE values provided by the Wood Science Laboratory. Using this method, a range of average MOE values was determined and only joists within this range were selected. These joists were positioned within the floor in a random order. Once the position of each joist was determined, it was recorded as the numbers indicate in Fig. 2.7. The end with the joist identification number was always placed on the north side of the floor.

Normal practice in house construction is to place all joists with the crowned edge or slight curvature in the longitudinal direction up. Joists with abnormal cracks or knots in their bottom fibers are often not used by the builder or are placed in noncritical areas. In this study the above procedure was followed. When a joist of this quality was encountered it was placed in position 01 or 13 where it would be fully supported.

Once the joist position was determined, the joist was toe-nailed to the sill plate. The center-to-center joist spacing was sixteen inches for all four floors. Depending upon joist splitting either one or two sixteen penny nails were used to toe-nail the joist ends. Several of the joists and headers were notched for the bolt inserts holding the sill plates to the frame. At each end of the joists a

sixteen-foot header or ribbon was attached. Three sixteen penny nails were used to attach the header to 2 x 6 joists. Four nails were used with the 2 x 8 joists, and five with the 2 x 12 joists.

At this point in the floor construction all joists were load tested as beams to determine a measure of the joist stiffness described in Section 2.3.

The plywood selection procedure for each floor or T-beam was similar to that of joist selection. Selection for three floors was done using the top six sheets from a particular stack. The average MOE values were used to select plywood for floor F2-8D16-1. Uniform plywood selection was done, as with the joists, by setting an acceptable range of MOE values and selecting only plywood within these limits. Once the position of the plywood was determined, it was recorded using the letters indicated in Fig. 2.7. All joists after the first floor were pre-cut to 12 feet 2 inches in length as described in Section 2.2. The addition of a header made the total floor length 12 feet 5 inches. Three standard sheets of plywood placed across the joists covered 12 feet, leaving a 2 1/2 inch gap at each edge of the floor as shown in Fig. 2.8.

Various nailing schedules for attaching the plywood sheeting to the joists used either cement-coated or common eight penny nails as tabulated in Table 2.1. The plywood was driven tightly together at every joint before it was attached to the joists. Joist nail spacing was varied on each floor, but a typical spacing was eight inches. The penetration of each nail into the joist was checked. When a nail missed or slanted out of the joist, it was pulled and replaced with another.

As shown in Fig. 2.6, some of the floor had joists 01 and 13 supported only on a blocked 4 x 4. Due to the crown of the joist,

full support directly upon the 4 x 4 was not possible . To provide full support over the length of the joist, shingle shims were driven approximately every six inches in between the 4 x 4 and end joists, for floor F2 and F4.

(c) T-beams

The construction of T-beams was very similar to that of the floor construction. Only differences for the T-beam construction will be discussed.

The T-beams consisted of two parts: the standard 12 foot 2 inch long joists and the attached plywood flange. When two joists were used to construct a twin T-beam representation of a floor with 16 inch joist spacing, a flange width of 32 inches was used, refer to Fig. 2.9. The plywood layer of the T-beams was placed with the face grain parallel to the joists, not perpendicular to the joists as was in the floor systems. This layout was chosen to provide more distance for strain measurements over the beam span without the influence of a plywood joint. This configuration of plywood placement is shown in Fig. 2.9.

The T-beams were also supported on the concrete frame. Sill plates were grouted to the frame using white hydrocal. The sill plate lengths were varied depending upon the number of joists. For single joist T-beams, the plywood and joist were selected randomly or using the average MOE values. For twin T-beams the joists were matched using the Wood Science Laboratory MOE values. Header joists, with the same length as the T-beam flange, were attached at both ends of the joists.

2.5 Description of Individual Specimens

(a) Floors

Each floor contained many variables, some previously discussed in the sections on materials and specimen construction. Table 2.1 lists most of the parameters for the four floors constructed. The end blocking entry in Table 2.1 refers to the support along the twelve-foot dimension provided by the 4 x 4 as shown in Fig. 2.6. To provide full support on all four edges, two floor specimens were shimed under the end joists. The other two floors were not shimed, and the gap below the joists was open due to the crown of the end joists. This small gap did not seem to have any large effect on the strength or stiffness of the floors.

The first floor, F1-6E16-1, was primarily a practice floor. The individual joists and plywood sheets were selected at random from the top of the storage stack. The MOE values for these joists and plywood were not determined by the Wood Science Laboratory. The sill plates were bolted but not grouted to the concrete base. Eight penny cement-coated nails were used to nail the plywood to the joists. The nail spacing was 8 ± 1 inch along the joists away from the plywood edges and 6 ± 1 inch at joist along the edges of the plywood. The joists of this floor were only eleven feet nine inches long which resulted in a floor with a total length of twelve feet.

The second floor, F2-8D16-1, was a standard floor as described in Section 2.4. The joists and plywood of this floor were selected for uniformity. The range of average MOE values of the joists as determined by the Wood Science Laboratory was 1.569 to 1.658×10^6 psi. The simple beam tests on the joists in place indicated that the variation in MOE values when the joists are standing upright may have been considerably

TABLE 2.1
INDIVIDUAL FLOOR SPECIMENS

Floor number	Joists			Plywood					
	species	nominal size	grade	species	thickness	type	nail spacing	nail type (8 penny)	End blocking
F1-6E16-1	Engelmann spruce	2 X 6	No. 3	Douglas fir	3/4 inch	Tongue and Groove	8 + 1 inch 6 + 1 inch edges	cement coat	No shims
F2-8D16-1	Douglas fir	2 X 8	No. 3	Douglas fir	3/4 inch	Tongue and Groove	8 + 1/2 inch	cement coat	shimmed
F3-8D16-1	Douglas fir	2 X 8	No. 3	Douglas fir	3/4 inch	Tongue and Groove	8 + 1/4 inch	common	No shims
F4-12E16-1	Engelmann spruce	2 X 12	No. 3	Engelmann spruce	5/8 inch	Tongue and Groove	6 + 1/4 inch	common	shimmed

larger. The average static MOE range for plywood along the face grain was 1.40 to 1.42×10^6 psi. In this floor eight penny cement-coated nails were used to fasten the plywood.

Floor number three, F3-8D16-1, was built using random material selection. Both plywood and joists were selected by using the top pieces off the storage stacks and were positioned in the floor at random. Common eight penny nails were used to attach the plywood to the joists. The nail spacing was again eight inches but the accuracy was increased to $\pm 1/4$ inch by snapping chalk lines to determine nail positions.

The fourth floor, F4-12E16-1, contained 2 x 12 Engelmann spruce joists. Both the plywood and joists were selected and positioned randomly. The plywood sheets were 5/8 inch thick tongue and groove Engelmann spruce with in-place dimensions of eight feet and three feet eleven one-half inches. This increased the edge gap outside the plywood and along the edge of the floor to 3 and 1/4 inches. Common eight penny nails were used at a spacing of $6 \pm 1/4$ inches.

(b) T-beams

Plywood, joist, and nail properties were varied in the construction of T-beams as recorded in Table 2.2.

The first T-beam, T1-8D16-1, was built with two joists to provide stability, and with joists chosen for uniformity. The average MOE machine graded values were 1.542 and 1.412×10^6 psi. Cement-coated eight penny nails at a spacing of $8 \pm 1/2$ inch were used to attach the plywood to the joists.

The second T-beam, T2-8D48-1, was built using a select structural graded joist. Only one joist was used and care was taken during

TABLE 2.2
INDIVIDUAL T-BEAM SPECIMEN

T-beam number	Joists			Plywood				flange width
	species	size	grade	species	thickness	nail spacing	nail type (8 penny)	
T1-8D16-1	Douglas fir	2 X 8	No. 3	Douglas fir	3/4 inch	8 \pm 1/2 inch	Tongue and Groove cement coat	16 inches
T2-8D48-1	Douglas fir	2 X 8	Select structural	Douglas fir	3/4 inch	8 \pm 1/2 inch	Tongue and Groove cement coat	48 inches

construction and testing not to displace the plywood flange. A 48 inch flange was attached with cement-coated eight penny nails placed every $8 \pm 1/2$ in.

CHAPTER 3

TESTING PROCEDURE

3.1 Introductory Remarks

During this study floors and T-beams were load-tested using a concentrated load applied using a four by four inch steel pad. Testing arrangements are described in Section 3.2. The method of applying the load during each test is discussed in Section 3.3. The method of recording the deflected shape of the loaded floor is described in Section 3.4. Some strains of the plywood surface were measured using techniques discussed in Section 3.5.

3.2 Testing Arrangements

All floor and T-beam tests were conducted in the Structures Laboratory at the Foothills Engineering Research Center. A concrete platform was constructed to support each test specimen. An MTS structural testing system was used in applying the concentrated load. The actuator was supported by a steel frame which allowed loading at any point on the specimen surface. This testing equipment is detailed in Appendix A.

A numbering system was developed to identify points on all the floor surfaces; specified first by its row or location along the joist and then by the joist itself. Row numbers were one foot apart with the first row number assigned at the north line of support and with the seventh row placed at the midspan location. Row and joist locations are numbered as shown in Fig. 2.7. The center joist is number 07, therefore position 0707 describes the exact center of the floor, and position 1313 is the far corner of the floor.

A T-beam numbering system was also developed and is fairly consistent with that of the floor system. The only difference is that each position is specified first by its joist and then by its row or location along the joist. For example, position 0206 is a point on the second joist, one foot north of midspan or six feet from the near (north) joist support.

Each floor was load-tested to failure. The center point, 0707, was the first point loaded to failure on each floor. Locations of additional test points were dependent upon the pattern of distressed joists. Points 0704, 0710, and 0711 were usually also tested to failure. Floor F3-8D16-1 was also loaded in between several joists to determine the ability of plywood to distribute the load to adjacent joists.

3.3 Application of Load

A load was applied to the floor specimen using a hydraulic loading system, MTS No. 908.75, which is discussed in detail in Appendix A.3. The load was applied directly to the floor using a 1 in. diameter ball bearing and a 1/2 in. thick and 4 x 4 in. steel pad. With this loading setup the load was always applied perpendicular to the floor surface.

Load positioning was accomplished by moving the actuator in the north-south and/or east-west directions. The north-south, joist direction, mobility was accomplished by mounting the actuator on a trolley which rolled on the bottom flange of a steel W 14 x 78 beam. The east-west mobility was obtained by suspending the ends of this same steel beam from the fixed east and west beams of the reaction frame using a half trolley setup. The rigid steel reaction frame surrounded the concrete support platform. Positioning of the load was done

manually by pushing the actuator and movable beam to the desired location. All trolleys were then clamped in position for applying the load. This positioning procedure is diagramed in Appendix A.2.

Fifteen individual points, tested by concentrated loads causing response within the elastic range, were used as a standard set of tests for each floor. This loading pattern included loads at joists 03, 05, 07, 09, and 11 at row locations 05, 07, and 09. In order to stay within the elastic range, the load value was usually limited to one thousand pounds. Several points of the fourth floor, which had 2 x 12 joists, were loaded to 2500 pounds and the floor response was found to remain linear and elastic. Other points on the floor were also loaded to obtain additional information about the deflected shape.

Load was normally applied to the floor in increments of 250 or 500 pounds. Each increment was gradually placed on the floor during five or ten second periods respectively. Time dependent effects of wood during these tests in the elastic range were found to be negligible. The average time needed to read deflection dials in the elastic range was one and one-half minutes.

A twenty-inch long load distribution bridge or beam was used to apply load on both joists of a twin T-beam. The seven-inch deep channel beam loaded each joist on a 4 x 4 inch aluminum pad. The actuator load pad was then placed in the middle of this bridge. Figure 3.1 shows this load distributing bridge. The loading bridge arrangement also provided the space required to place strain transducers on the plywood flange and along the loaded row.

3.4 Deflection Measurements

(a) Mechanical Detection

Deflection dial indicators were used to obtain most of the deflection data. These dials were supported under the floor as shown in Fig. 3.2. A supporting bridge was constructed and attached under the floor by the standard coil inserts placed in the concrete beams. Fifteen dials were attached to the support and positioned under the joists at the fifteen standard load locations. These were at the intersections of rows 05, 07, and 09 and joists 03, 05, 07, 09 and 11. These fifteen locations were considered as the standard deflection grid system. Four more deflection dials could be placed at other grid points and were used to increase the number of readings around the point of load application.

Deflection dials were also placed underneath each T-beam. Deflection dials were attached to another supporting bridge which was also supported by the concrete inserts. The deflection dials were located under each joist at every row line from 03 to 11 in order to describe the deflected shape of each joist. This deflection dial setup is shown in Fig. 3.3.

The deflection dials were read to the nearest one-thousandth of an inch. The deflection range of the dials were one or two inches. The first step in reading deflections was to position each dial so that the initial reading was at least 0.030 inch. All dials were then read with no load applied on the floor to determine a zero reading. After application of a load increment each dial was tapped lightly and the new reading recorded. The net deflection corresponding to an applied load is then the reading taken with that load applied minus the zero reading.

(b) Electrical Measurement of Deflection

Linear variable differential transformers were used in plotting the continuous load versus deflection curves discussed in Section 4.2. Two LVDTs, always used in conjunction with deflection dials, were attached beneath the test specimen as shown in Fig. 3.4. The actuator also contained an LVDT and load versus deflection curves were plotted from it. The actuator's LVDT also indicated the deflections of the steel frame, and therefore these frame deflections could be subtracted from the total deflection.

The electrical setup included a cable from each LVDT beneath the floor extending to a transformer box. From each transformer box, the deflection signal entered into an X-Y plotter. Each LVDT, along with its transformer and X-Y plotter, was calibrated over the linear range of the LVDT. The load signal was obtained from the MTS Console No. 850. This signal was split three ways and calibrated on all three plotters. On the third X-Y plotter, the deflection output of the actuator LVDT was recorded after calibration was completed. This signal was obtained from the MTS console. These X-Y plotters are shown on Fig. 3.5. Calibrations on these X-Y plotters were checked for accuracy several times between specimen tests.

(c) Optical Detection

A Zeiss self-leveling level was used to measure the deflected shape of the floor around the loaded point at and near failure. Deflection dials and LVDTs, with the exception of the actuator LVDT, were used exclusively for loads within the elastic range. Engineering scales with 50 divisions per inch were attached to the joists immediately around

the point of load application, Fig. 3.6. With this arrangement deflections were measured to the nearest one hundredth of an inch.

Deflection readings were recorded until the load punched through the plywood sheathing. In the floor tested the joist directly under the load always failed before the loading pad punched through the plywood sheathing. Deflection measurements from the attached scales reflect the deflection of the bottom of the joists. These values will not always equal the floor deflection after the joist cracks or splits. This must be considered when examining the deflection data from the load tests to failure.

3.5 Strain Indication

One of the objectives of the project is to determine the extent of flange participation in wood floors. The experimental studies needed to meet this objective were started during this research. Questions to be answered include how much does the plywood flange actually add to the stiffness and load carrying capacity of the floor system and what width of this flange is effective.

To determine the extent of the effective flange width, clip-type strain transducers were attached across a T-beam flange. Figure 3.7 shows ten of these clip gages positioned across a T-beam and Fig. 3.8 shows a close up view of one of the clips. Four strain gages, Micro Measurements type EA-13-125AD-120, were glued onto each clip, one on each side of the clip legs. Each transducer was notched on each leg and attached to the floor with a pair of aluminum blocks. One block had a tongue on one end which fit into the notch in the clip gauge. The other side of the clip gage was supported by a machine

screw which also fit into the notch and extended through the support block. These blocks were attached to the plywood flange by wood screws placed two inches apart. The machine screw in one of the blocks was advanced to apply an initial compressive load to the clip. The initial readings for these transducers were then recorded. As load was applied to the test specimen, bending moments caused increased compression in the plywood flange and the resulting compression strain could be measured using these strain gage clips.

The first procedure in obtaining strain readings was to calibrate each transducer to determine the strain gage indicator output versus known strain relationship. Once the initial calibrations were made, periodic recalibration was completed to insure accuracy. Transducers were then attached at the desired locations and given an initial compression as described in the preceding paragraph. A switch and balance unit along with a strain indicator were used to indicate the strain readings, see Fig. 3.9. With no load, each clip gage strain output was recorded as a zero reading. After load application, all strain output readings were recorded. The difference between the resistance at an applied load and the zero reading multiplied by the calibration constant of the clip gage provided the actual strain for the plywood over the two-inch length.

CHAPTER 4

SPECIMEN BEHAVIOR

4.1 Introductory Remarks

Loadings within the elastic range and loadings to failure were applied on the floors and T-beams. The results of the loadings within the elastic range are discussed in Section 4.2. Included in this section are a check on how well the observed deflections satisfy Maxwell's reciprocal theorem, a discussion of load-sharing among the joists, load versus deflection curves, and isometric deflected surfaces of the loaded floor.

The inelastic behavior including failure of the floors when heavily loaded is discussed in Section 4.3. This phase of the load tests is subdivided into three parts: (1) the deflected floor surface at overloads, (2) the inelastic behavior and initial joist failure, and (3) the description of final floor failure.

4.2 Elastic Deflections(a) Deflection Diagrams

Maxwell's reciprocal theorem states that the deflection at point i due to a load at point j is equal to the deflection at point j when this same load is placed at point i . The observed deflections, resulting from loads up to one thousand pounds, have been compared to the requirements of Maxwell's theorem. It was found that the deflections of the floors satisfied the reciprocal theorem within an average of four percent. Some departure from Maxwell's law resulted from the localized inelastic action in the nailed connections.

An example illustrating Maxwell's reciprocal theorem is presented in Figures 4.1(a) and (b). Figure 4.1(a) shows the deflection of various positions due to a 1000 pound load applied to point 0707 on floor F4-12E16-1. The values included in Fig. 4.1(b) are the deflections at position 0707 resulting from load applied at the location of deflection value given. For example, the number listed in position 0507 in Fig. 4.1(a) is the deflection at that point due to a load at position 0707. The deflection listed at that same position in Fig. 4.1(b) is the deflection at 0707 due to a load applied at 0507. The values would be the same in both figures if Maxwell's reciprocal theorem was exactly satisfied. Differences are normally due to inelastic behavior.

Continuous load-deflection curves of the floors were plotted using the LVDTs and associated equipment described in Section 3.4(b). A curve for each floor with the load applied at position 0707 is shown in Figures 4.2, 4.3, 4.4, and 4.5. Several phenomena illustrated by these curves should be noted. The load-deflection curves were reasonably linear even at fairly high load levels, for example a load of 2500 pounds for floor F4-12E16-1 (Fig. 4.5). Each curve was generally linear, up to the point of first joist failure, as will be discussed in Section 4.3. The extent of the elastic behavior of each specimen is also depicted by the hysteresis loops shown in Figures 4.2 to 4.5. Examination of the curves reveals that the joists after being unloaded return near to their original position, but that some residual deflection remained. This small amount of residual deflection, approximately 3 percent, was retained within the specimen several hours after unloading.

Isometric drawings of the deflected floor surface were plotted using a routine available through the CSU Computer Center. These

drawings show the deflected floor shape, deflected surfaces around the actuator, and stages of deflection resulting from increasing load. The orientation of the floors in these figures is consistent with that of Fig. 2.7; the upper-right line is joist 01 and the upper-left line is row 13. The vertical scale, showing deflection, is exaggerated by a factor of 24. The arrow in these figures indicates the position of the load. Deflection measurements were not taken at every point during all load tests. To obtain complete isometric drawings, some dummy deflection values obtained from assuming symmetrical values within the floor were input at needed locations. The vertical line indicating the deflection has been omitted at positions where dummy deflections were inserted. An example drawing of a deflected floor is shown in Fig. 4.6. The deflected shape for each floor resulting from a load applied at the center (position 0707) is presented in Figures 4.7, 4.8, 4.9, and 4.10.

(b) Empirical Load Sharing

An equation for calculating the load carried by each joist in a floor system was developed in the study by Polensek, Atherton, Corder, and Jenkins (19). This empirical equation was obtained after examination of data from forty-four laboratory-built wood-joist floors loaded with a 300 pound concentrated force applied at joist midspans. They concluded that, in most of their test floors, the concentrated load of 300 pounds resulted in deflections of six neighboring joists three on each side of the loaded joist. To determine the load sharing coefficients, Equation 4.1 was proposed and requires direct use of deflection data obtained in the concentrated load tests. The load-sharing coefficient, q_i , specifies the percentage of the concentrated load which is carried by the neighboring joist i .

$$q_i = \frac{m_i y_i}{\sum_{k=1}^n m_k y_k} \quad (4.1)$$

where m_k = factor depending on the type of load contribution of the joist k ,

y_k = midspan deflection of joist k obtained in testing,

n = number of deflected joists,

k, i = subscripts denoting joists.

The factor m_k used in Equation 4.1 was established by considering two shape functions for load distribution across the joists. The loaded joist was assumed to carry a concentrated load at midspan. The corresponding m_k value of 48 relates to the constant in the denominator for the equation for midspan deflection, $\Delta = PL^3/48EI$. The adjacent joists loaded by the plywood bridging across the joists were assumed to have a shape function of half a sine wave. This yields a m_k value of 62. The m_k value for other distributed loading patterns having a maximum value at midspan include m_k equal to 63 for a parabolic loading and 60 for an isosceles triangular loading (page 57 of Ref. 19). The assumption that the loaded joist carries only a concentrated load at midspan is shown to be incorrect in Section 5.2(b). The equation may however be a good approximation for calculating load-sharing coefficients.

Joist midspan deflections resulting from loads applied up to 1000 pounds at point 0707 for the four floors tested are presented in Figures 4.11, 4.12, 4.13, and 4.14. The load-sharing coefficients were calculated from these midspan deflections using Equation 4.1 for each floor at loads within the elastic range and the results are contained in Table 3.1.

TABLE 4.1

LOAD-SHARING COEFFICIENTS

Average coefficients of load-sharing, q_i , of the concentrated load applied in the mid-span of joist i , in percent.

Floor number	Load (pound)	Loaded joist i	First joist from i	Second joist from i	Third joist from i	Fourth joist from i
F1-6E16-1	500	25	21	11	3	2
"	1000	25	23	11	3	1
F2-8D16-1	250	32	24	8	2	0
"	500	33	23	9	2	0
"	750	33	24	8	2	0
"	1000	33	24	8	2	0
F3-8D16-1	250	35	24	8	0	0
"	500	34	25	8	0	0
"	750	34	24	8	1	0
"	1000	34	24	7	2	0
F4-12E16-1	250	45	25	4	0	0
"	300	45	25	4	0	0
"	750	45	25	4	0	0
"	1000	45	24	5	0	0

Table 3.1 indicates that in floor No. 1, consisting of 2 x 6 joists, the load was shared by nine joists. A joist was considered to be participating in the load sharing if it supported more than 1 percent of the applied load. Floors number 2 and 3 with 2 x 8 joists had load distribution to a total of five and sometimes seven joists. Floor number 4, with 2 x 12 joists, distributed the load to only five joists with 45 percent being supported by the joist at the point of application. These results show that as the joist size increases, compared to the sheathing, the load-sharing becomes localized and the joist under the applied load supports an increasing proportion. This behavior results from the decreasing ability of the plywood to spread load laterally to other joists as the ratio of the plywood stiffness to joist stiffness decreases.

4.3 Mode of Failure

(a) Deflected Surfaces at Overloads

The load-sharing by the joists became more localized with increased load because of inelastic behavior within the specimen. Figure 4.15 shows how the midspan deflection of the floor joists changes as the load on joist 07 is increased to failure. Seven joists shared in the load distribution for the floor with 2 x 6 joists when a load of 500 pounds was applied. At 3500 pounds applied load, five joists participated in resisting the load. Joists 04 and 10 carried only an insignificant percentage of this increased load. An approximate lower limit value for deflections remaining within the elastic zone is included in Fig. 4.15. This value was obtained from previous tests in which 1000 pounds was applied and the load-deflection curve indicated the floor returned to very near its undeflected shape when the load was

removed. Only joists 06, 07, and 08 deflected beyond the known elastic range. Figures 4.16 and 4.17 show the overload deflection behavior for floor numbers two and three, which included 2 x 8 joists.

This localization of the floor resistance and joist failure was even more pronounced in floor F4-12E16-1. Figure 4.18 shows the midspan deflections of 2 x 12 joists of this floor when the load was applied at position 0707. Only three joists show significant load-sharing effects when the loads produced deflections within the elastic range. At joist failure, only the loaded joist deflected beyond the known elastic range.

Isometric plots have also been drawn to show the deflection surface around the load actuator. To produce these surfaces, comprehensive deflection data were collected during the failure of floor number F4-12E16-1. Figures 4.19, 4.20, and 4.21 show the stages of deflection with increased load until the loading pad punched through the plywood sheeting. Figure 4.19 shows the stages of deflection with applied loads of 1000, 2000, 3000, and 4000 pounds. Figure 4.20 shows joist 07 after it had broken and the increased deflection of joists 06 and 08 which had to accept additional load when the load carrying capacity of joist 07 dropped. In Figures 4.20 and 4.21, joist 07 has failed and the deflected shape of joist 07 is no longer the same as the floor surface. Therefore, on these figures joist 07 is shown in its deflected configuration immediately before failure.

(b) Description of Inelastic Behavior up to Initial Joist Failure

Inelastic behavior developed with increasing load which resulted in distress within the joists and plywood. At these increased loads nonlinear response was exhibited through inelastic stress and

the formation of splitting in and near knots located in the bottom portion of the joists which acted as stress raisers. This was usually the first distress noted in the overload tests. When the grain angle deviated by more than about five degrees from the longitudinal axis of the joist, splits developed parallel to the grain and extending from the bottom fibers. Small splits parallel to the edge and near the middle of the joist depth, due to horizontal shear, sometimes developed when the grain angle was along the joist.

As joists deflected under load, horizontal shear forces in the joist-plywood layered beam system caused slip between the plywood and joists. To resist this slip, some bending of the nails and local crushing of the wood fibers around each nail occurred. Increase loads caused additional horizontal shear resulting in lateral deformation forces in the nails fastened to the joists near the loaded point. These withdrawal forces caused the nails to either withdraw from the joists, or to tear through the plywood sheeting. An additional discussion of nail-slip characteristics is contained in Section 5.2. This inelastic behavior continued to develop with increasing load until the joist failed.

However, the load-deflection curves remained nearly linear up to initial joist failure even though the floor obviously was experiencing some inelastic behavior. Figure 4.22 shows the linearity of a typical load-deflection curve of a joist loaded to failure.

The usual manner of joist failure was for a crack, following the diagonal grain angle, to propagate until it extended through the entire joist depth. Figure 4.23 shows this type of joist failure. Another type of failure was for the joist to split in half due to

horizontal shear developing a crack along a grain angle parallel to the joist edge. Figure 4.24 shows a joist which split at near midheight.

A less common joist failure mechanism was cross grain tension failure. This type of failure usually occurred when the joist was partially split with only a few inches at the top of the joist remaining. This occurred when the angle of grain was parallel to the joist and knots were absent from the immediate area.

(c) Description of Final Floor Failure

The failure of the loaded joist did not mark the maximum load carrying capacity of the floor. After this initial failure, the plywood was able to bridge across the broken joist and redistribute the load to the neighboring joists. The magnitude of this plywood bridging effect is dependent upon the plywood stiffness and strength as well as joist spacing. Strength and stiffness of the plywood is in turn dependent upon species, grade, and thickness. Nearly twice the load which produced initial joist failure was often supported by the remaining floor system. The analysis of the floor load carrying capacity is discussed in Section 5.2.

The final configuration of the floor at failure was found to be dependent upon the position of the load. The two basic load placements studied were load placed over a joist at the middle of an attached plywood sheet (example: position 0707 on the floor), and load placed over a joist on the joint of the plywood sheeting (example: position 0704 on the floor).

When the load was placed away from the edge of a plywood sheet, the plywood could bridge as a continuous beam across the broken joist to the neighboring ones. As the load was increased, the two neighboring joists

deflected and, depending on the floor configuration of joist and plywood sizes, sometimes reached the inelastic range. In the floors constructed with 2 x 8 joists, the joist adjacent to the loaded joist sometimes also failed. The nails fastening the plywood to joists 06 and 08 also showed distress in all floors loaded to failure at point 0707. Horizontal shear stresses also caused slip between the two layers of these neighboring joists. The two neighboring joists also tended to twist toward the applied load which caused further nail slip and pullout as shown in Fig. 5.1. The failure load tests were terminated when the 4 x 4 inch loading pad punched through the plywood at the maximum applied load as shown in Fig. 4.25. A typical load-deflection curve for load applied at position 0707 on the floor, and plotted until plywood failure, is shown in Fig. 4.26.

When the load was placed on a plywood joint, the plywood was forced to distribute the load in the lateral direction primarily by cantilever beam action. Additional lateral load distribution was developed because nails attaching the plywood to the broken joist allowed the plywood near the load to support some load through a tensile membrane or suspension action. Again this load redistribution after initial joist failure caused bending and inter-layer slip in the neighboring joists. With increasing load, the suspension action of one plywood sheet was usually lost when the nails attaching the plywood to the loaded joist withdrew or were pulled through the plywood. The one plywood sheet remaining attached to the broken joist was then forced to resist a majority of the load. Eventually with increased load the loading pad sheared through the remaining plywood sheet. Figure 4.27 shows this type of failure at a plywood joint. A load-deflection

curve of floor F3-8D16-1 loaded at position 0704 to failure is plotted in Fig. 4.28.

CHAPTER 5

STRENGTH ANALYSIS

5.1 Introductory Remarks

Chapter 4 described the ability of a flooring system to support load after the failure of the joist directly under the loaded point. This ability of the floor to redistribute load to neighboring joists and eventually support more load than that causing initial joist failure is discussed in more detail in Section 5.2(a). Included in this section is a comparison of the load carrying capacity determined from conventional design of wood floors with the load causing failure of the first joist. A brief discussion of a possible method of designing wood floors to include the added strength due to the T-beam action and load-sharing is also contained.

The load-sharing coefficients calculated in Chapter 4 and the assumption that the loaded joist simply carries a concentrated load is discussed in Section 5.2(b). Also, the load distribution actually observed for this joist will be described. In the same section the application of the nail-slip tests performed by the Wood Science Laboratory is compared with the stresses applied to the nails of a floor system subjected to a concentrated load. Finally, the way in which a floor system resists concentrated loads approaching its ultimate capacity is examined, and a model including membrane action of the plywood is discussed.

5.2 Analysis

(a) Flexural Strength of Loaded Joist

A discussion of strength requires a definition of what constitutes failure. The point of failure is often obvious and unique. However, failure could be defined at several load levels for the wood floor systems tested. One definition of failure would be the point at which the applied load can no longer be supported, which for a wood floor is when the load punches through the plywood. This load will be discussed later in this section and is the most variable measure of failure load. A second definition of floor failure is the load causing the initial joist to fail. The point defining this failure is obvious, but the resistance to load may not fall appreciably and can be considerably less than the maximum capacity of the floor. Continued load carrying capacity is possible and is dependent upon the plywood's ability to bridge between the neighboring joists. Another occurrence that can be considered a failure of the floor is the reaching of a deflection limitation or a serviceability failure.

An important factor to an owner or occupant is to limit deflections of wood floors. A floor which vibrates and deflects enough that it feels inadequate can result in the floor being judged unacceptable even if its actual strength far exceeds the loads it must carry. The deflection limit for floors with ceilings is usually set at the span divided by 360, or 0.4 inch for a 12 foot span (4). Using this limit and neglecting load-sharing and T-beam action, the usual procedure in floor design, allowable concentrated loads were computed for each of the floors and these values are shown in Table 5.1. Also listed in this table are the actual loads causing a deflection of 0.4 inch for each

TABLE 5.1
 EXPERIMENTAL LOAD COMPARISONS
 Conventional design loads versus the experimental load values
 for concentrated loads applied at midspan

Design criteria	Method of determining load	Values of individual floors				Common units
		F1	F2	F3	F4	
Deflection or span/360	Conventional design	134	459	459	1144	pounds
Deflection or span/360	Experimental measurements	850	1550	1600	2825	pounds
Deflection or span/360	Percent increase of experimental measurements	534	238	249	147	percent
Allowable bending stress	Conventional design	184	496	496	773	pounds
	Measured load at failure	4000	4250	3450	4000	pounds
Allowable versus failure	Percent increase of experimental measurements	2074	757	596	417	percent

floor, obtained from the average midspan deflections of several loading tests. Comparison of the two values reveals the increase in load, above that allowed by conventional design, which can actually be supported before the deflection limitation is reached. With the floor using 2 x 6 joists, an increase in load of 534 percent was supported, and with 2 x 12 joists, an increase in load of 147 percent was supported before a midspan joist deflections of 0.4 inch was reached.

In the conventional design technique, three conditions are checked to determine the allowable loads. Shear stress must be computed and compared with allowable values. However, this is usually not the controlling factor for floor design. The second check is concerned with deflection limitations of the floor and is discussed in the preceding paragraph. The third check is to show the bending stresses do not exceed the allowable values. This was the controlling factor for all four floors. Table 5.1 lists the allowable loads determined by conventional methods and limitations on bending stress from the National Design Specifications (8). A load duration factor of 1.6 was included in the conventional method to account for an approximate loading time of 10 minutes. The loads averaged from each floor tested, which were required to cause joist failure are also presented in Table 5.1. The percent increase of joist carrying capacity over that computed as allowable is listed in Table 5.1. The joists supported 4 to 21 times more load than conventionally considered allowable.

How can this large discrepancy between conventionally-designed and experimentally-measured loads be explained? In determining allowable stresses, considerations are made for load duration, a strength ratio for defects, moisture content, and special grading (5). Each one of

these limits has a maximum and therefore is a conservative value for most pieces of lumber. Therefore, the safety factor is a combination of each conservative value. All these allowable values are then based on those exceeded by 95 percent of all specimen tested. It must be noted here that conventional design procedures are for uniform loads and include an increased allowable bending stress for repetitive members. However, conventional design techniques for wood flooring systems leave out two essential factors, the load-sharing by neighboring joists and the T-beam interaction of joist and plywood. Section 4.2(b) discusses empirical data on concentrated loads showing that load-sharing alone could increase allowable loads by 200 to 300 percent.

The added stiffness and strength of the floor due to T-beam action can be illustrated by examining results of the T-beam tests. Test results of T-beam T2-8D48-1 are shown in Table 5.2. The test results for this T-beam are examined because this T-beam had only one joist and therefore, one non-overlapping effective plywood flange. Loads were applied to the joist before and after the plywood was attached. Therefore, any increase in stiffness can be attributed directly to the contribution of the plywood flange. The average increase in stiffness for this T-beam was 34 percent. The study done by NAHB (14) also found a similar increase, 35 percent, in the stiffness for the floors, using similar plywood and joists, that were load-tested during their research.

The load carrying capacity of a wood flooring system will normally exceed the load required to fail the first joist, when supporting a concentrated load. This can be considered as an added safety factor. Section 4.3(c) describes the two types of failures observed during this

TABLE 5.2
T-BEAM STIFFNESS

T-beam number T2-8D48-1 deflections at joist midspan

Load (pounds)	Deflections without plywood attached	Deflections with plywood attached	Percent increase of stiffness with plywood
250	0.139	0.101	34.5
500	0.287	0.215	33.5
750	0.446	0.334	33.6

research. In one, the plywood was continuous over several joists on each side of the load. For loads applied near the center of a plywood sheet an increase of at least 2000 pounds above the load causing first joist failure could be supported before the load punched through the plywood.

The second type of failure resulted when the plywood was butted together over the loaded joist. Loads applied over the plywood joint required only an average load of 115 percent of that causing initial joist failure before the load punched through the floor. This small increase results from the plywood discontinuity and leads to an earlier failure of the plywood attached to the joist. The increase is also strongly influenced by the configuration of the failed joist. If the joist splits close to parallel with its longitudinal axis and does not drop away from the plywood, the nails can remain within the joist. This yields suspension and cantilever actions from the two plywood sheets. However, if the joist cracks diagonally through the joist and

close to the applied load, the failure configuration will cause the joist to pull away from the plywood sheeting. Then the nails can no longer hold the two plywood sheets together and to the joist. Therefore, only cantilever action supports the load over a narrow width of plywood. Only a slight increase in load then leads to the actuator pad punching between the two bending plywood sheets.

(b) Membrane Action with Nail-Slip and Pullout

Test results show that a concentrated load applied over a joist is supported by 3, 5, or 7 joists, depending upon the ratio of plywood thickness to joist depth of the flooring system. The neighboring joists are loaded by the deflection of the plywood. Figure 5.1 illustrates the load distribution to the other joists. The joist being loaded was assumed in Section 4.2(b) to be loaded only by a concentrated load. Because some load must be transferred from the loaded joist to the plywood causing bending of the plywood, the assumption of concentrated load only is incorrect. An exaggerated diagram showing the actual loading which is applied to this joist is contained in Fig. 5.2. This shape was observed experimentally and verified with mathematical models when overloads were placed on the floor and just before joist failure. Nails were withdrawn from the floor as much as $3/4$ inch by the tensile forces loading the plywood. From this loading diagram in Fig. 5.2, it is obvious that the concentrated load assumption used in calculating load-sharing coefficients results in only an approximate technique.

Another conclusion based on the loading pattern shown in Fig. 5.2 concerns the nail-slip characteristics. Due to bending of the floor and the resulting horizontal shear, inter-layer slip occurs between the joists and sheathing. Bending of the plywood in a direction perpendicular

to the joists causes the nails to be stressed in tension and as noted above, high loads can result in the withdrawal of the nail from the joist. Therefore, because the nail connector is loaded both in shear and withdrawal, an interaction between these two loads probably exists. The semi-standard nail-slip tests, completed by Patterson (17) and others (1), do not apply tension to the nails. The loaded joist is the major one with the upward distributed load shown in Fig. 5.2, which produces tension in the nails and the nail-slip constants are likely most in error for this joist. Further study should be conducted on nail-slip characteristics to determine how much effect tension in the nails can change the nail-slip constants.

Examination of the geometry of an over-loaded flooring system near failure shows that a configuration forms in which membrane stresses are very important. The application of load at the center of a plywood sheet produced an area of tensile stresses around the loaded point supported by inplane compressive forces in the plywood still further from the load. Figure 5.3 illustrates these tension stresses throughout the plywood sheet which are transmitted through the nails to the joists. These stresses have a component parallel to the joist which causes interlayer slip and another component which tends to bend the joist toward the point of load application. These stresses may also result in strains in neighboring plywood sheets when they are partially transferred through the nails in the joists at the edge of the sheet. This configuration of tension and compression regions within the floor is also illustrated in Fig. 5.3. For a load applied on a plywood joint, a similar stress field is illustrated in Fig. 5.4.

The load was applied directly over a joist in all the load-tests described thus far. During the testing of floor F3-8D16-1, a concentrated load was also applied at position 0211.5, a point half way between joists 11 and 12. As the load was increased, a continuous beam failure was readily observed in the plywood. This failure mechanism developed into three hinges; one over each neighboring joist and one under the load. A similar failure mechanism was developed when the load was applied in the middle of a plywood sheet after the joist beneath the load had failed. Large tension cracks were observed in the plywood at each hinge, on top at the negative hinges and underneath at the positive hinge. The load positioned at 0211.5 which finally allowed the 4 by 4 inch loading pad to punch through the plywood was 5000 pounds, and occurred at a combined joist and plywood deflection of approximately 1 1/2 inches.

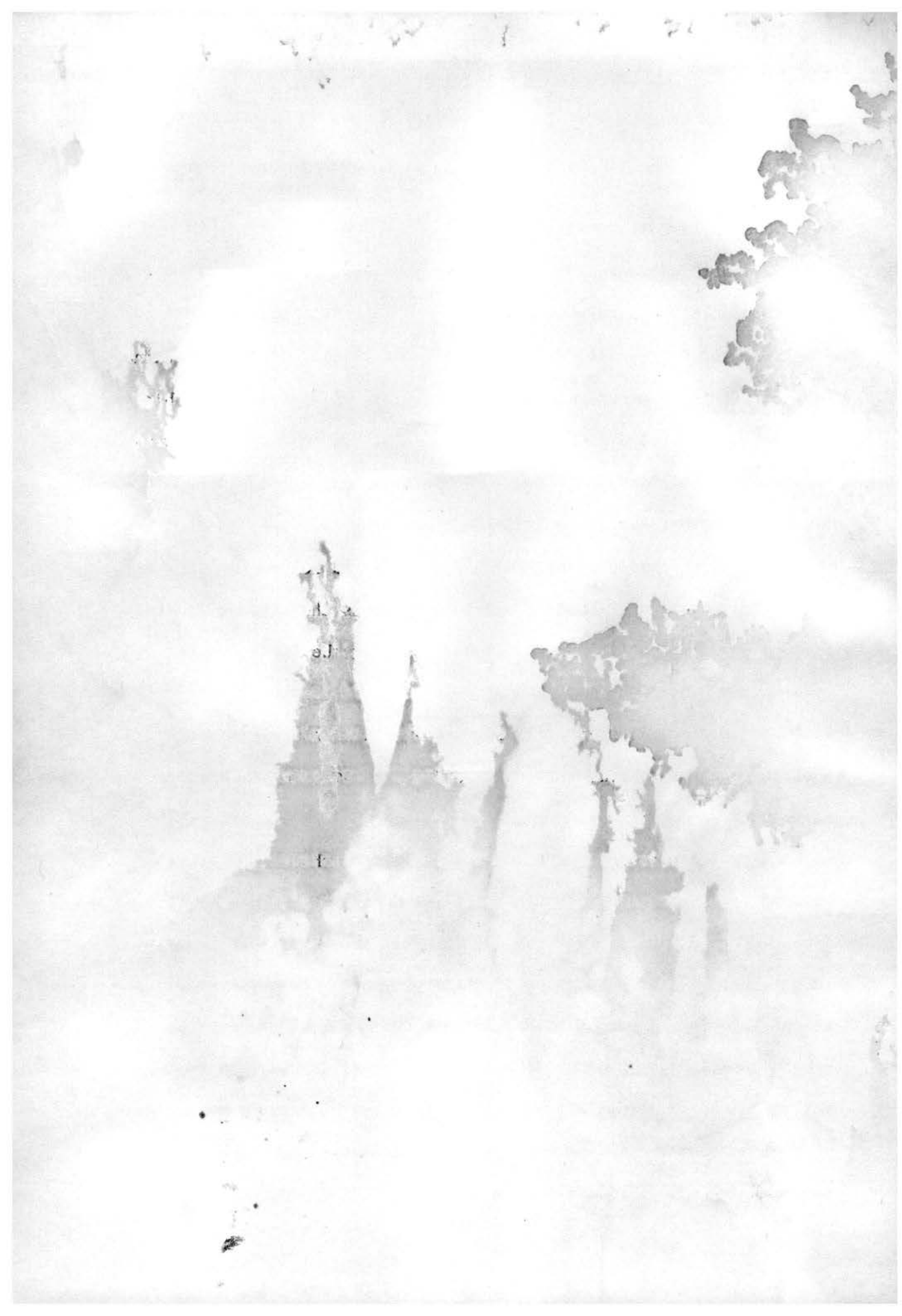
CHAPTER 6

SUMMARY AND CONCLUSIONS

6.1 Summary of the Testing Program

During this study, four floors and two T-beams were constructed from wood joists and plywood and were subjected to concentrated load tests. Three of the floors had over-all dimensions of sixteen feet by twelve feet five inches as shown in Fig. 2.7. This latter dimension included a joist clear span of 12 feet, a bearing of 2 inches and a header joist attached for lateral stability. Variations between the floors included differences in joist size, species, and grade; plywood thickness, species, and type; and nail spacing and type. Table 2.1 lists the variations used within each floor. These floors were tested by applying a concentrated load at various positions on the floor and recording the joist deflections at numerous load increments. The ultimate load carrying capacity of each floor was also determined by applying increasing load until a punching failure occurred in the plywood.

Several studies have concluded that T-beam interaction occurs between each joist and the attached plywood within a flooring system (1, 6, 7, 8, 9, 10, 12, 14, 18, 19, 20, 21). To study this behavior in more detail, two T-beams were constructed with properties similar to those of the floors. Table 2.2 lists the material properties used within each T-beam. One objective of the T-beam testing was to determine the extent of stress within the plywood flange due to loading the T-beam as a unit. Once the stress distribution of a T-beam flange is evaluated, an effective flange of equal capacity can be assumed. To



determine the extent of the effective flange, strain measurements were recorded across the T-beam flange as load increments were applied.

6.2 Conclusions

Conventional design of wood flooring systems is completed by satisfying deflection limitations, allowable bending stresses, and allowable shear stresses. Test results, listed in Table 5.1, obtained during this study show that the load corresponding to the allowable deflection can be 300 percent above the allowable load computed with the usual assumptions. Even with these loads applied, the floor joists still had a margin of safety with respect to first joist failure of 1175 to 3150 pounds of additional concentrated load. The load corresponding to first joist failure was 4 to 21 times the allowable joist load computed from allowable stresses and using the usual design assumptions.

This large discrepancy between design loads and experimental failure loads is partially due to the design procedure's neglect of the two major factors of load-sharing and T-beam action. Experimental data on load-sharing, discussed in Chapter 4, reveals that a concentrated applied load is distributed to as many as seven joists, depending upon the floor material used. Table 3.1 and other studies (19) clearly show that load-sharing is dependent upon joist size, species, and grade as well as these characteristics of the plywood. One T-beam test provided results showing that a 34 percent increase in stiffness could be attributed directly to the effects of the plywood flange in a beam of reasonable proportions. From previous research (1, 19) and the test results obtained during this study it is suggested that simple constants

representing load-sharing and T-beam action could and should be developed for each type of flooring system. These constants could then be applied directly in the conventional design technique to incorporate the load-sharing and T-beam action within a loaded floor.

REFERENCES

1. Amana, E. J. and Booth, L. G., "Theoretical and Experimental Studies on Nailed and Glued Plywood Stressed-Skin Components," Journal of the Institute of Wood Science, Vol. 4, No. 19, Sept. 1967, pp. 43-69, and Vol. 4, No. 20, April 1968, pp. 19-34.
2. American Concrete Institute, "ACI Standard Building Code Requirements for Reinforced Concrete," The Institute, Detroit, 1971, (ACI 318-71).
3. American Institute of Steel Construction, "Manual of Steel Construction, seventh edition," The Institute, New York, 1970.
4. American Institute of Timber Construction, Timber Construction Manual, John Wiley and sons, Inc., New York, 1966.
5. American Society for Testing and Materials, 1968 Book of ASTM Standards, by the Society, Philadelphia, 1968.
6. Goodman, J. R., "Layered Wood Systems with Interlayer Slip," Wood Science, 1, (3):148-158, 1969.
7. Goodman, J. R. and E. P. Popov, "Layered Beam Systems with Interlayer Slip," Journal of the Structural Division, ASCE, Vol. 94, No. ST 11, Proc. Paper 6214, 2535-2547 pp., 1968.
8. Goodman, J. R., W. M. Henghold, and H. Y. Rassam, "Design Aspects of Mechanically Connected Composite Systems," accepted for presentation and publication, ASCE Specialty Conference on Selection, Design and Fabrication of Composite Materials for Civil Engineering, Carnegie-Mellon University, Pittsburg, Pa., November 1972.
9. Henghold, W. M., "Layered Beam Vibrations Including Slip," Ph.D. Dissertation, Colorado State University, Fort Collins, June 1972.
10. Henghold, W. M. and J. R. Goodman, "Static and Dynamic Behavior of Layered Beams Including Slip," Presented and published, Sixth St. Louis Symposium on Composite Materials in Engineering Design, May 1972.
11. Hurst, H. T., "The Wood-Frame House as a Structural Unit," National Forest Products Association, Washington, D.C., 1965.
12. Ko, Meng-Fang, "Layered Beam Systems with Interlayer Slip," M.S. Thesis, Colorado State University, Fort Collins, Colorado, December 1972.

REFERENCES - (Continued)

13. McClain, Thomas E., "Nondestructive Evaluation of Full Size Wood Composite Boards," M.S. Thesis, Colorado State University, Fort Collins, Colorado, 1973.
14. National Association of Home Builders Research Foundation Inc. "Static and Dynamic Performance of a Minimum Wood Joint Floor Construction," The Foundation, Rockville, Maryland, June 1970.
15. National Forest Products Association, "National Design Specification for Stress-Grade Lumber and its Fastenings," The Association, Washington, D.C., 1971.
16. O'Halloran, M. R., "Nondestructive Parameters for Lodgepole Pine Dimension Lumber," M.S. Thesis, Colorado State University, Fort Collins, Colorado, December 1972.
17. Patterson, David W., "Nailed Wood Joist Under Lateral Loads," M.S. Thesis, Colorado State University, Fort Collins, Colorado, 1973.
18. Polensek, Anton, "Static and Dynamic Properties of Glued Wood-Joist Floors," Forest Products Journal, Vol. 21, No. 12, December 1971.
19. Polensek, Anton, Atherton, G. H., Corder, S.E., and Jenkins, J. L., "Response of Nailed Wood-Joist Floors to Static Loads," Forest Products Journal, Vol. 22, No. 9, September 1972. pp. 52-61
20. Sliker, Alan, "Joist Deflection Simulated by a Computer Program," Forest Products Journal, Vol. 22, No. 9, September 1972. pp. 71-73.
21. U.S. Department of Agriculture Forest Service, "U.S. Forest Products Laboratory 1970 Progress Report on Lumber, Plywood, and Related Research," Forest Products Laboratory, Madison, Wisconsin, October 1970.

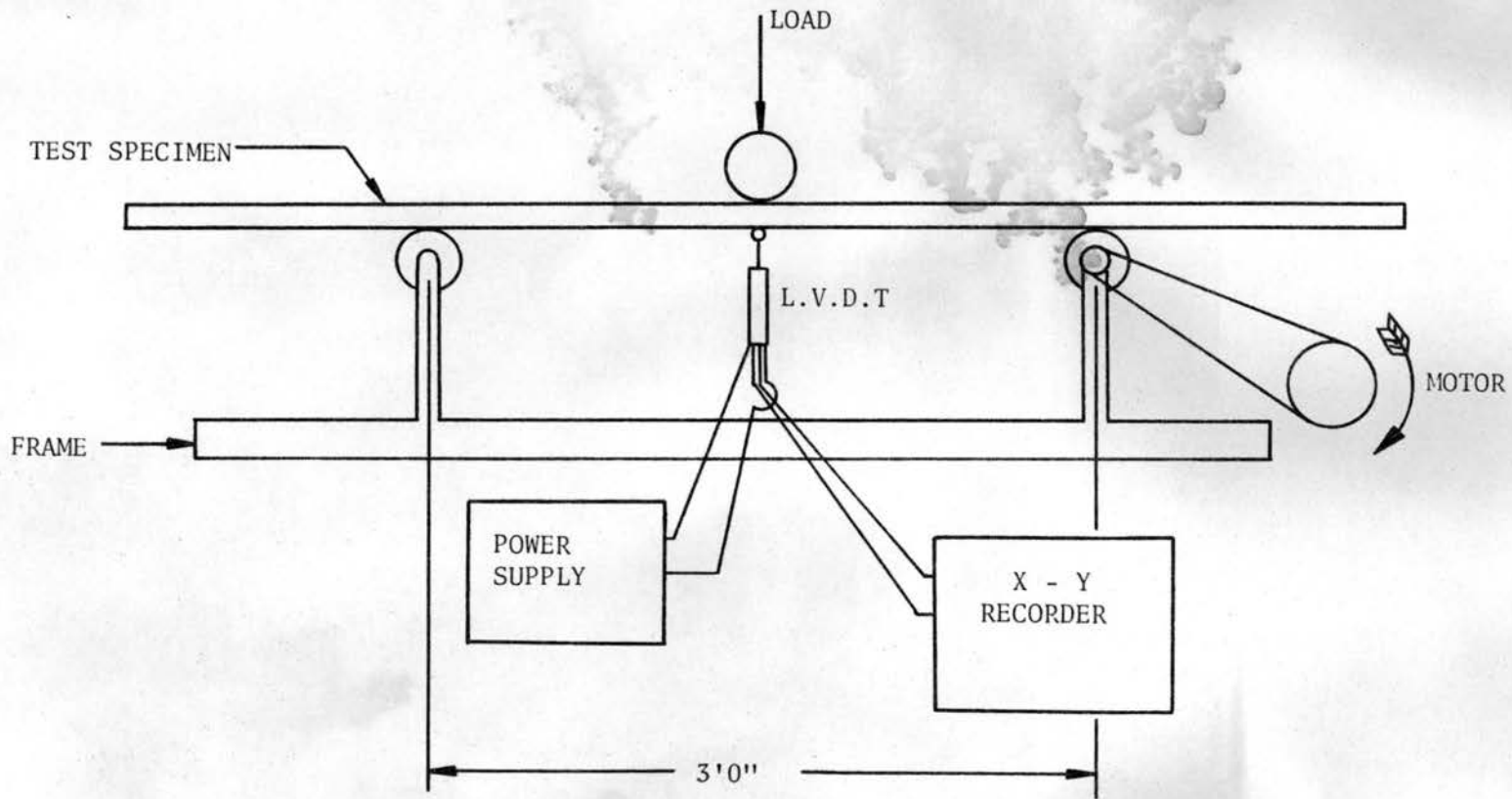


Fig. 2.1. Top view of continuous deflection testing machine for joists.

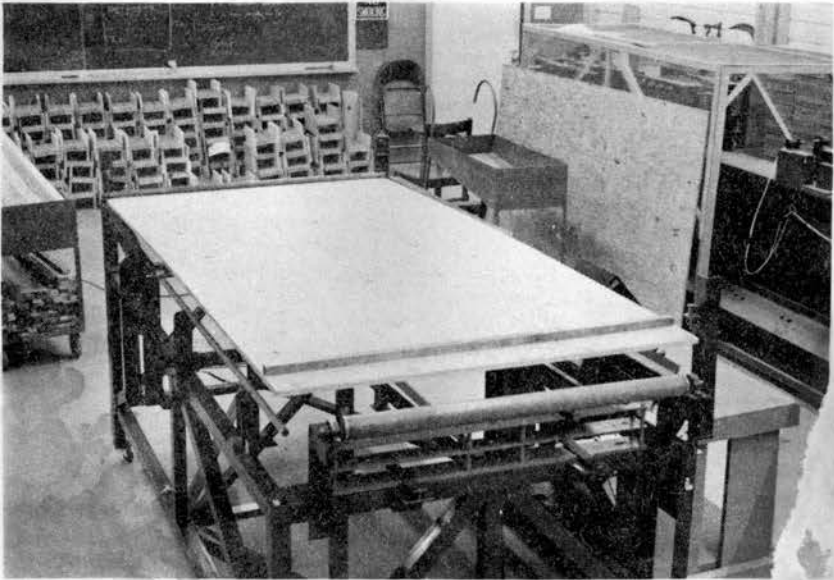


Fig. 2.2. Apparatus used in determining plywood modulus of elasticity values.

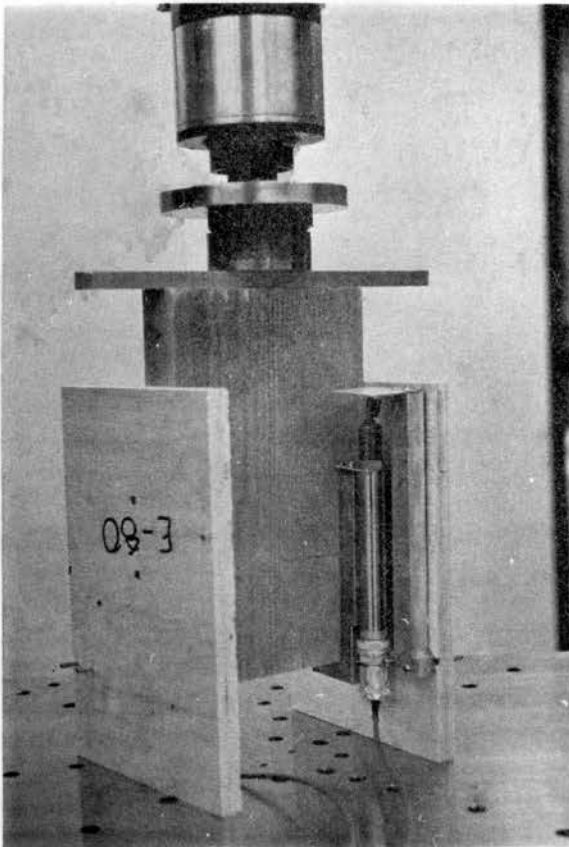


Fig. 2.3. Testing configuration used to obtain nail-slip curves.

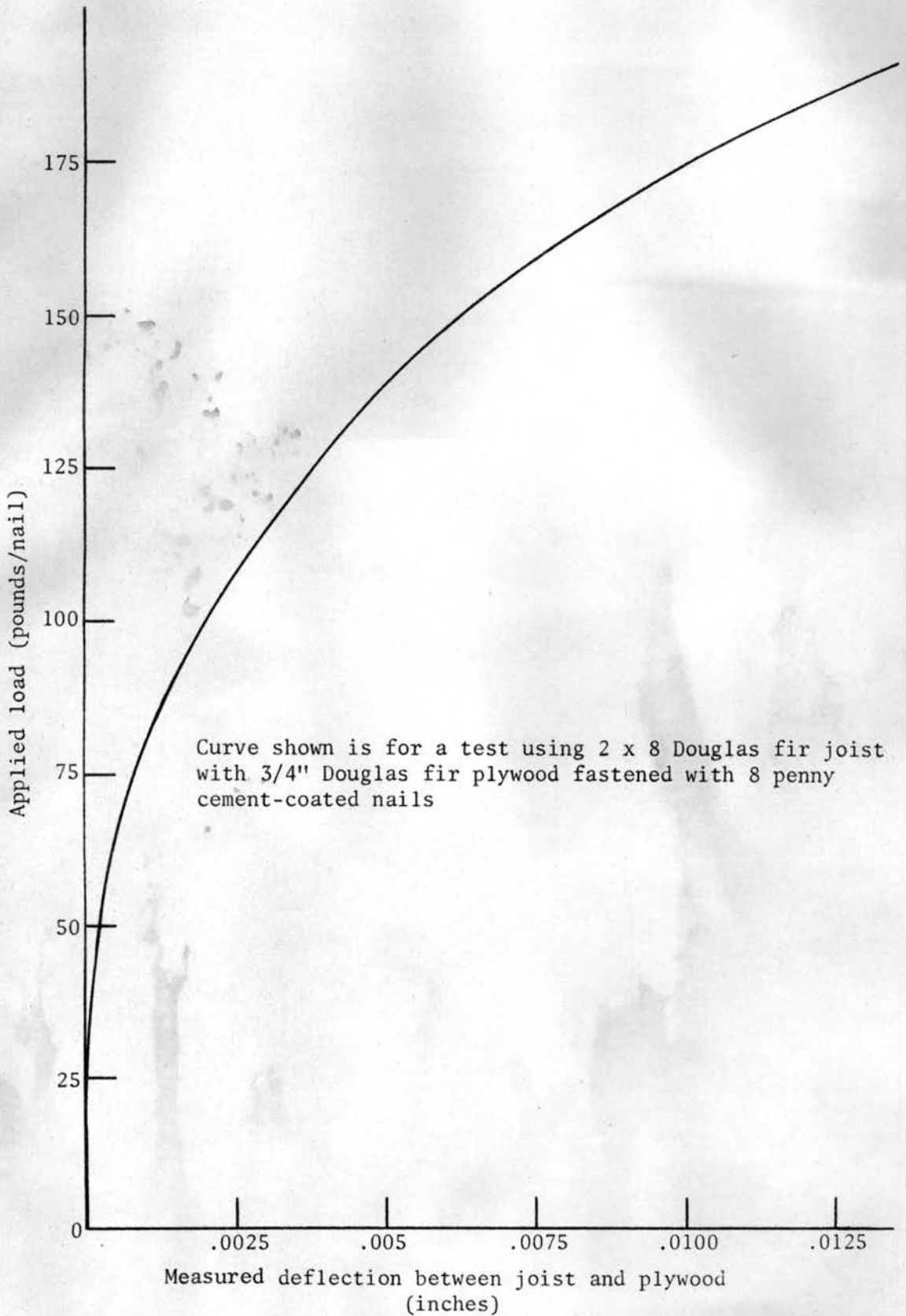


Fig. 2.4. Typical nail-slip curve between joist and plywood.

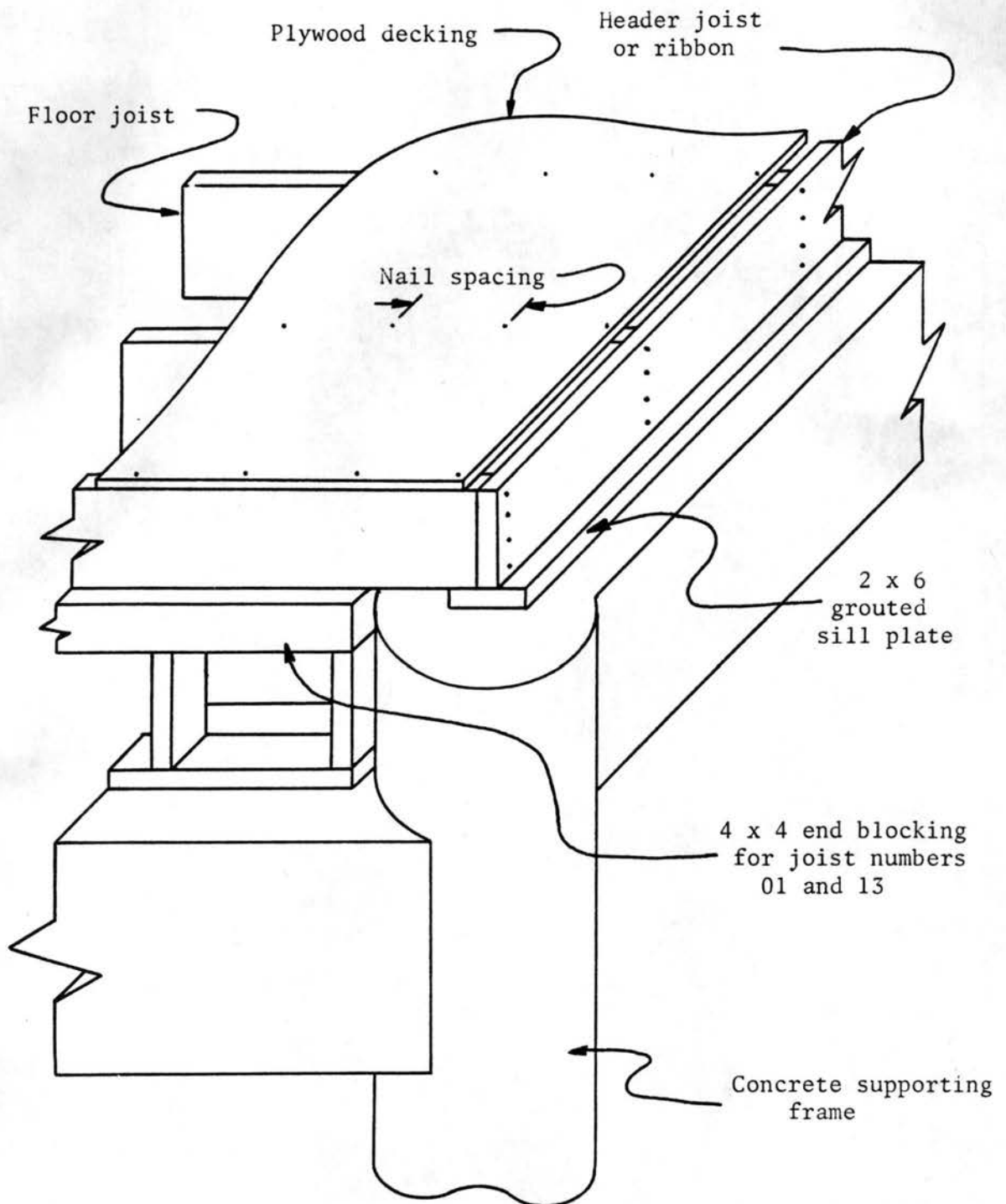


Fig. 2.6 Cut-away view showing floor construction and floor support.

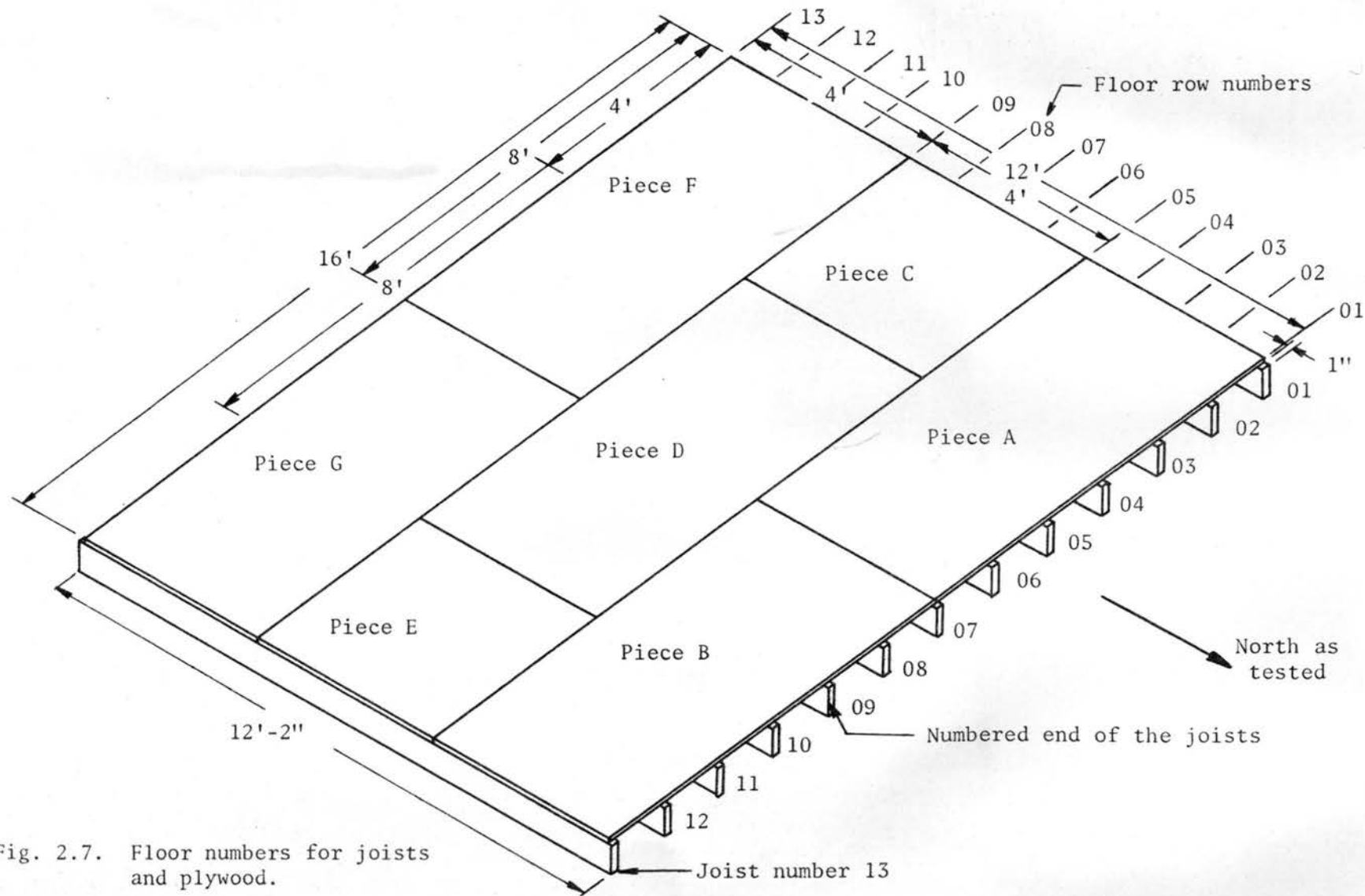


Fig. 2.7. Floor numbers for joists and plywood.

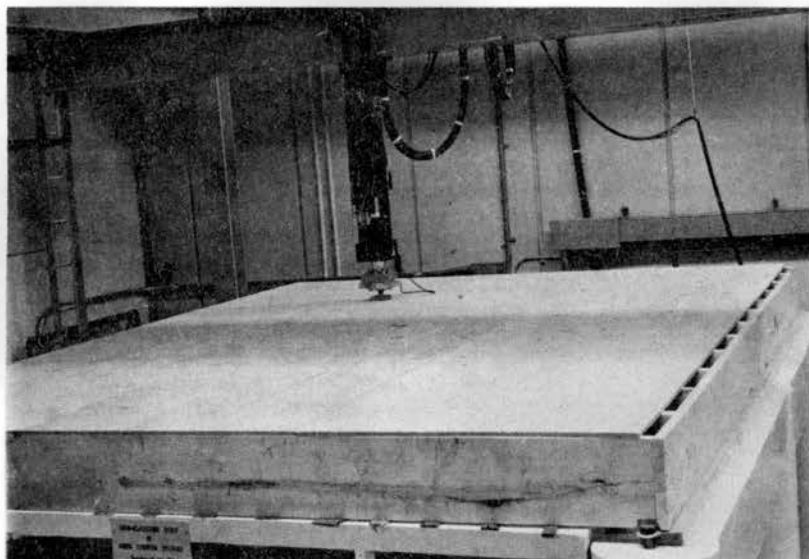


Fig. 2.8. Floor No. F4-12E16-1 mounted on the testing frame.

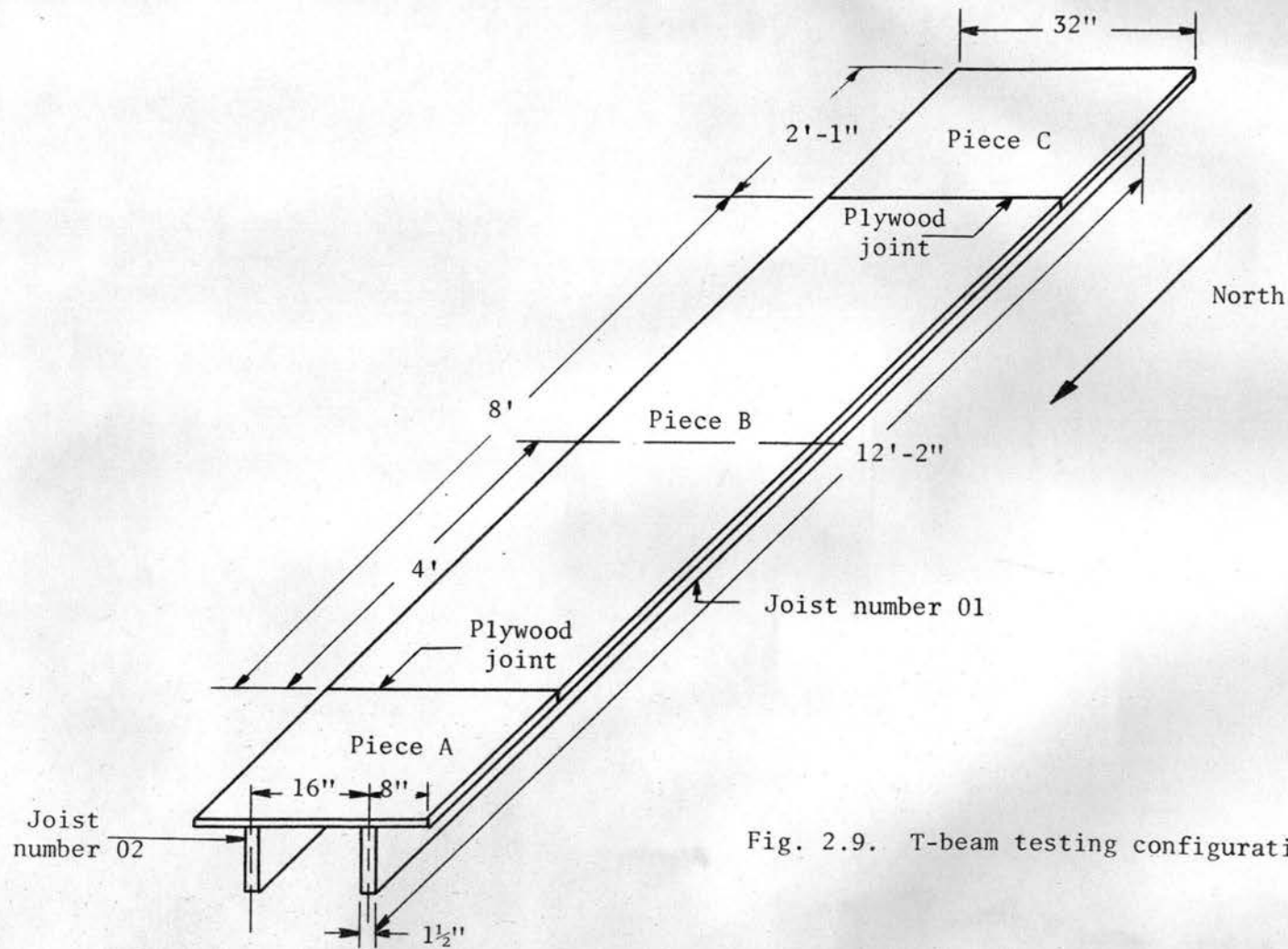


Fig. 2.9. T-beam testing configuration.

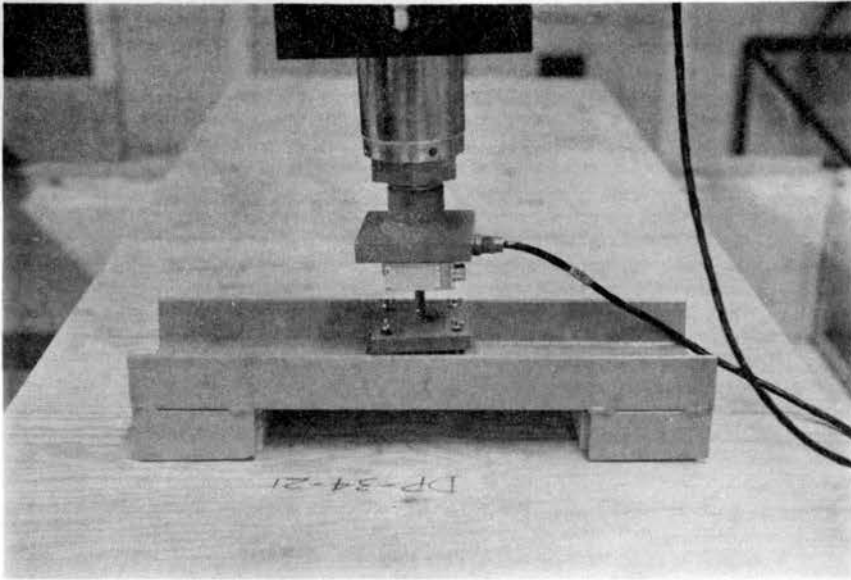


Fig. 3.1. Load distributing bridge used in T-beam testing.

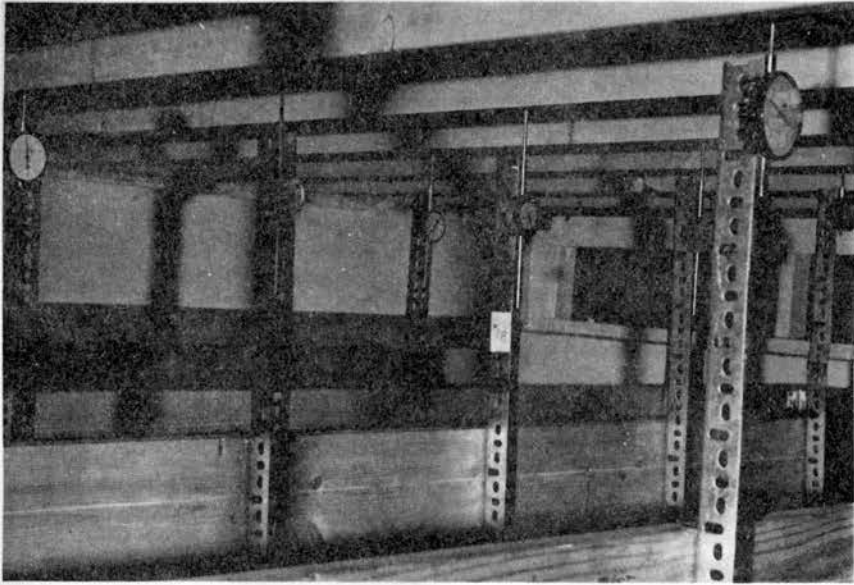


Fig. 3.2. Deflection dial indicators supported under the floor joists.

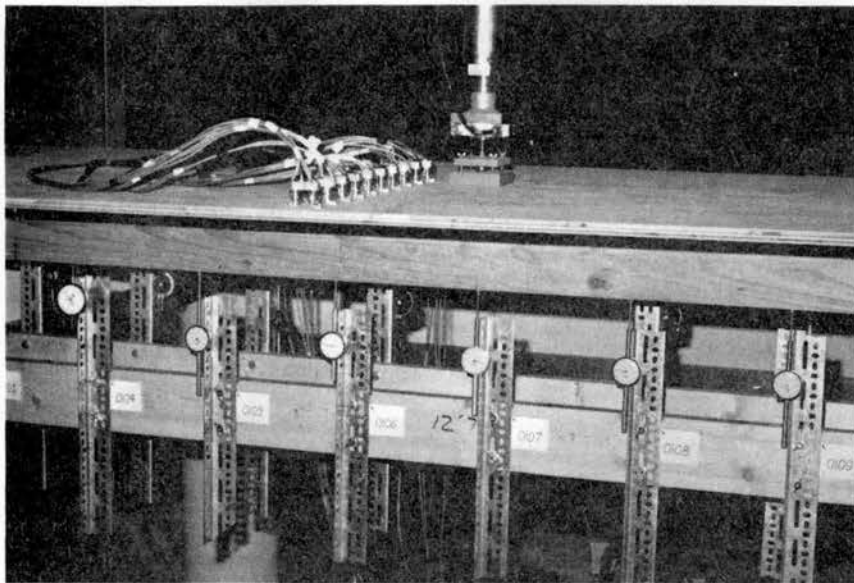


Fig. 3.3. Deflection dial indicators supported under the T-beam joists.

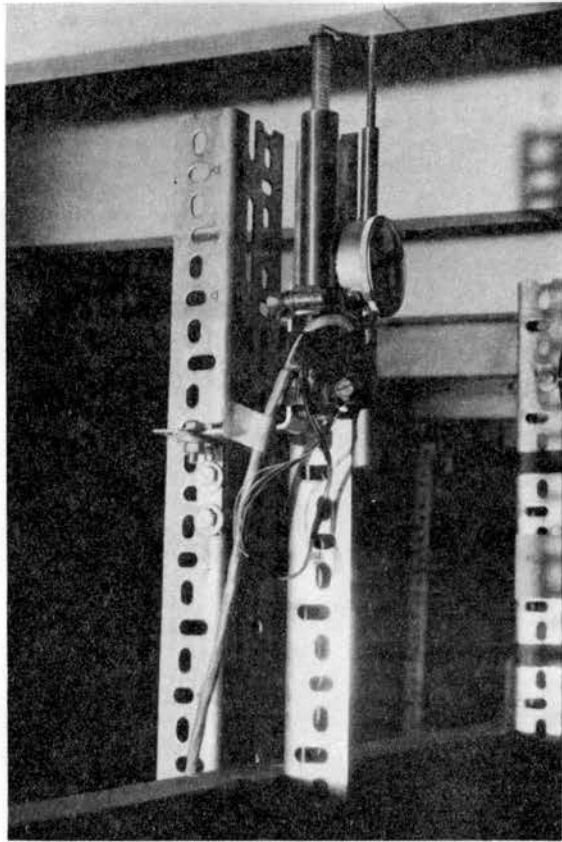


Fig. 3.4. A deflection dial indicator and LVDT positioned under a floor joist.

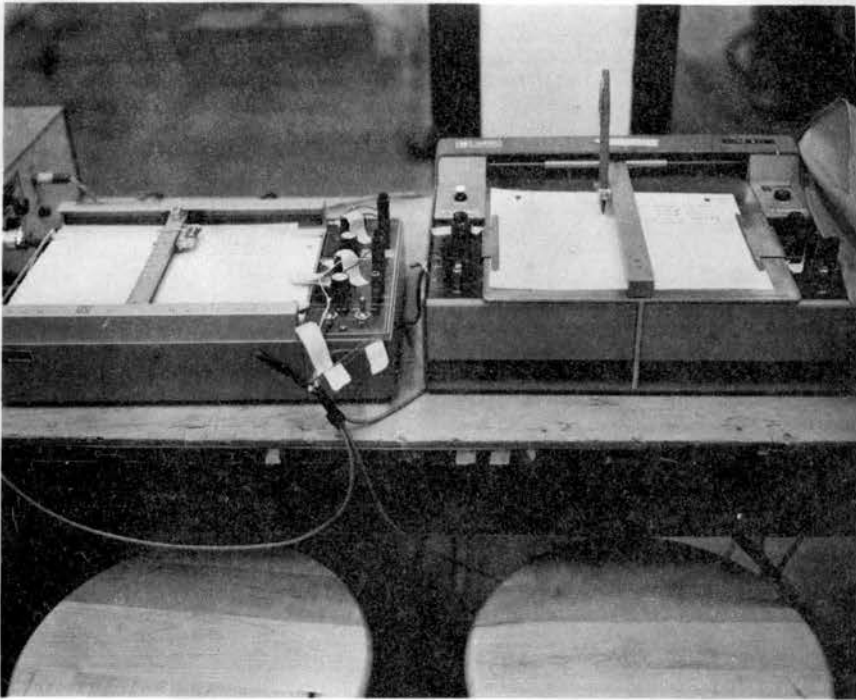


Fig. 3.5. X-Y plotters used to draw the continuous load versus deflection curves.

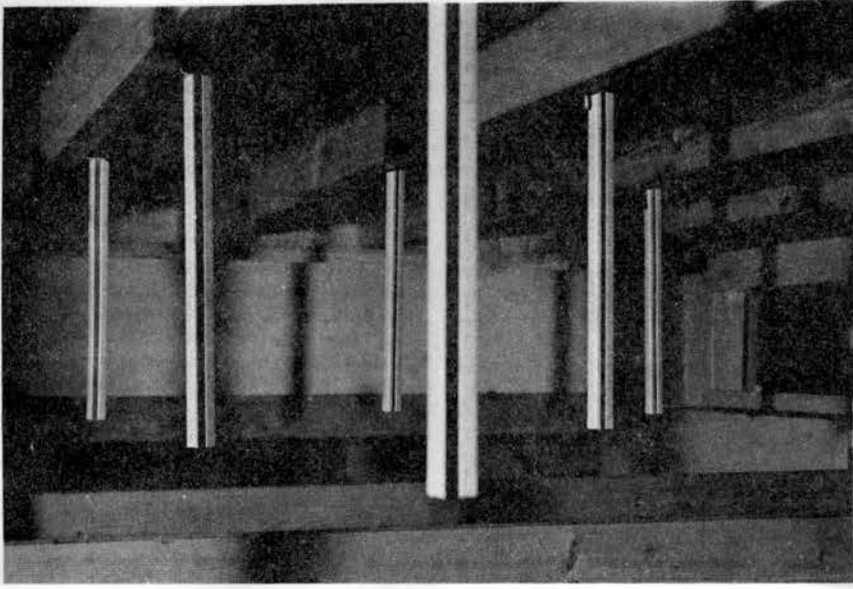


Fig. 3.6. Attachment of engineering scales to floor joists.

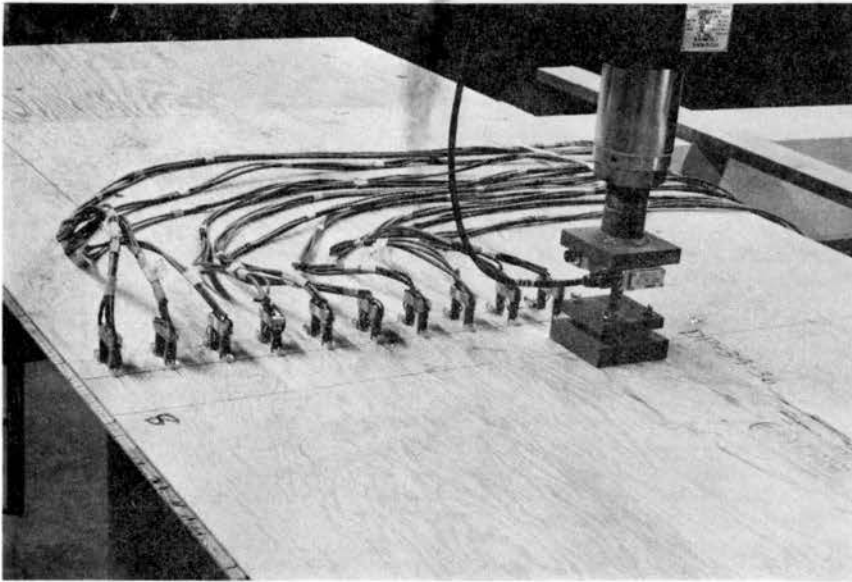


Fig. 3.7. Strain gage clips placed across a T-beam flange.

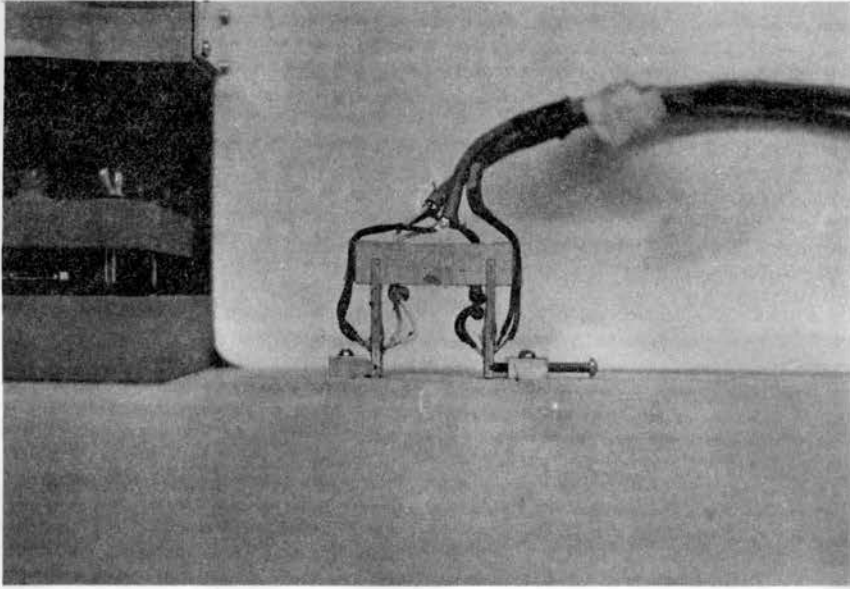


Fig. 3.8. Individual strain gage clip attached to the plywood Decking.

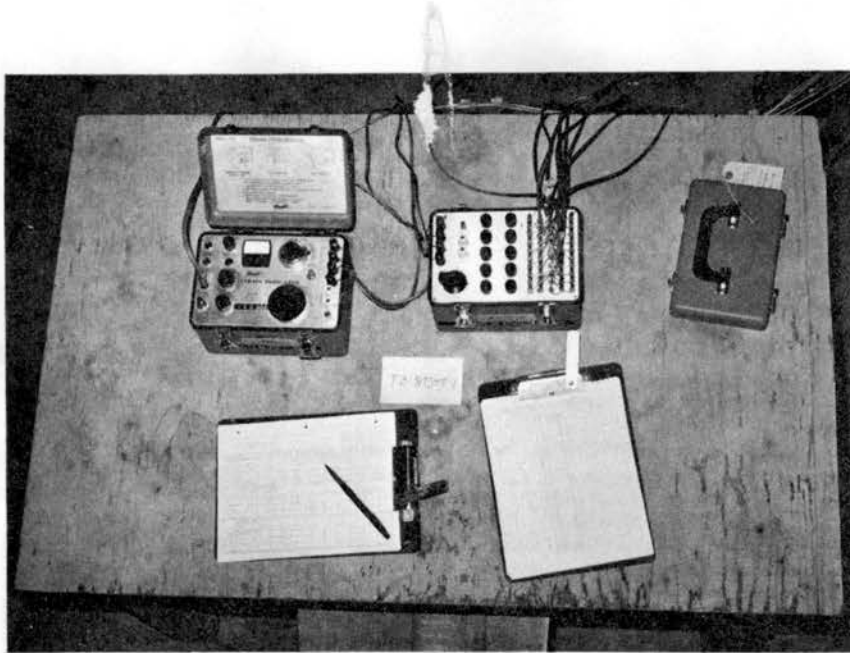
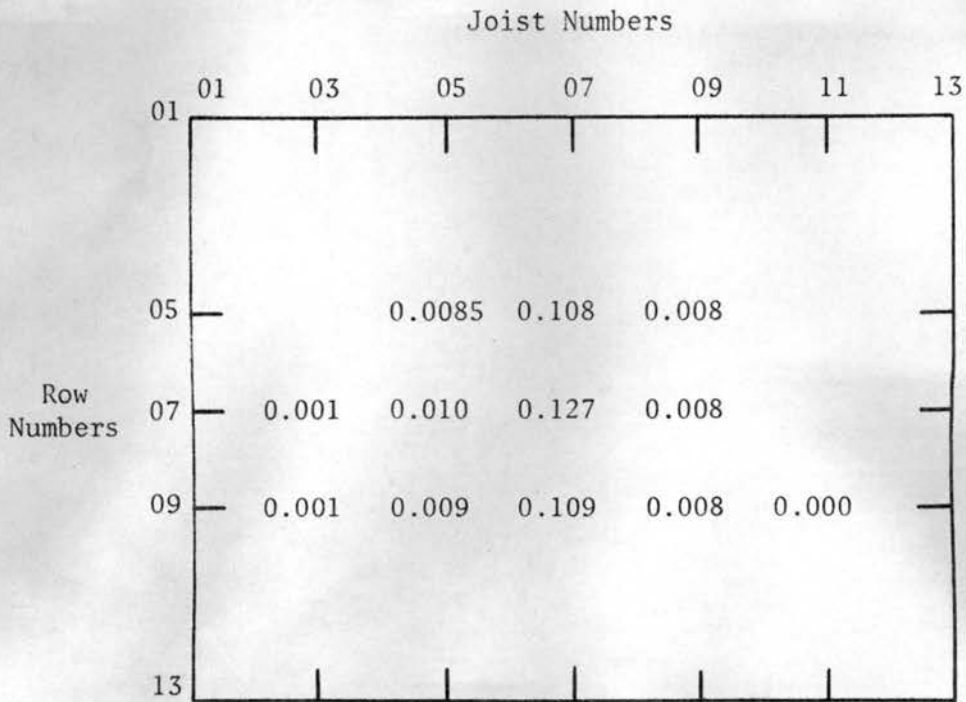
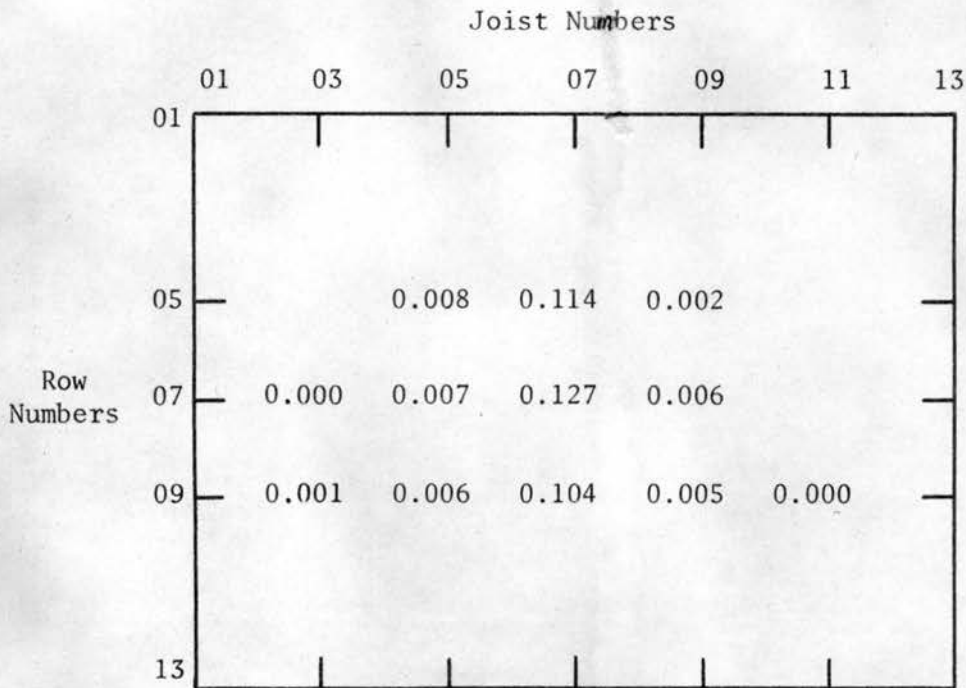


Fig. 3.9. Switch and balance unit along with a strain indicator used to measure strains.



a) Deflection at j (positions shown) due to a load applied at 0707.



b) Deflection at 0707 due to a load applied at j (positions shown).

Fig. 4.1. Illustration of Maxwell's Reciprocal Theorem on floor F4-12E16-1 with 1000 pounds applied.

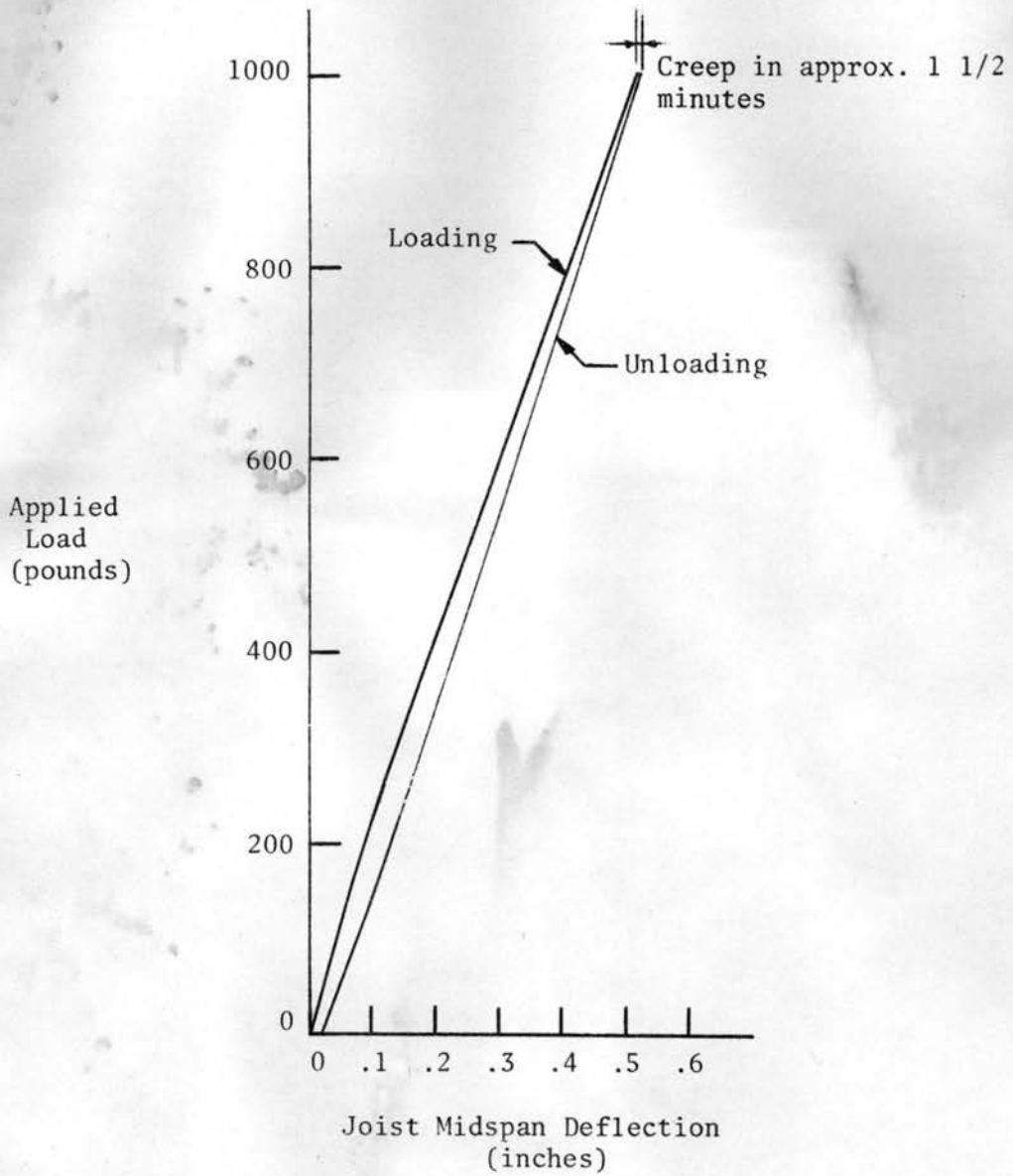


Fig. 4.2. Continuous load versus deflection curve for load applied at 0707 on floor F1-6E16-1.

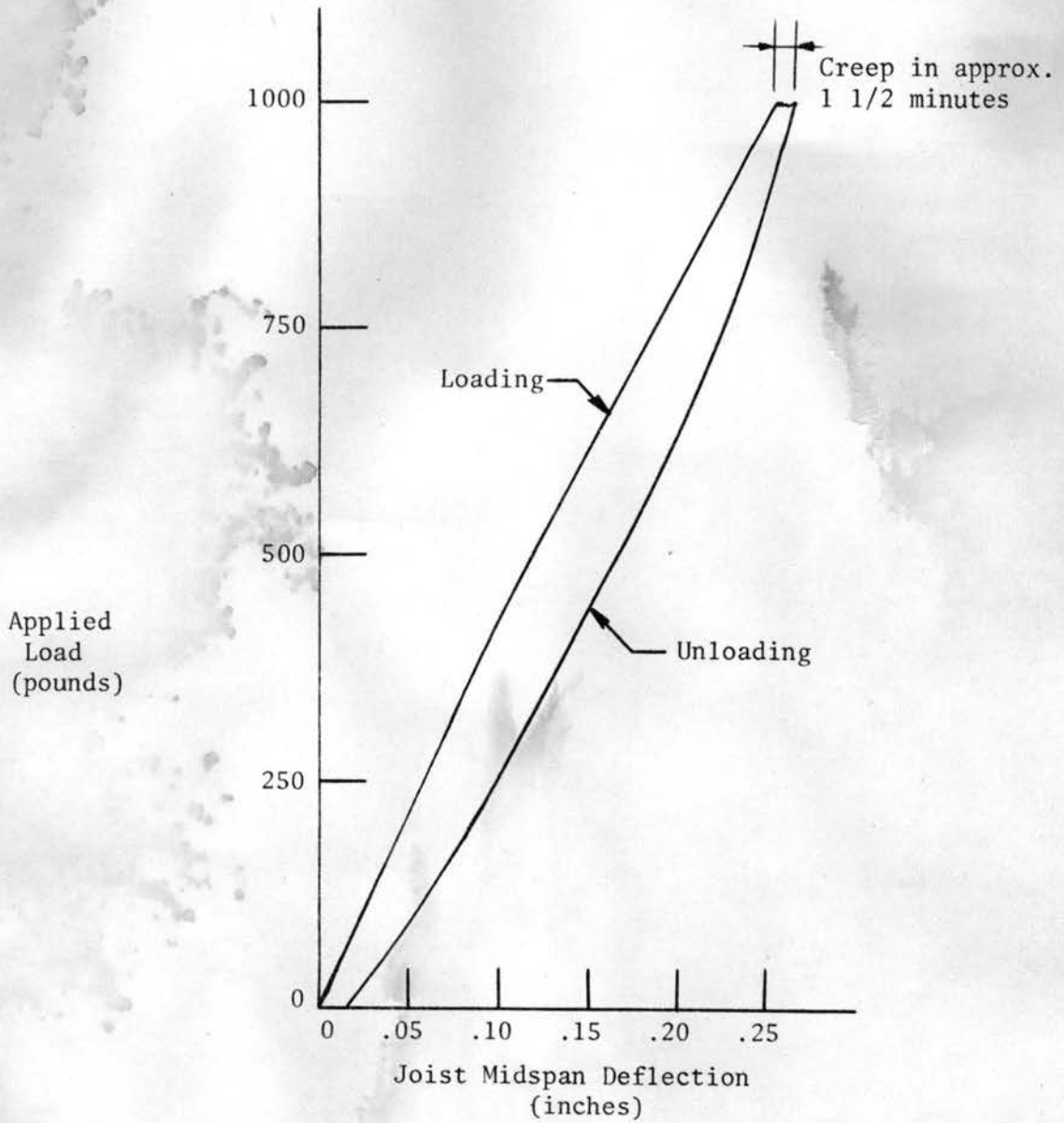


Fig. 4.3. Continuous load versus deflection curve for load applied at 0707 on floor F2-8D16-1.

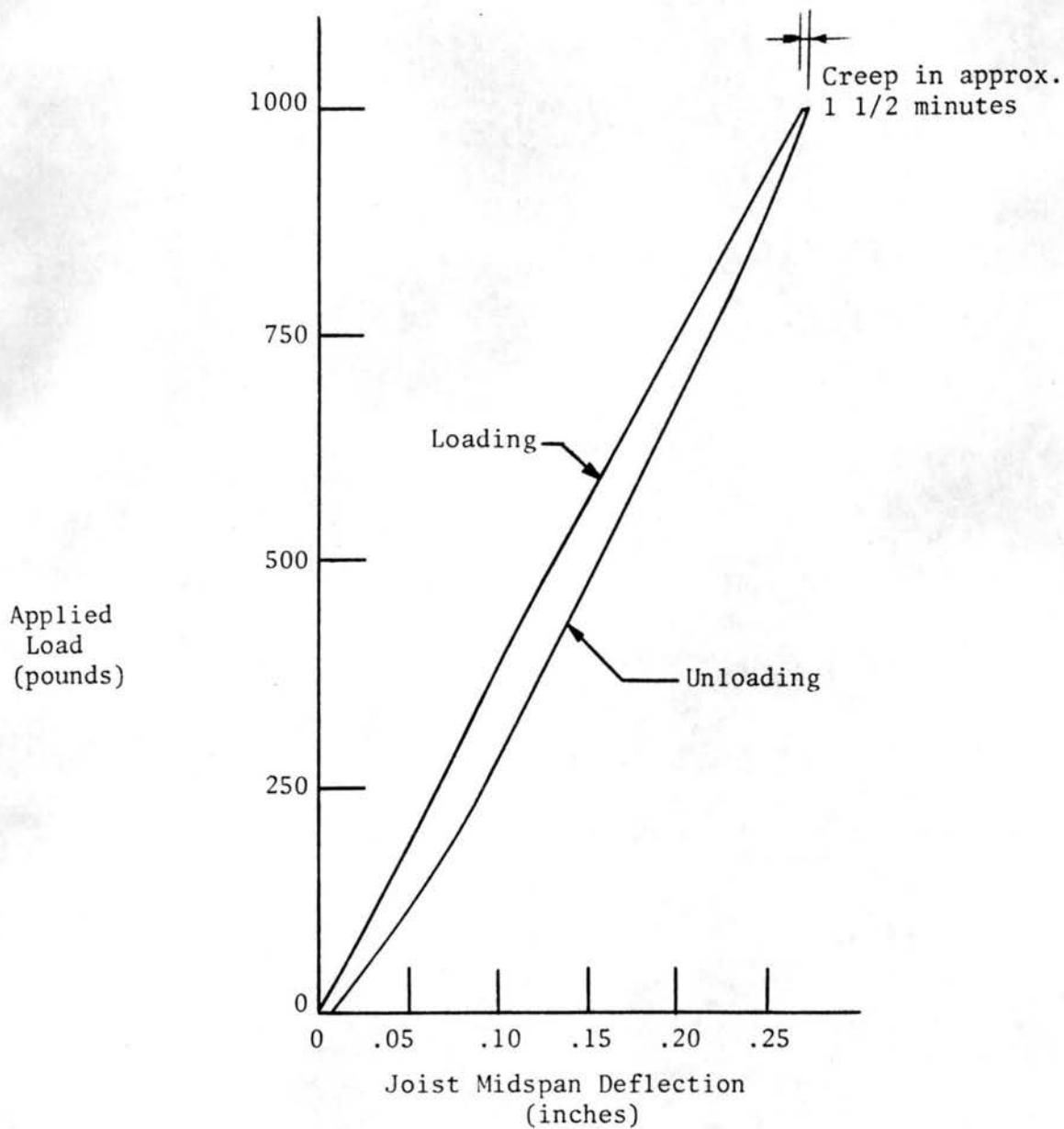


Fig. 4.4. Continuous load versus deflection curve for load applied at 0707 on floor F3-8D16-1.

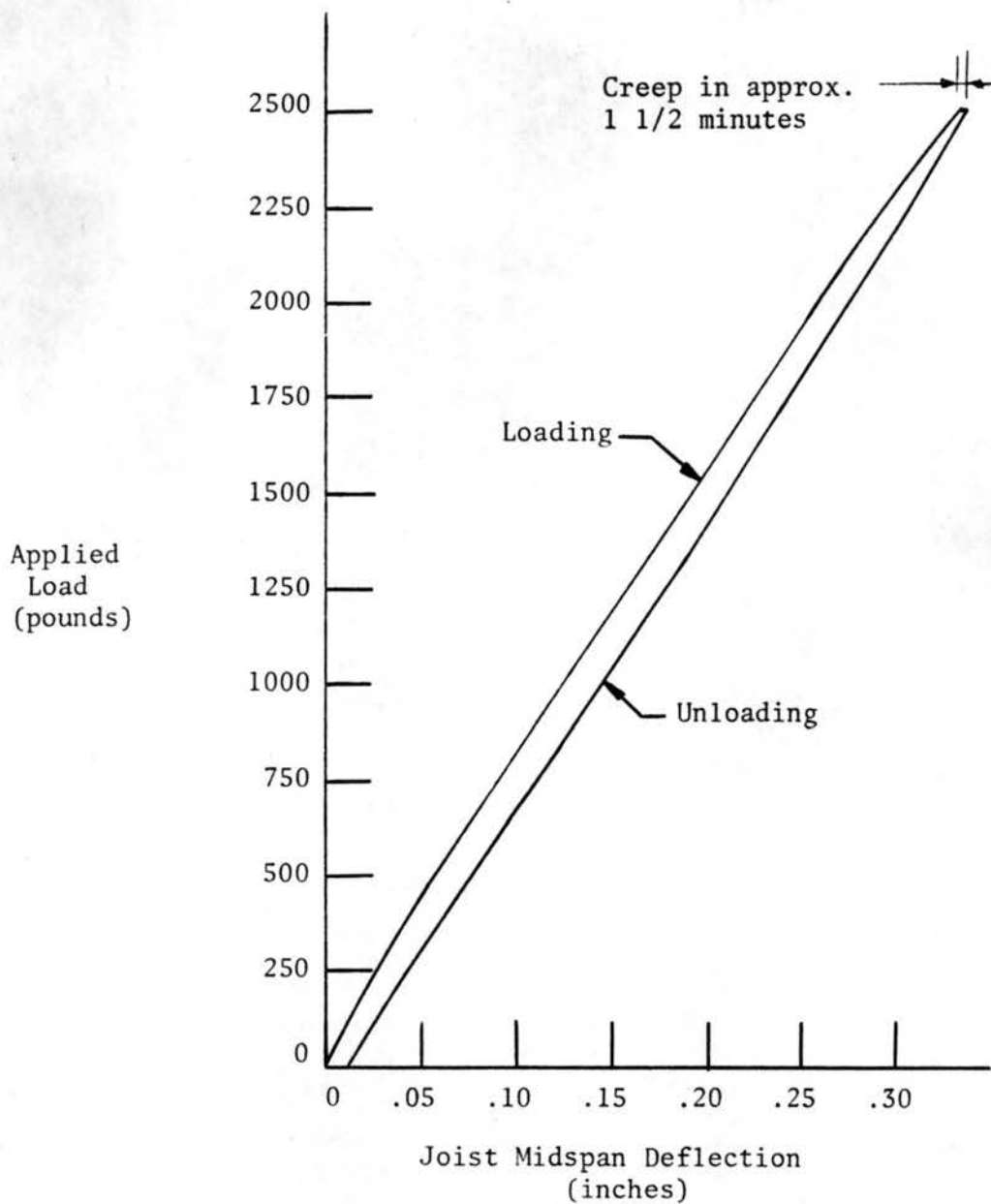


Fig. 4.5. Continuous load versus deflection curve for load applied at 0707 on floor F4-12E16-1.

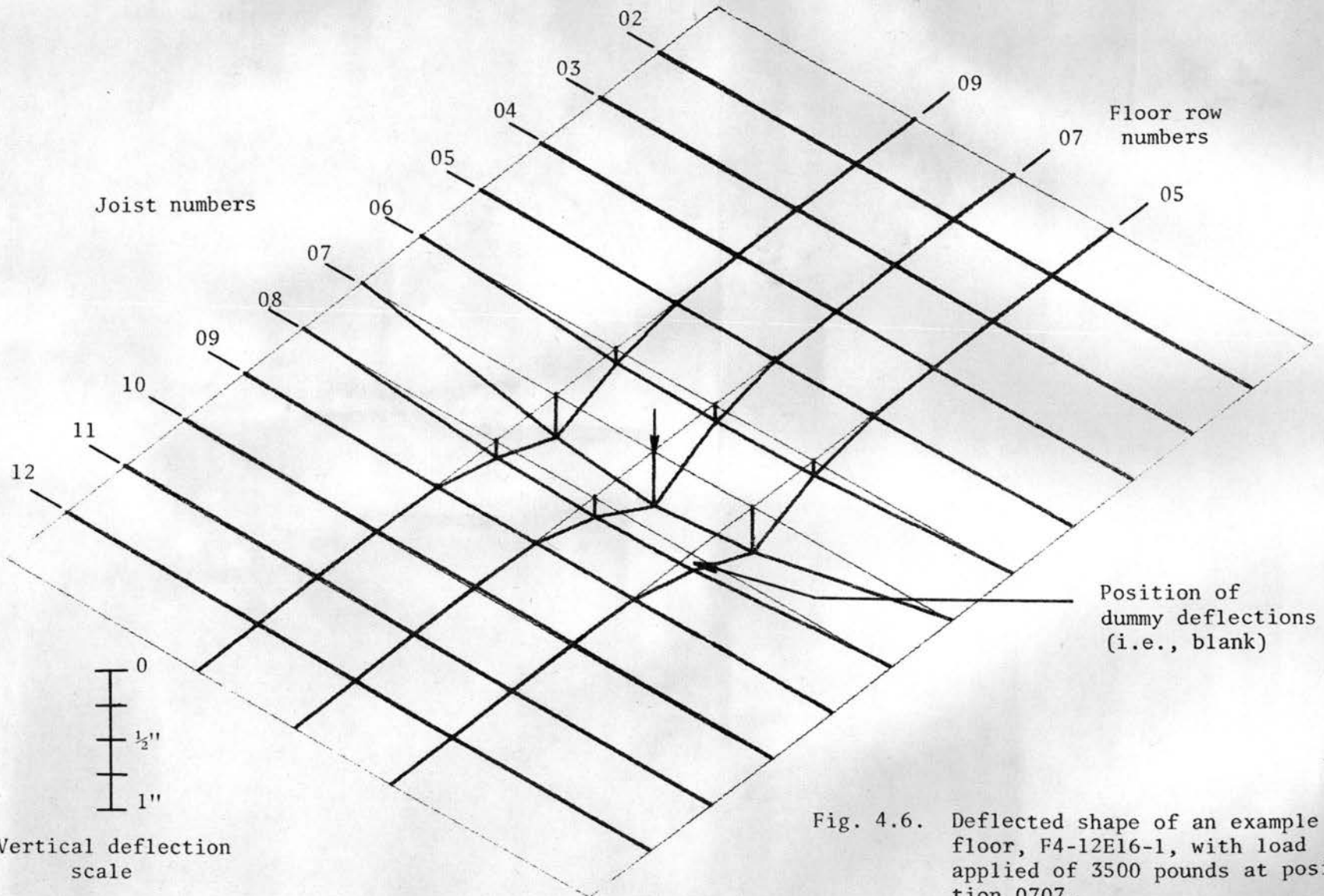


Fig. 4.6. Deflected shape of an example floor, F4-12E16-1, with load applied of 3500 pounds at position 0707.

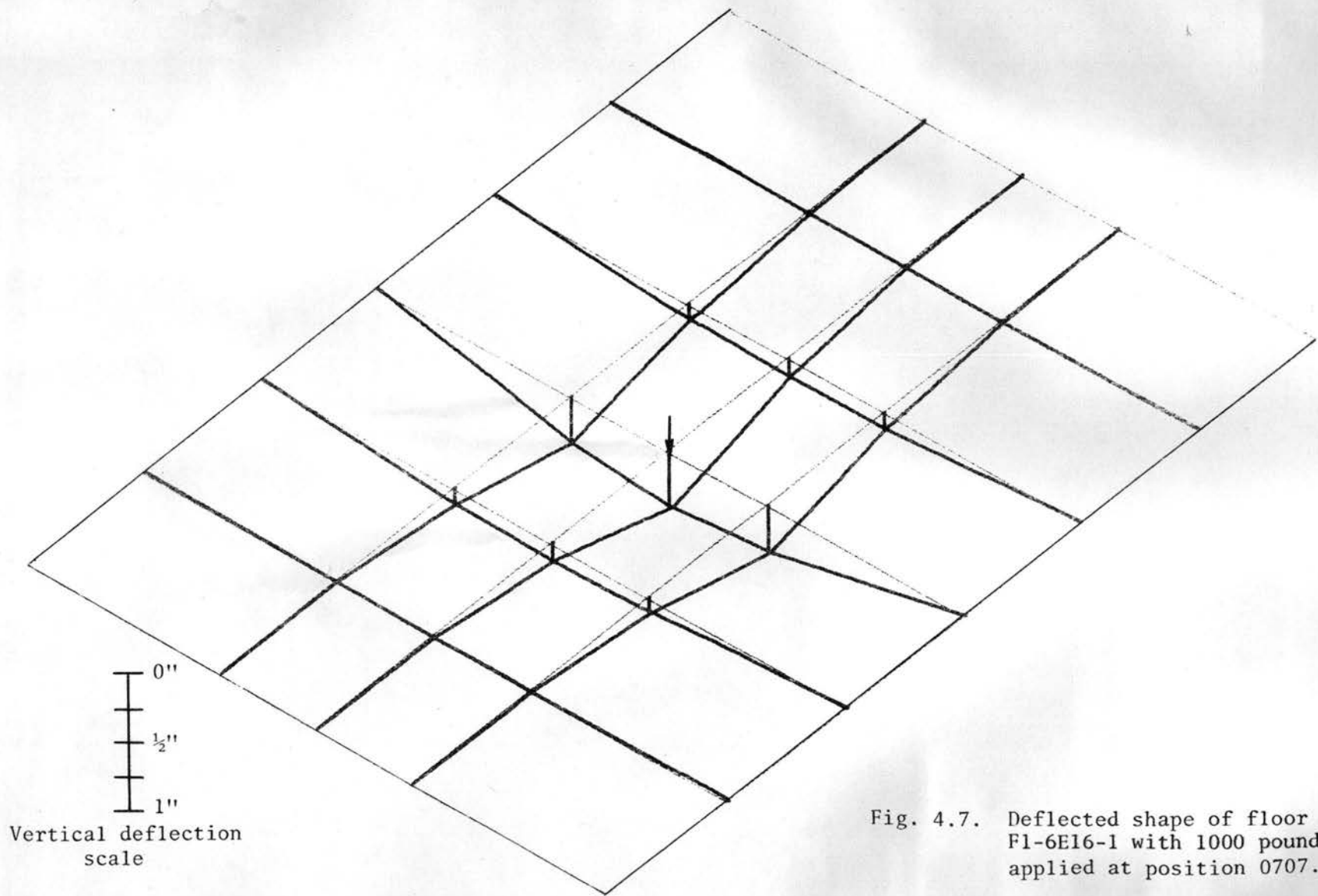
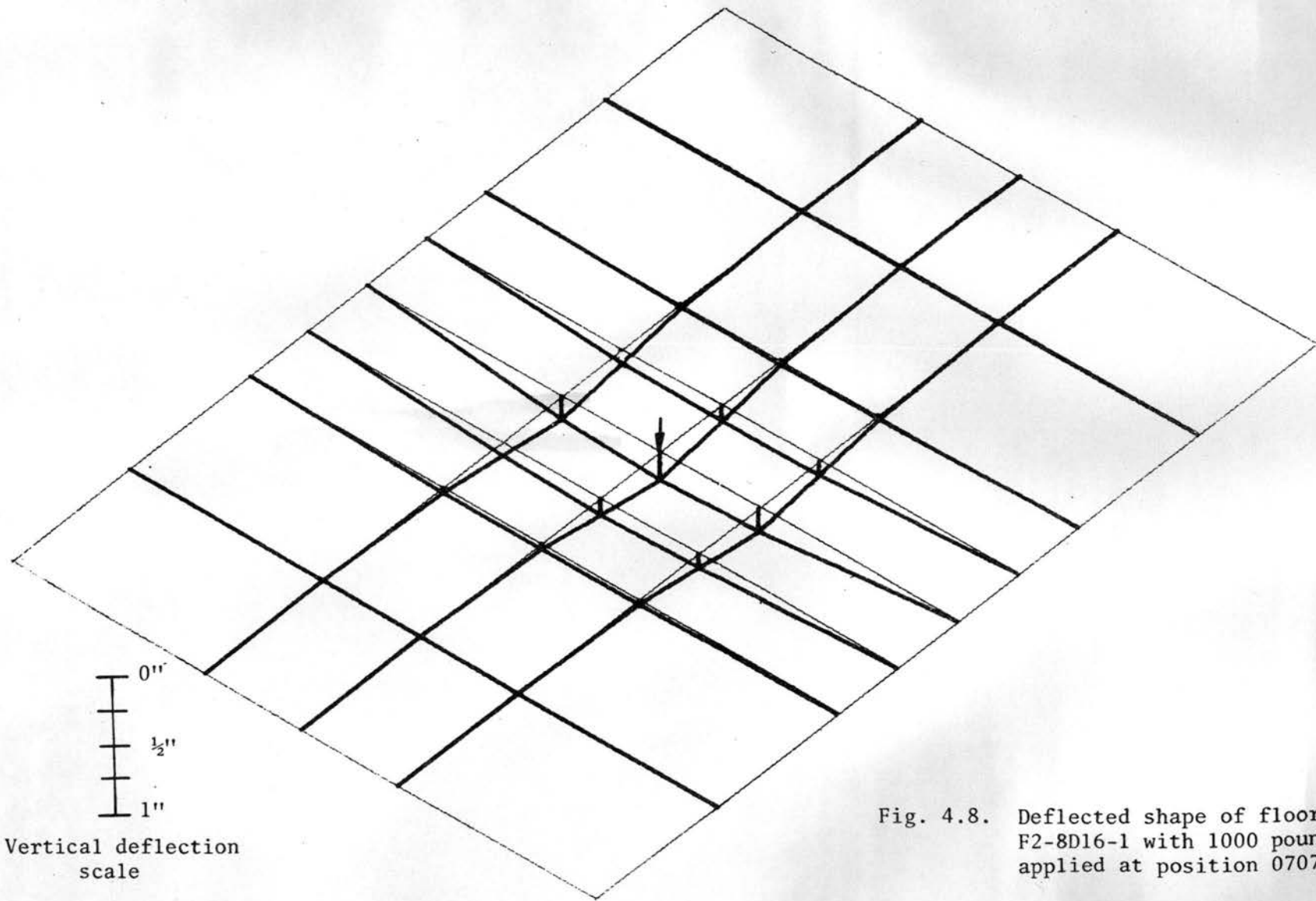


Fig. 4.7. Deflected shape of floor
F1-6E16-1 with 1000 pounds
applied at position 0707.



Vertical deflection
scale

Fig. 4.8. Deflected shape of floor
F2-8D16-1 with 1000 pounds
applied at position 0707.

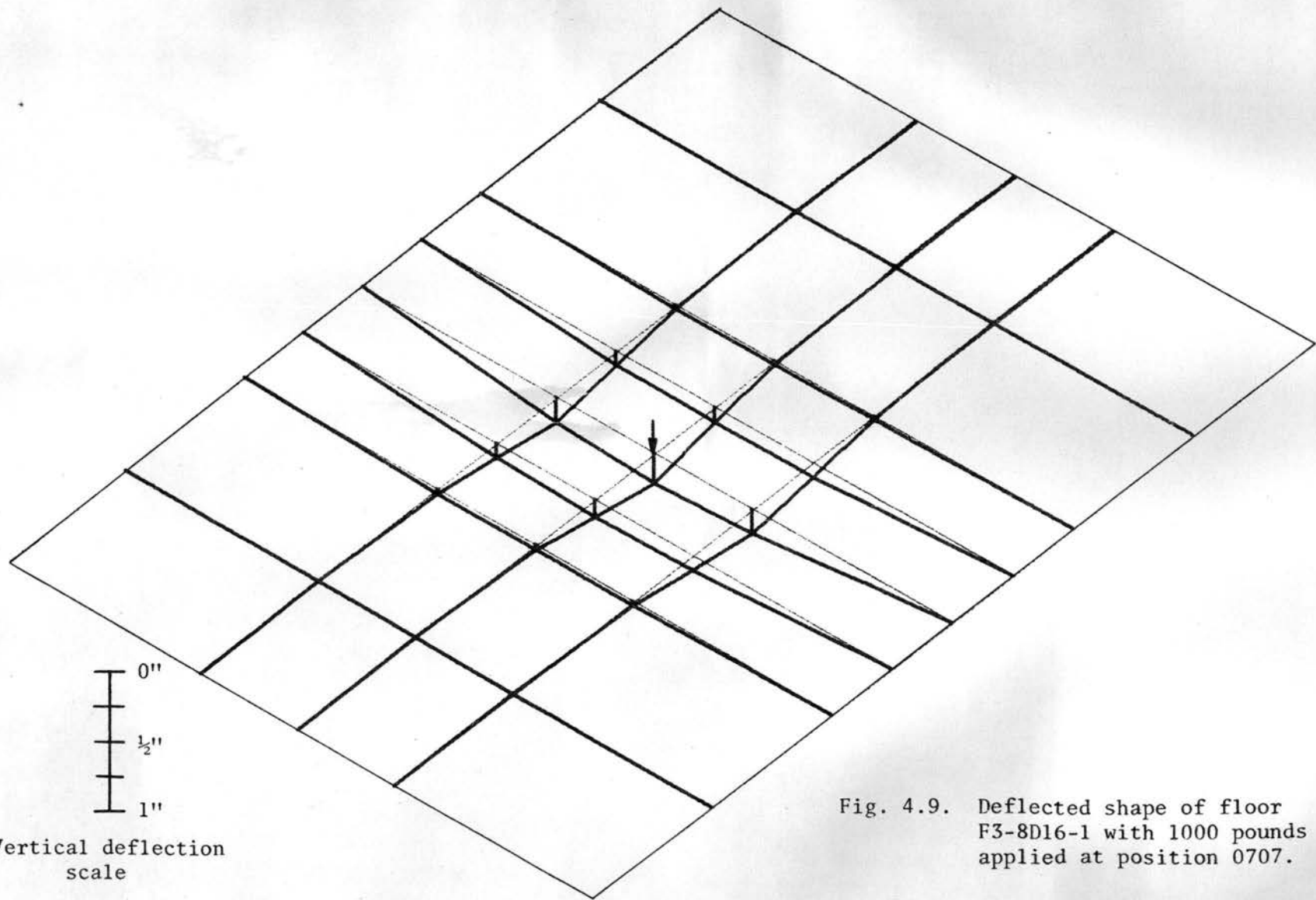
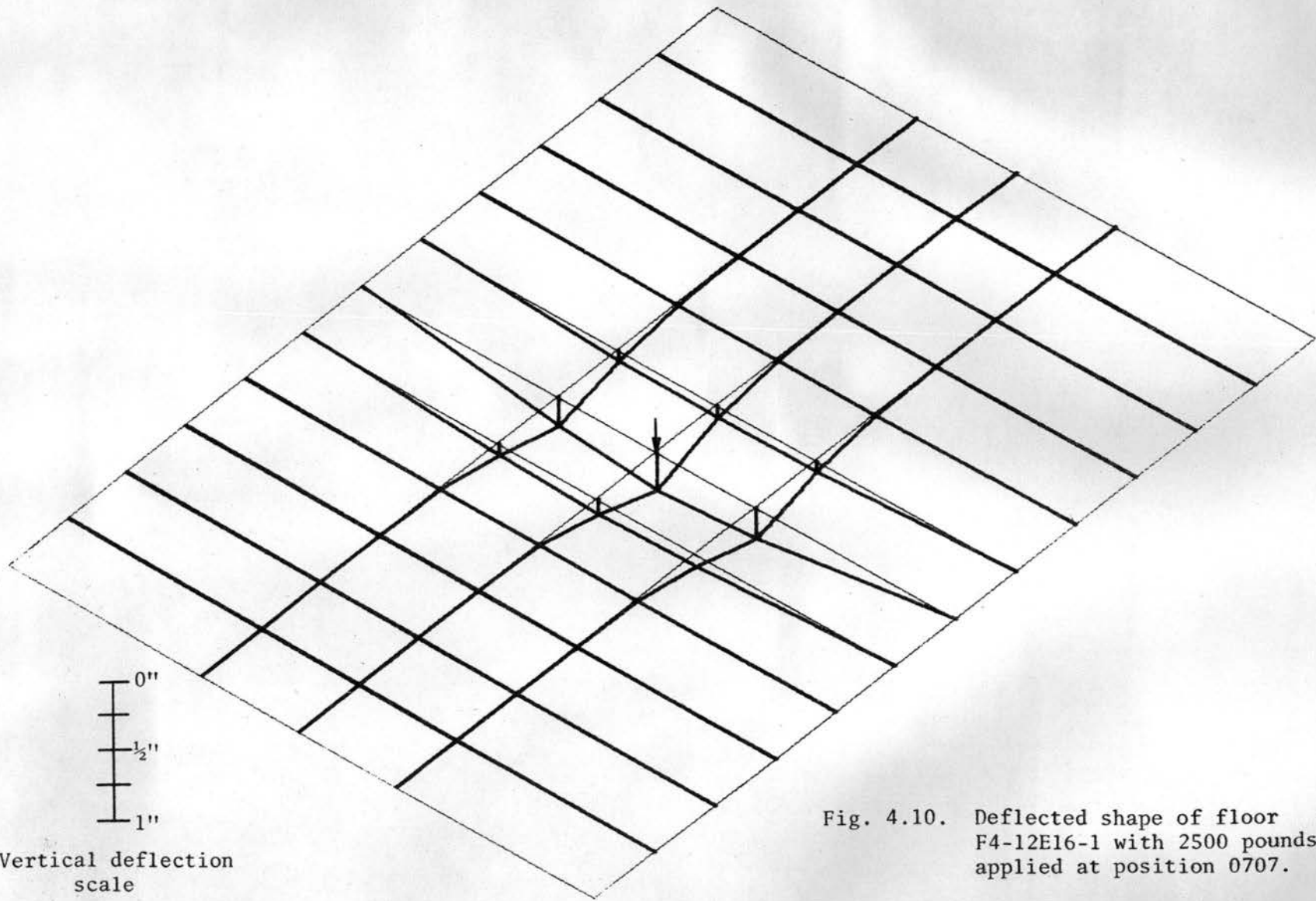


Fig. 4.9. Deflected shape of floor F3-8D16-1 with 1000 pounds applied at position 0707.



Vertical deflection
scale

Fig. 4.10. Deflected shape of floor
F4-12E16-1 with 2500 pounds
applied at position 0707.

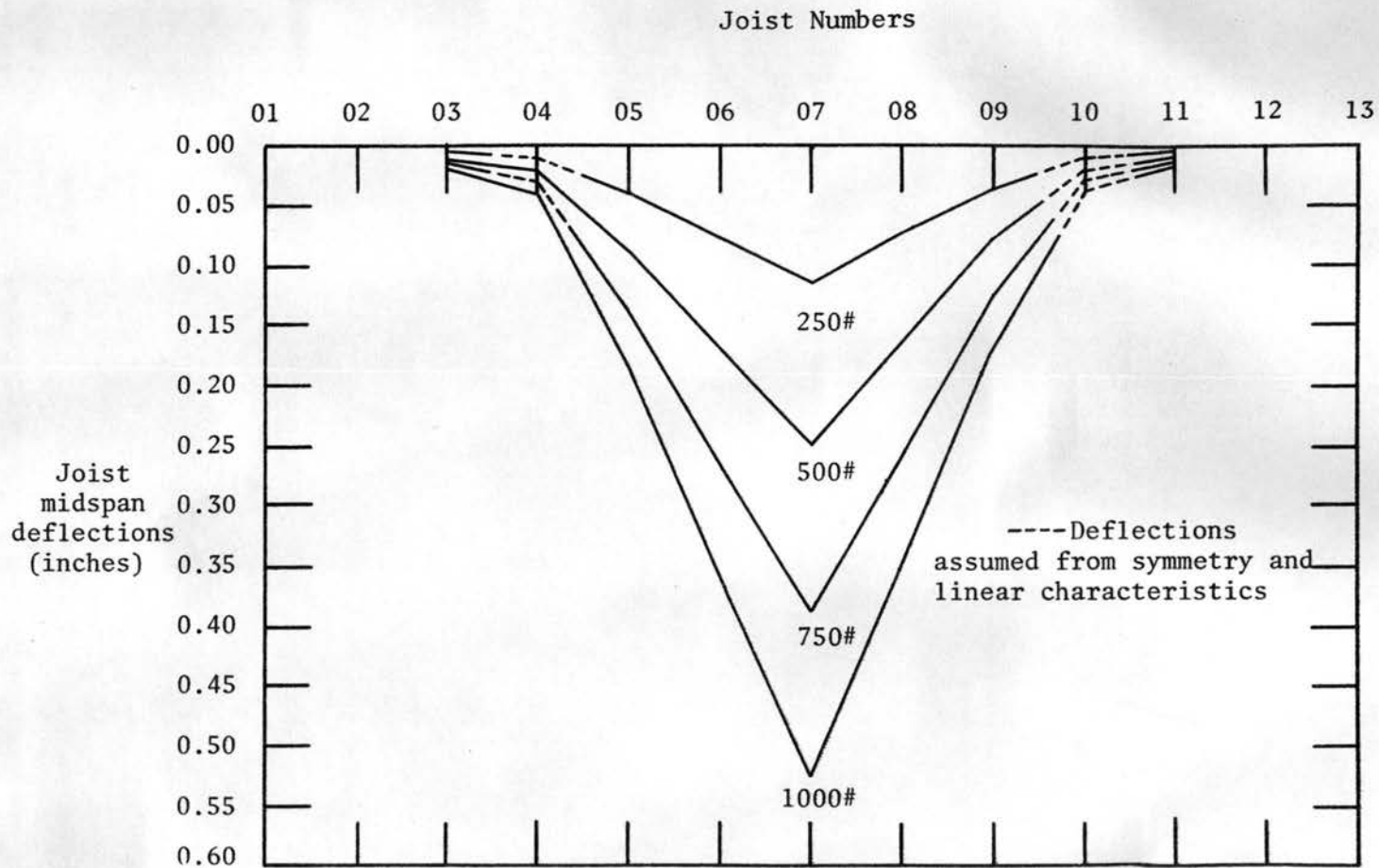


Fig. 4.11. Joist midspan deflections of floor F1-6E16-1 with load applied at 0707.

Joist Numbers

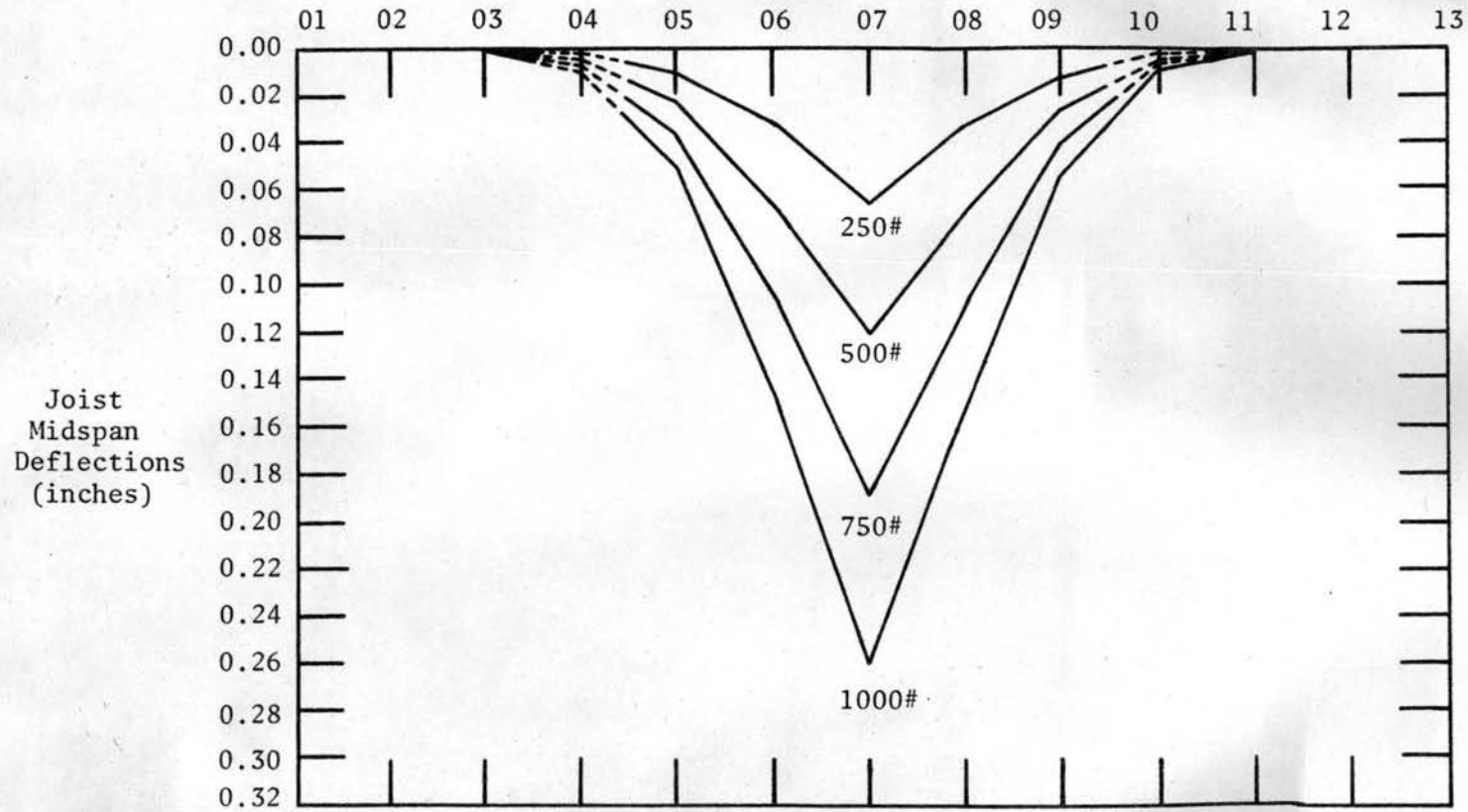


Fig. 4.12. Joist midspan deflections of floor F2-8D16-1 with load applied at 0707.

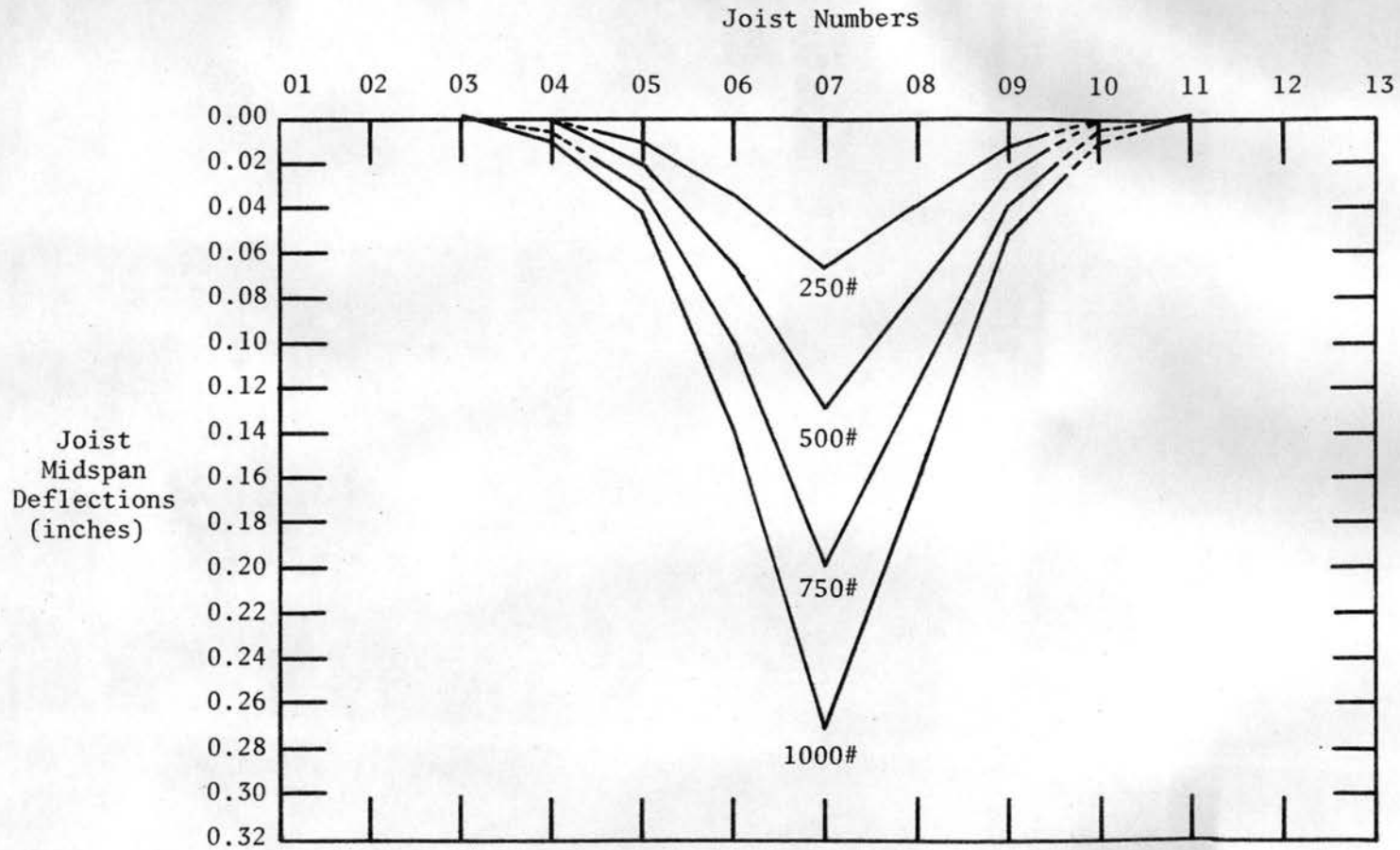


Fig. 4.13. Joist midspan deflections of floor F3-8D16-1 with load applied at 0707.

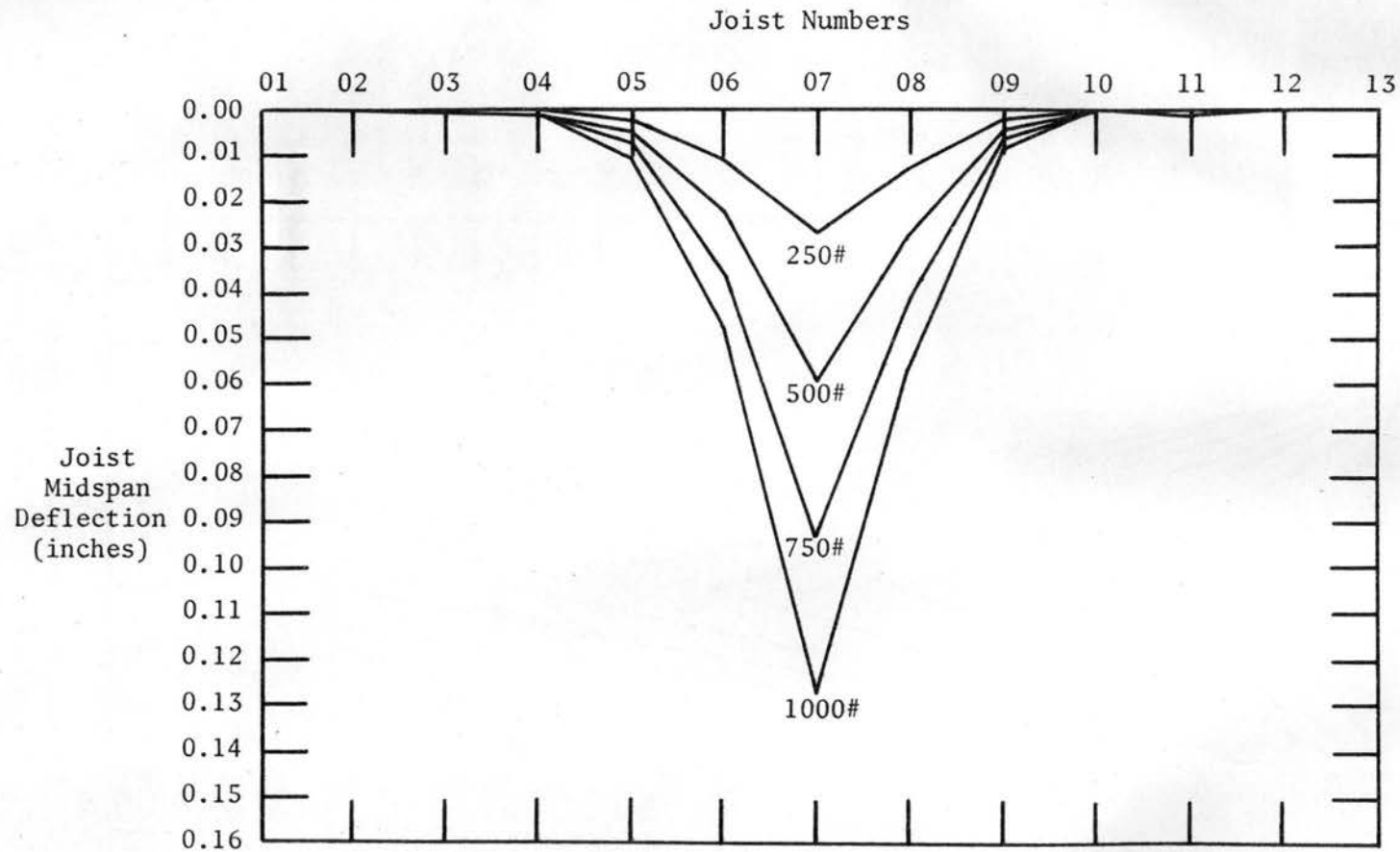


Fig. 4.14 Joist midspan deflections of floor F4-12E16-1 with load applied at 0707.

Vert

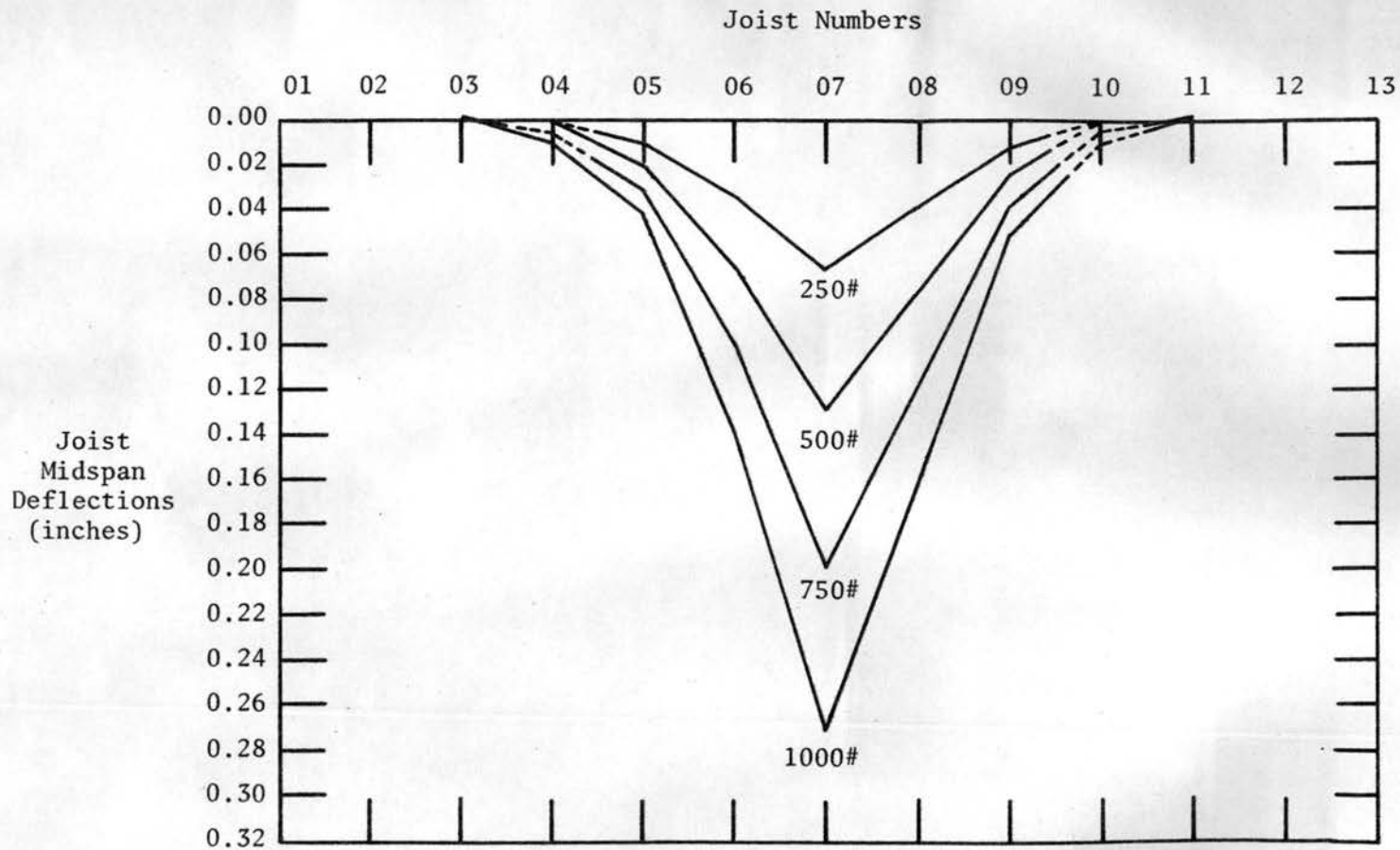


Fig. 4.13. Joist midspan deflections of floor F3-8D16-1 with load applied at 0707.

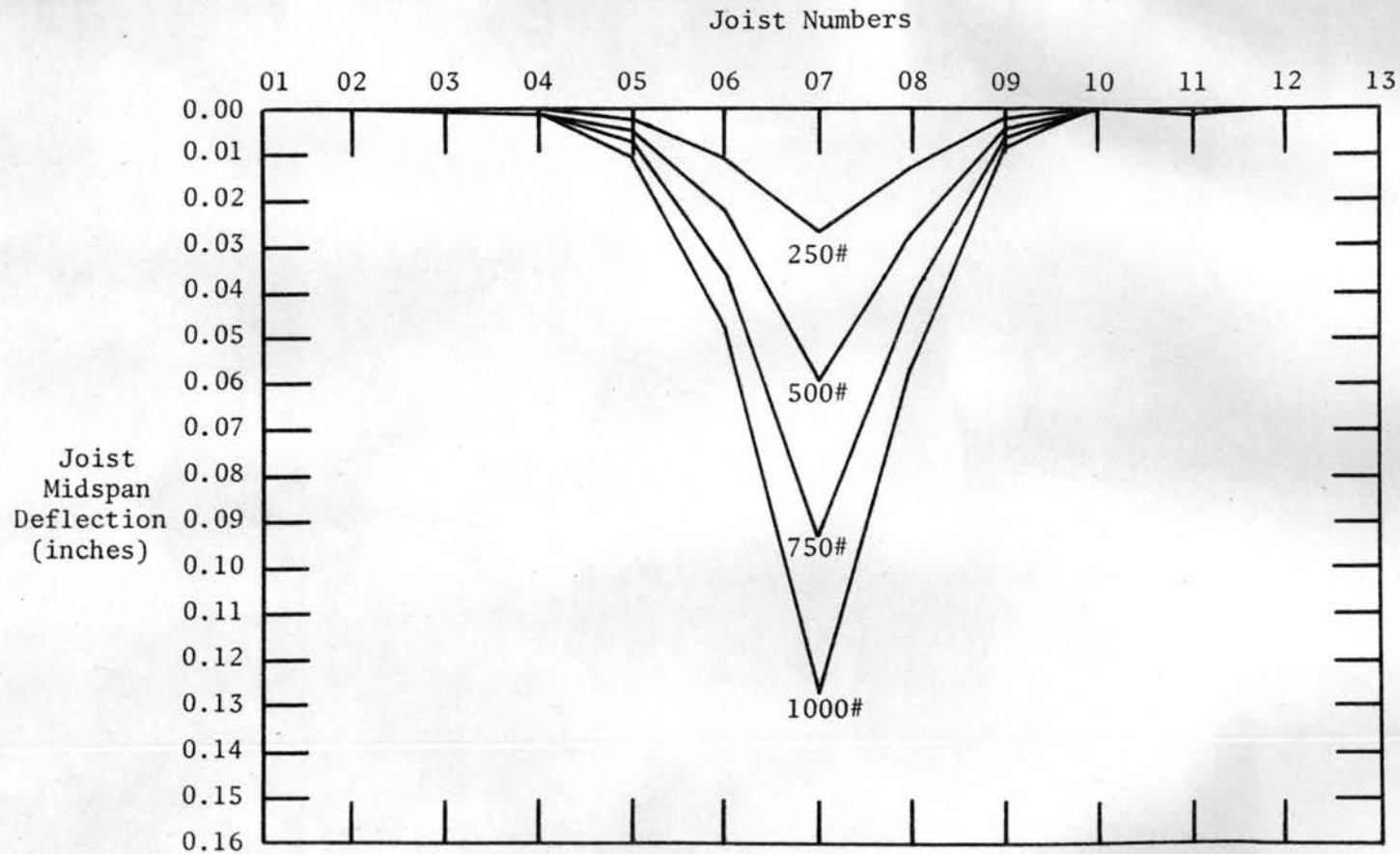


Fig. 4.14 Joist midspan deflections of floor F4-12E16-1 with load applied at 0707.

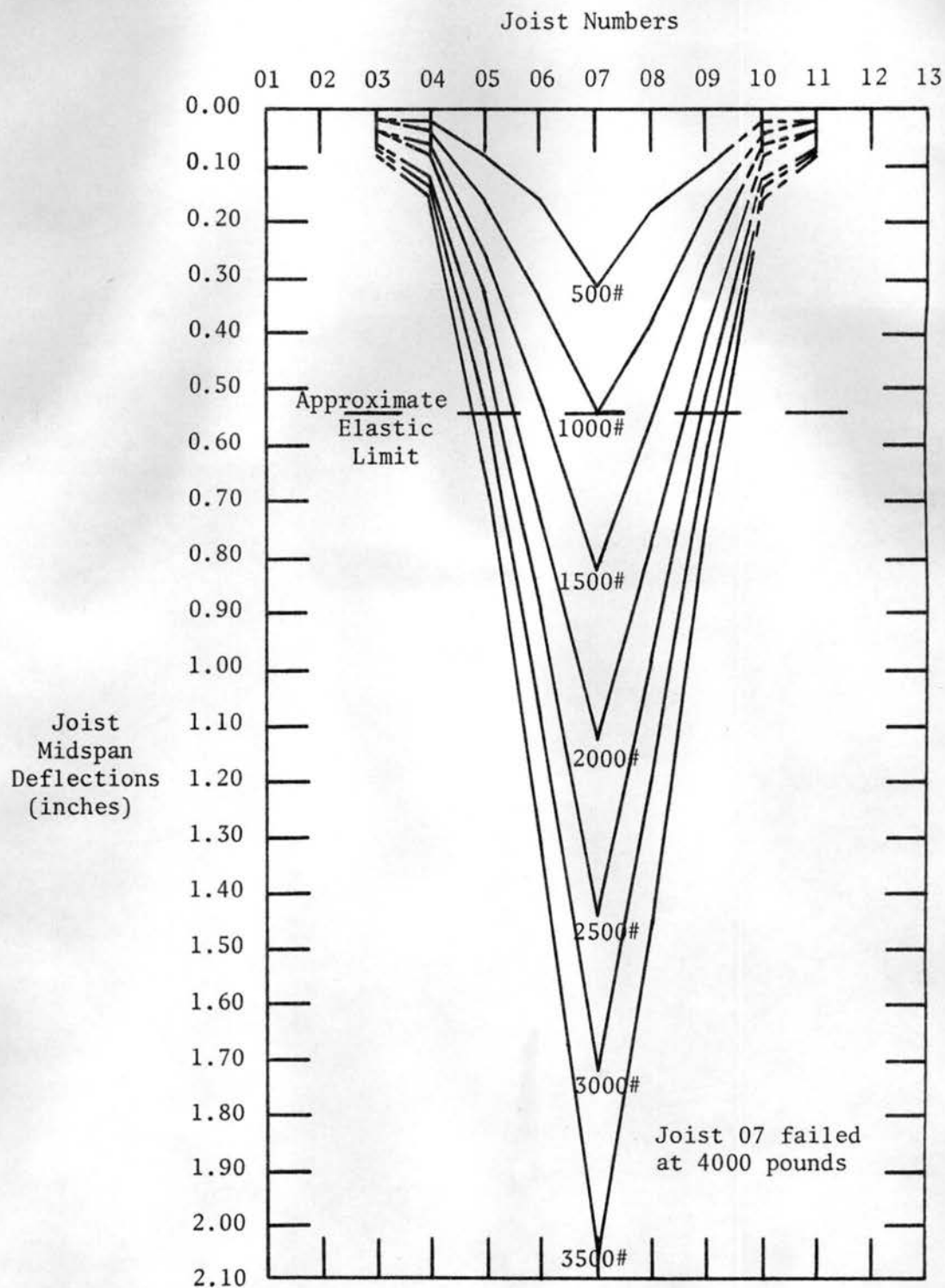


Fig. 4.15. Joist midspan deflections of floor F1-6E16-1 with load applied until joist failure.

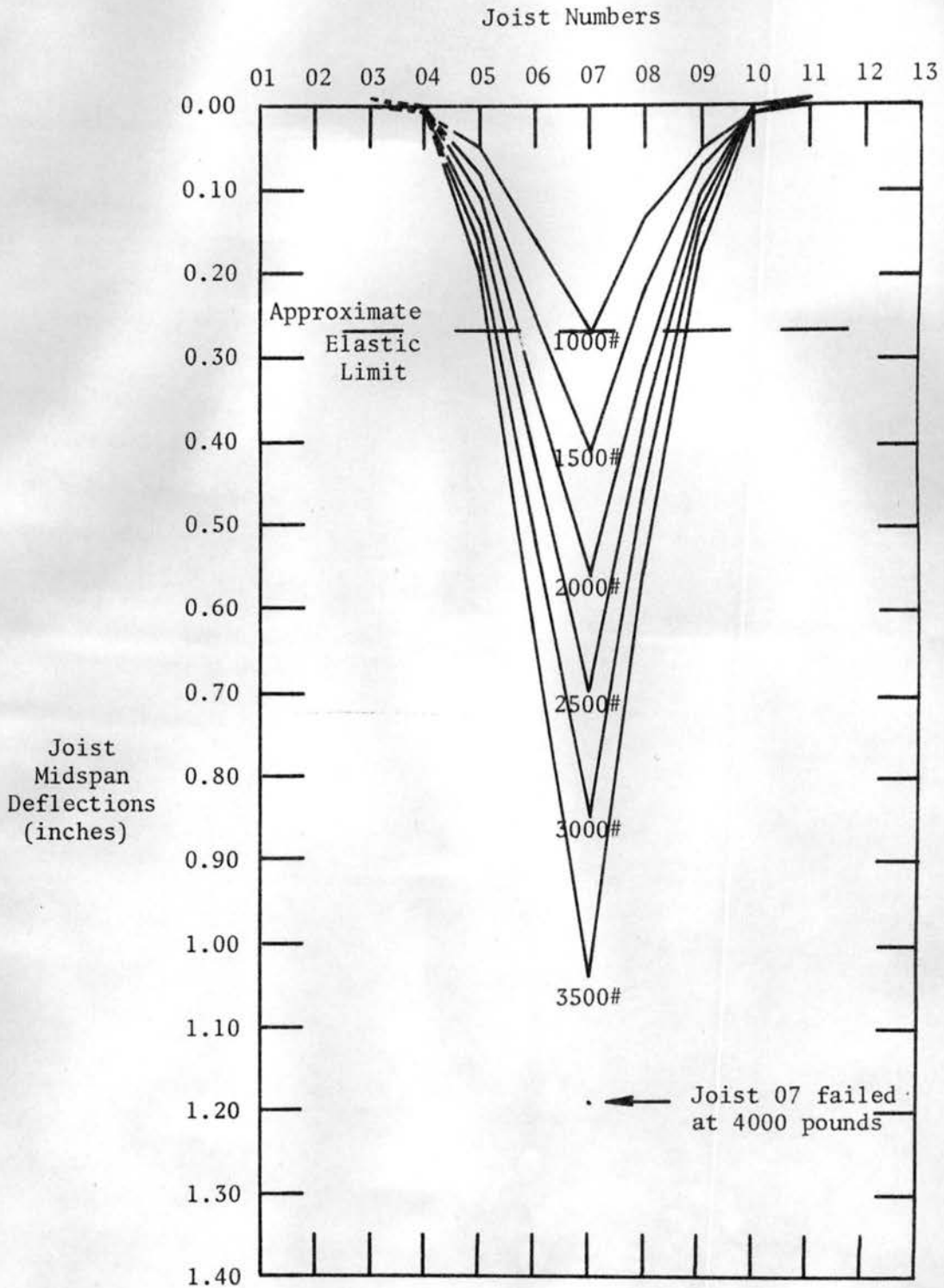


Fig. 4.16. Joist midspan deflection of floor F2-8D16-1 with load applied until joist failure.

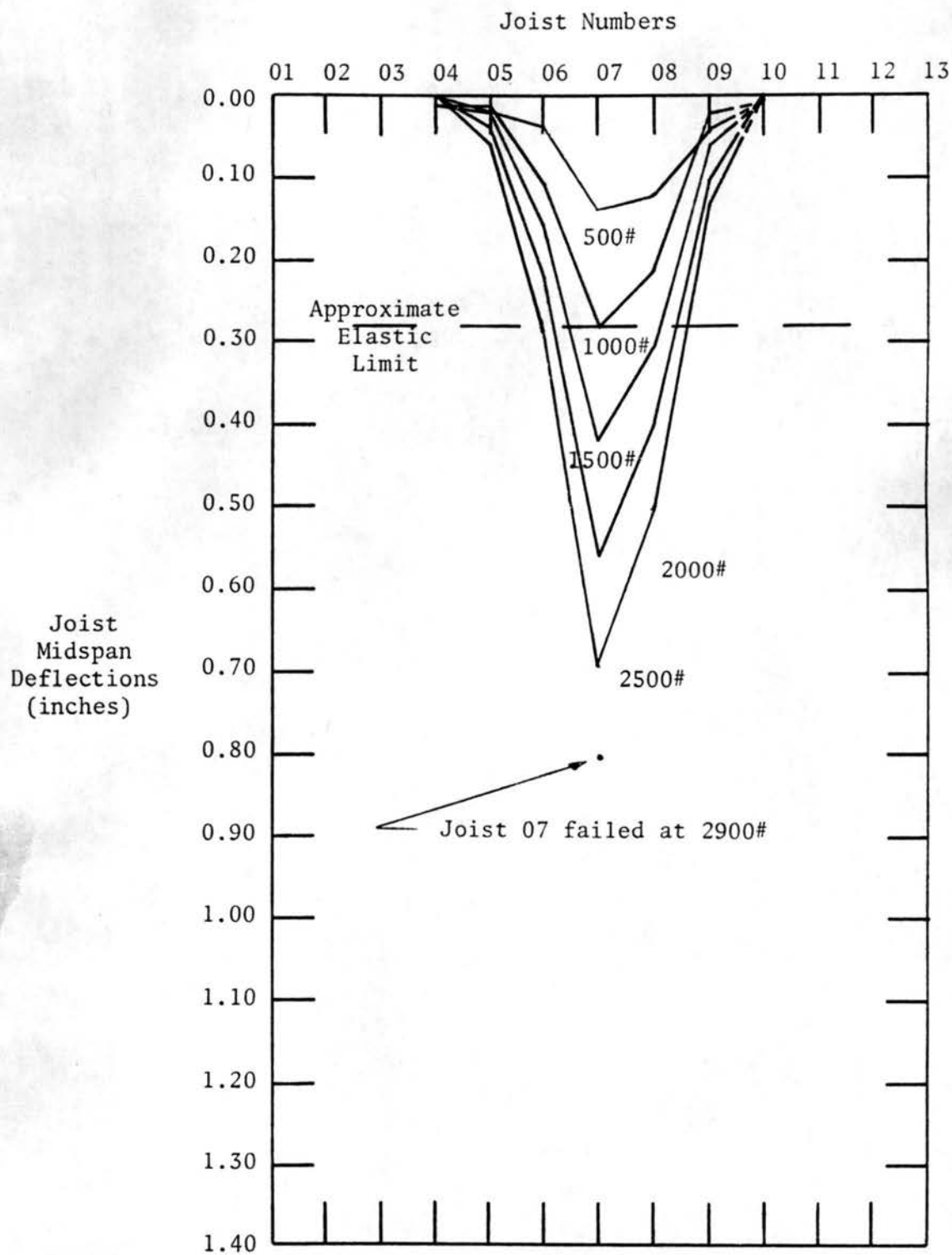


Fig. 4.17. Joist midspan deflections of floor F3-8D16-1 with load applied until joist failure.

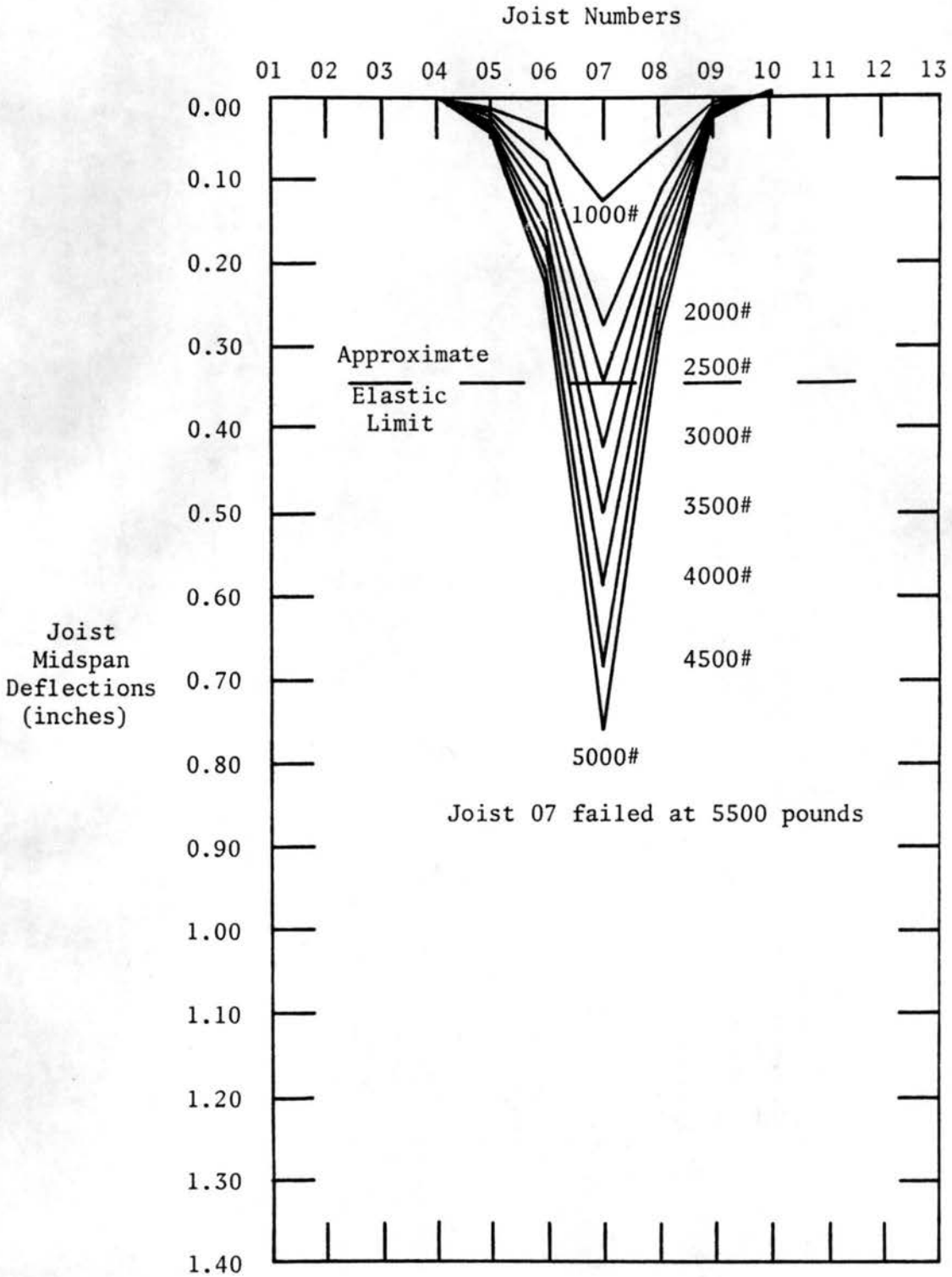
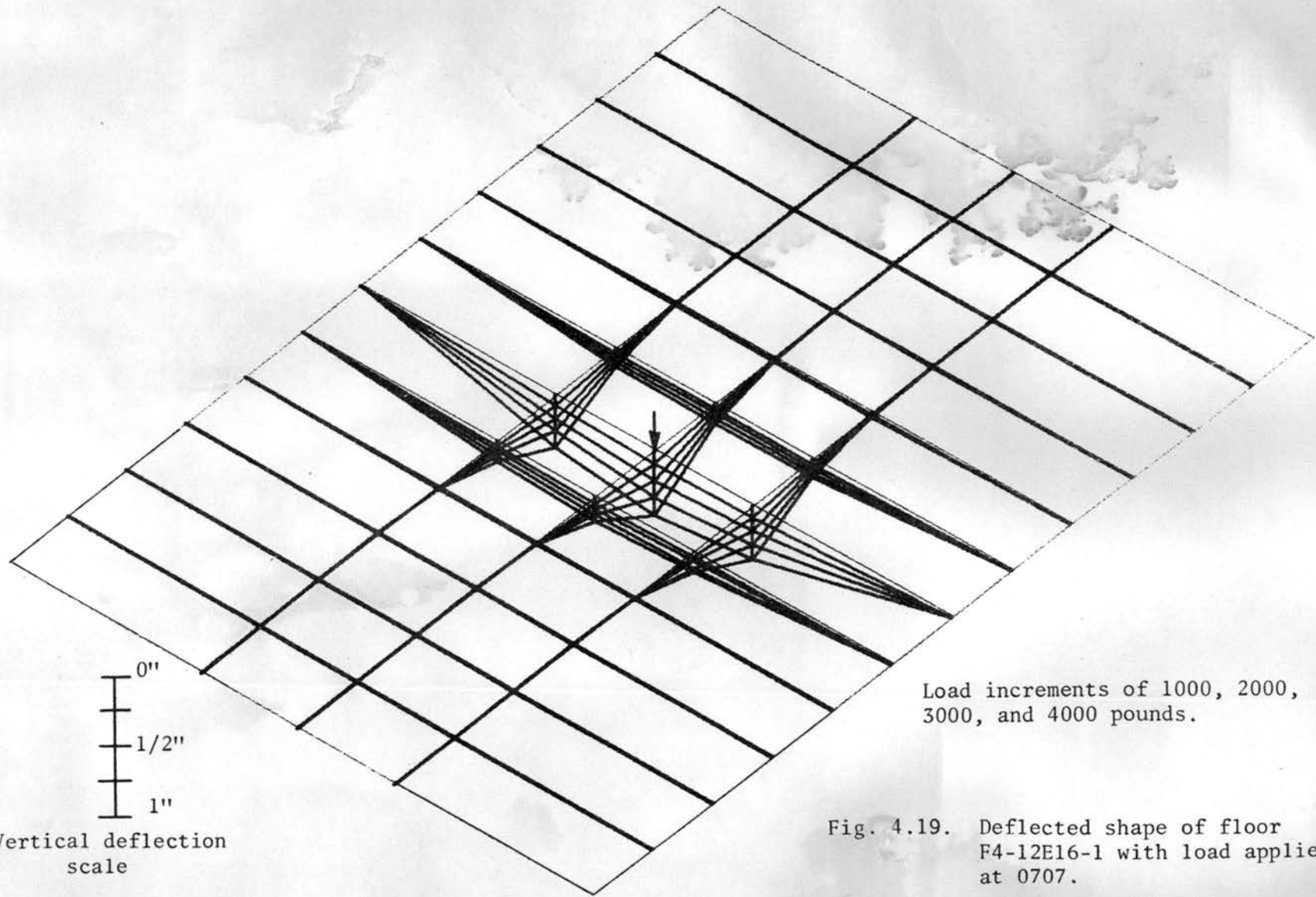


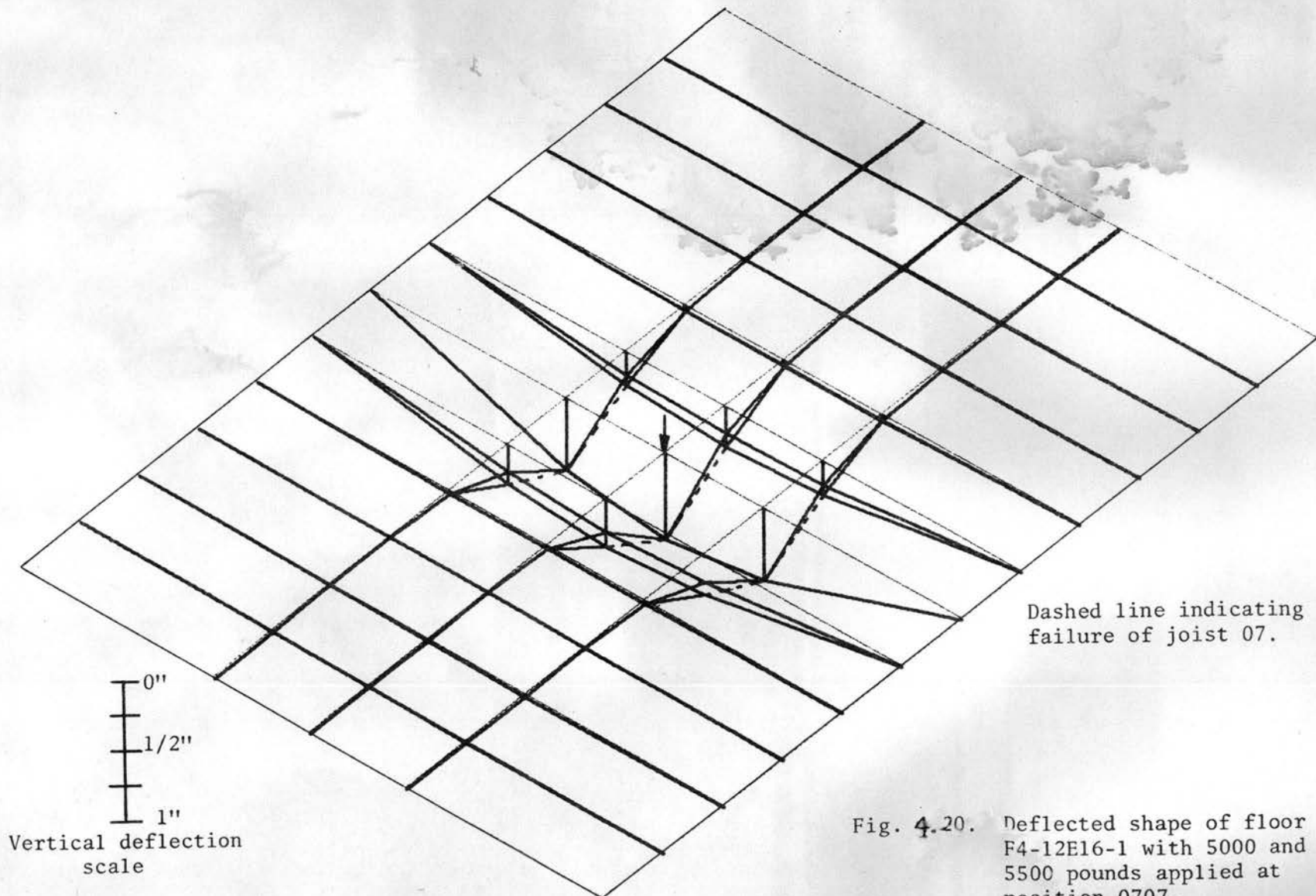
Fig. 4.18. Joist midspan deflections of floor F4-12E16-1 with load applied until joist failure.



0"
1/2"
1"
Vertical deflection
scale

Load increments of 1000, 2000,
3000, and 4000 pounds.

Fig. 4.19. Deflected shape of floor
F4-12E16-1 with load applied
at 0707.



0"
1/2"
1"
Vertical deflection
scale

Dashed line indicating
failure of joist 07.

Fig. 4.20. Deflected shape of floor
F4-12E16-1 with 5000 and
5500 pounds applied at
position 0707.

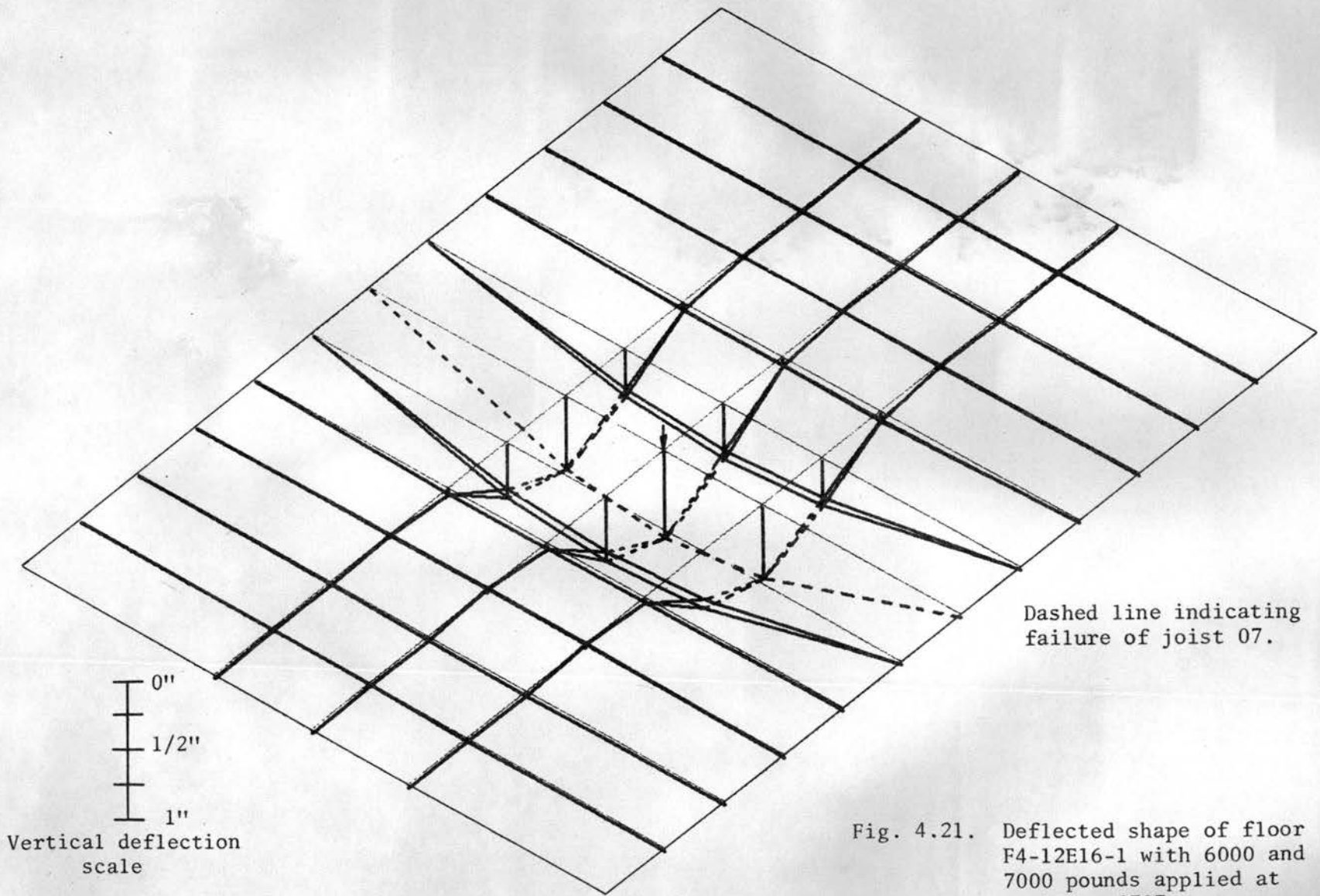


Fig. 4.21. Deflected shape of floor F4-12E16-1 with 6000 and 7000 pounds applied at position 0707.

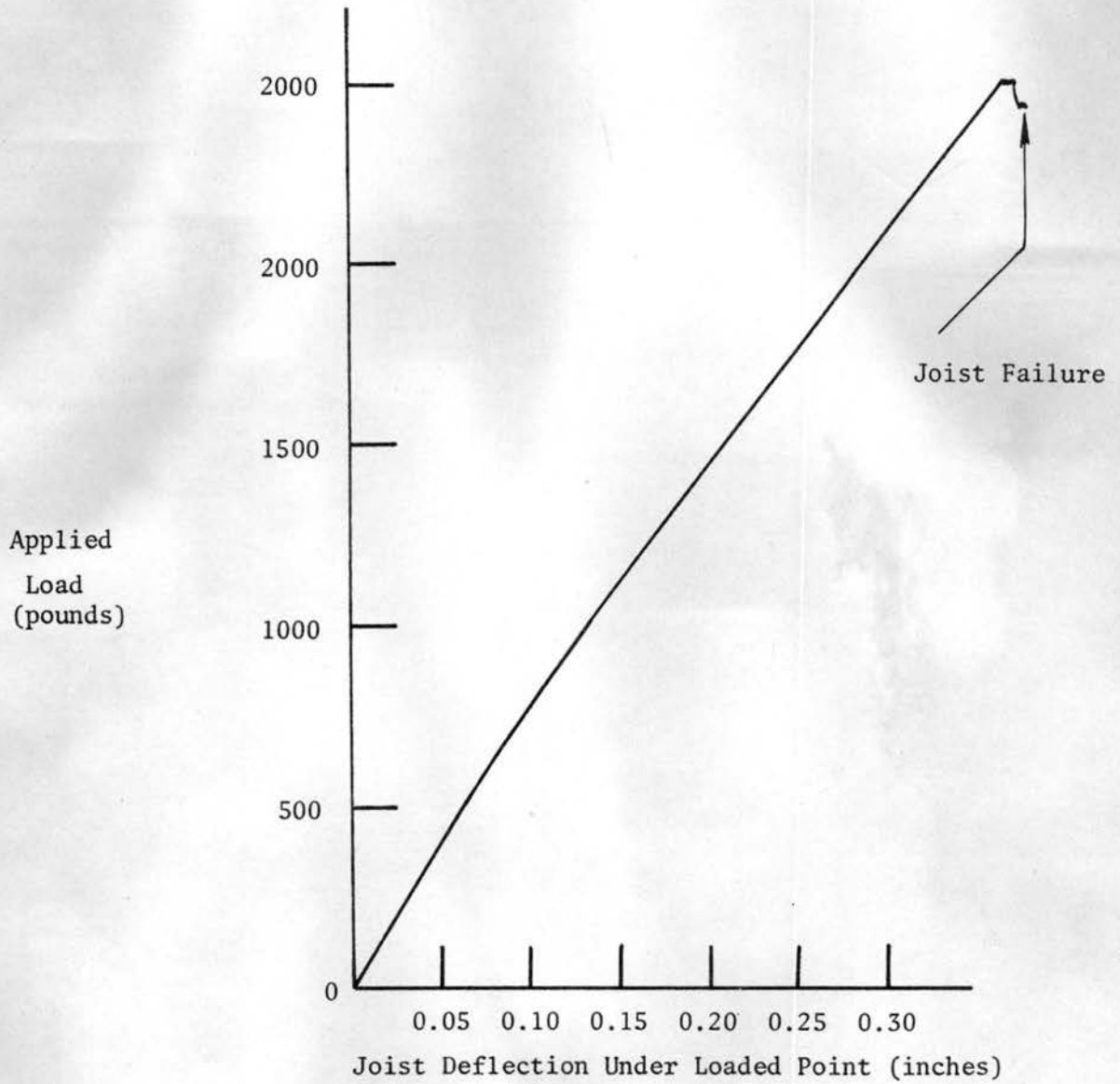


Fig. 4.22. Typical load-deflection curve plotted until joist failure, F4-12E16-1 loaded at position 0911.

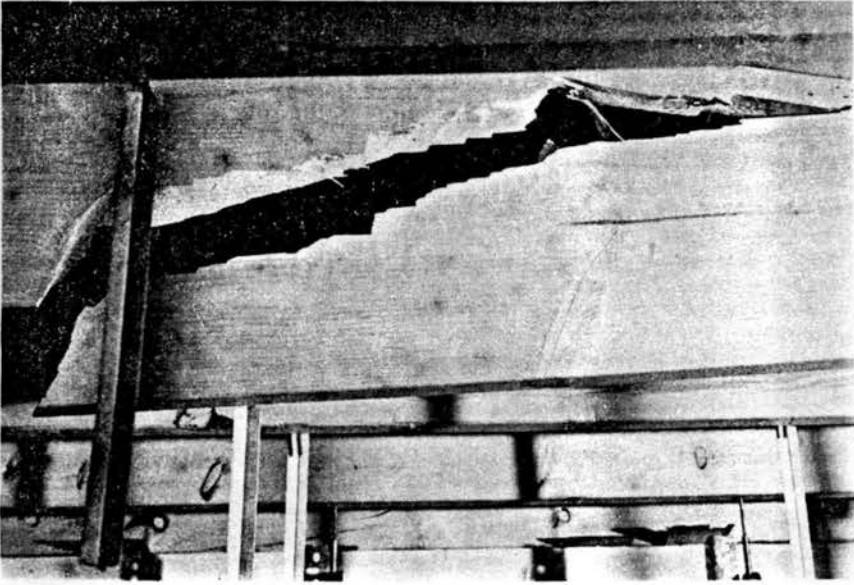


Fig. 4.23. Typical joist failure including cracking around knots and along the grain angle, and cross grain tension cracking.

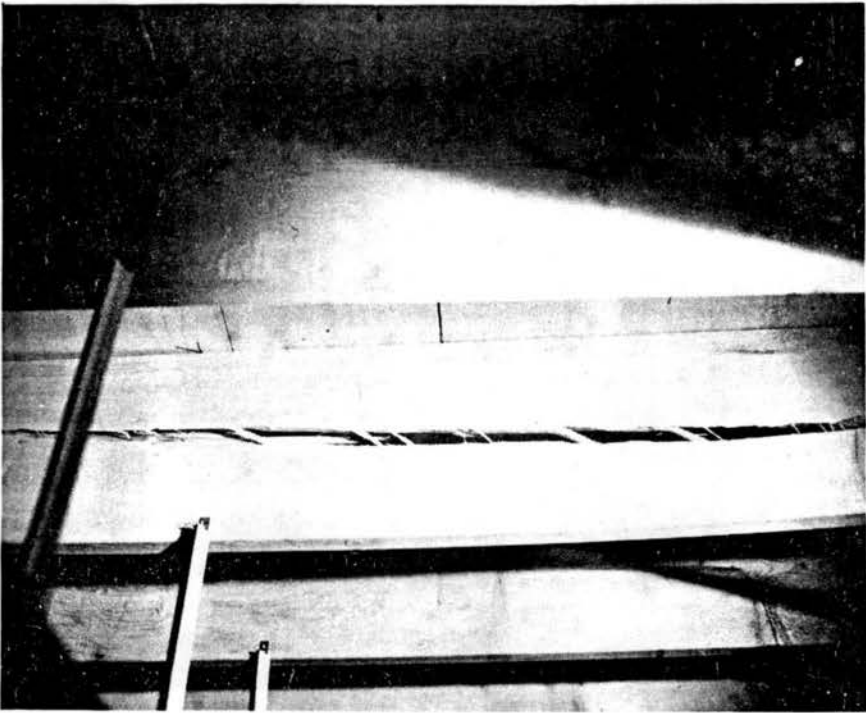


Fig. 4.24. Joist failure due to a horizontal shear crack at joist mid-depth.

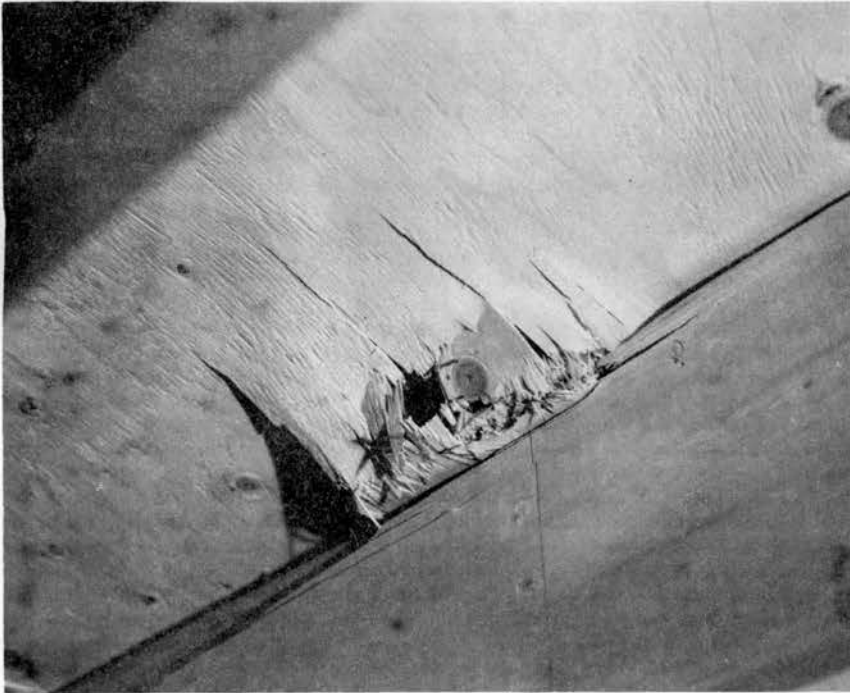


Fig. 4.25. Plywood failure with punching through of the loading pad at position 0707 on the floor.

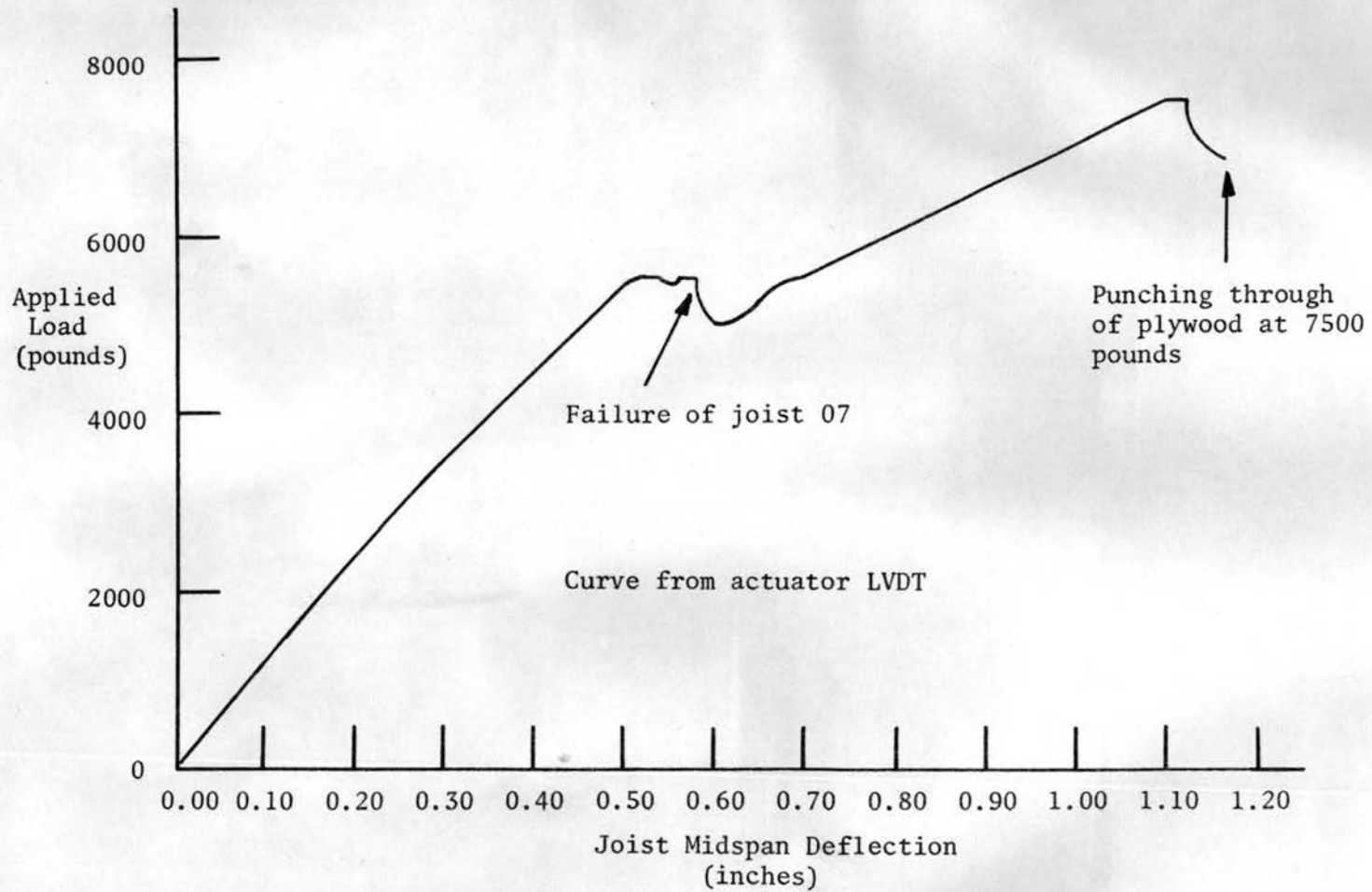


Fig. 4.26. Typical load-deflection curve plotted until punching through of the plywood, floor F4-12E16-1 loaded at position 0707.

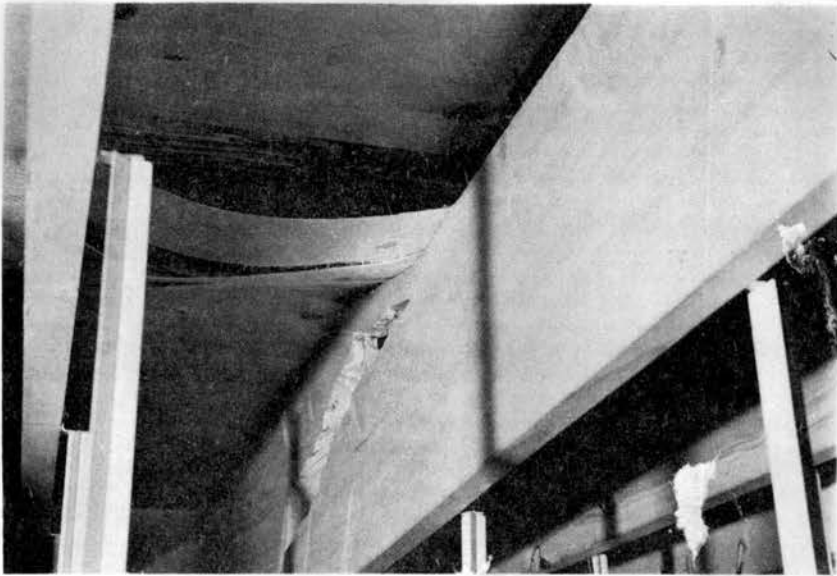


Fig. 4.27. Plywood failure with punching through of the loading pad at a joint, position 0704 on the floor.

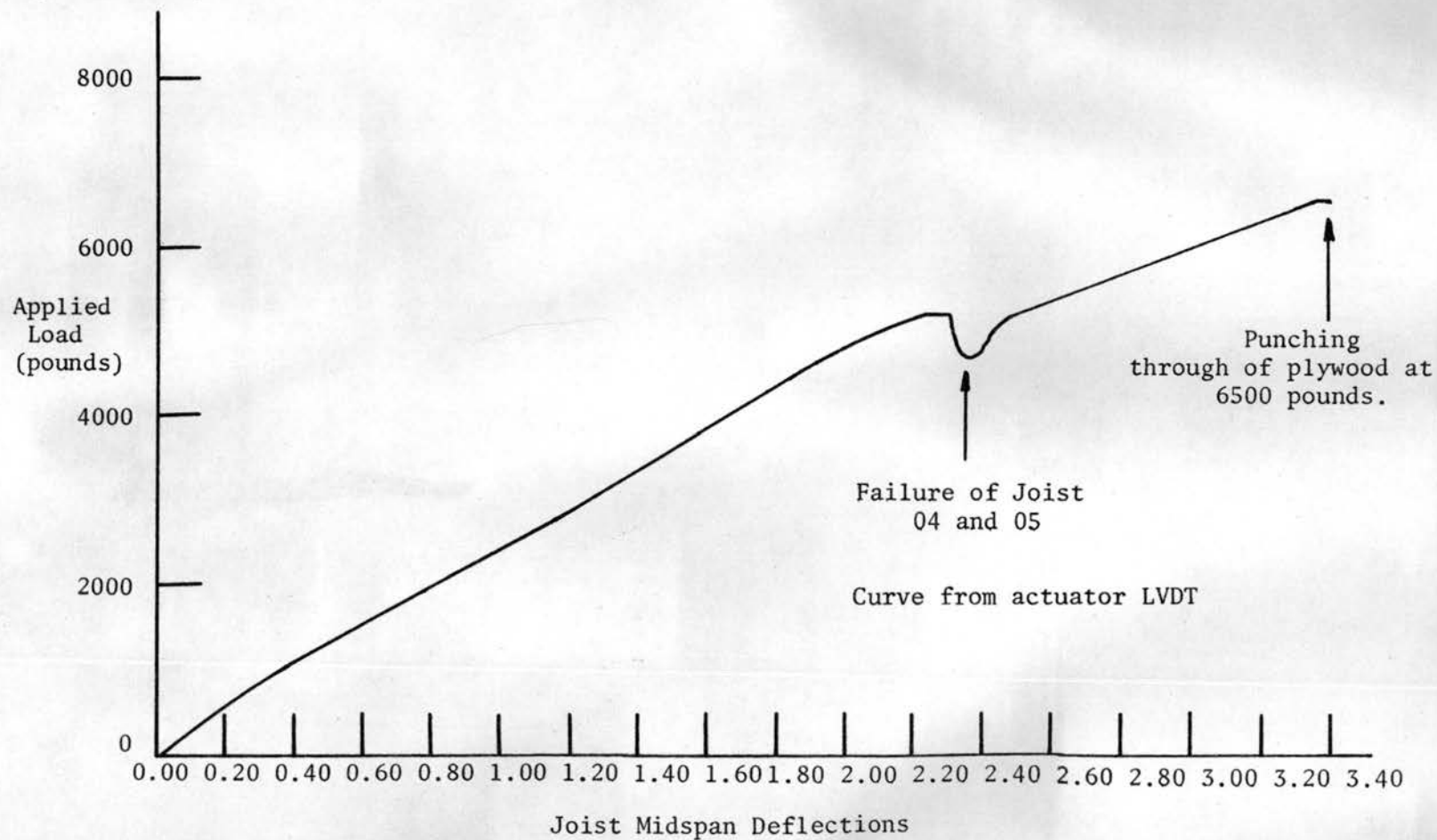


Fig. 4.28. Typical load-deflection curve plotted until punching through of the plywood, floor F3-8D16-1 loaded at position 0704.

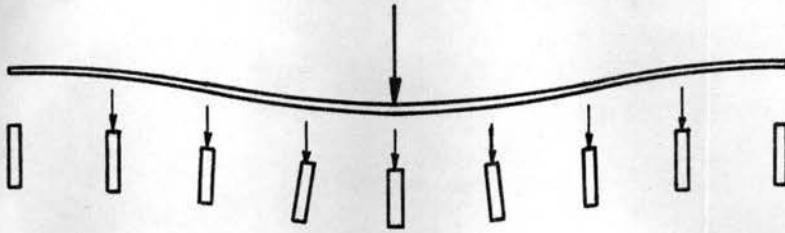


Fig. 5.1. Load distribution from the loaded point to neighboring joists.

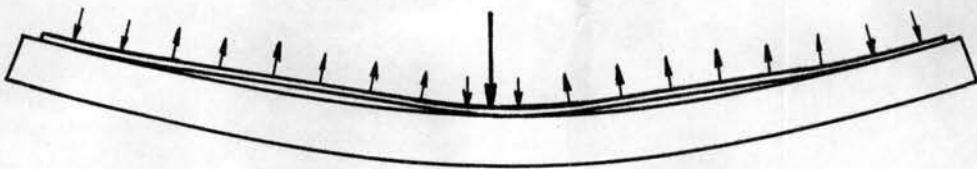


Fig. 5.2. Load distribution along the loaded joist due to plywood bending and the forces within the nail fasteners.

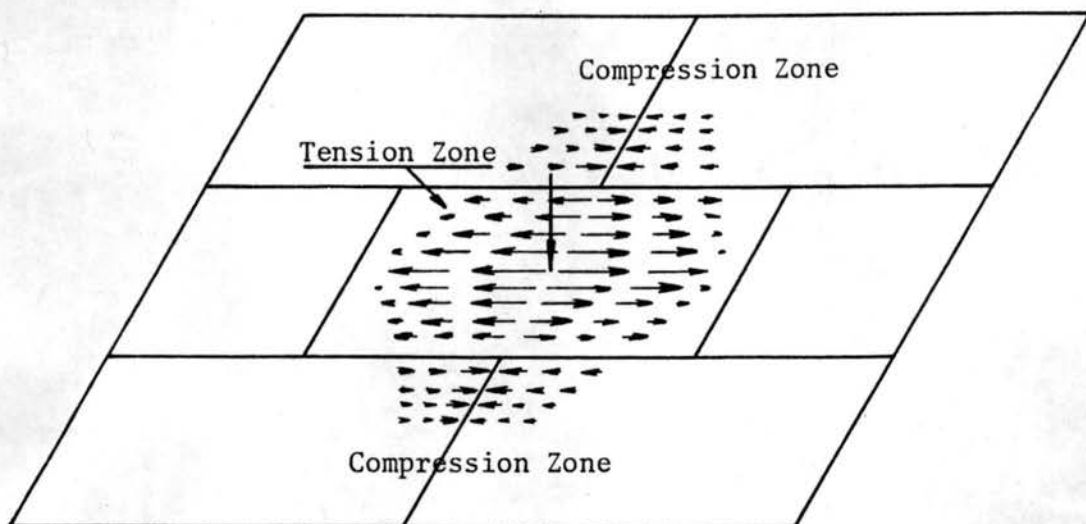


Fig. 5.3. Compression and tension regions of the plywood with a load applied at the center of a plywood sheet.

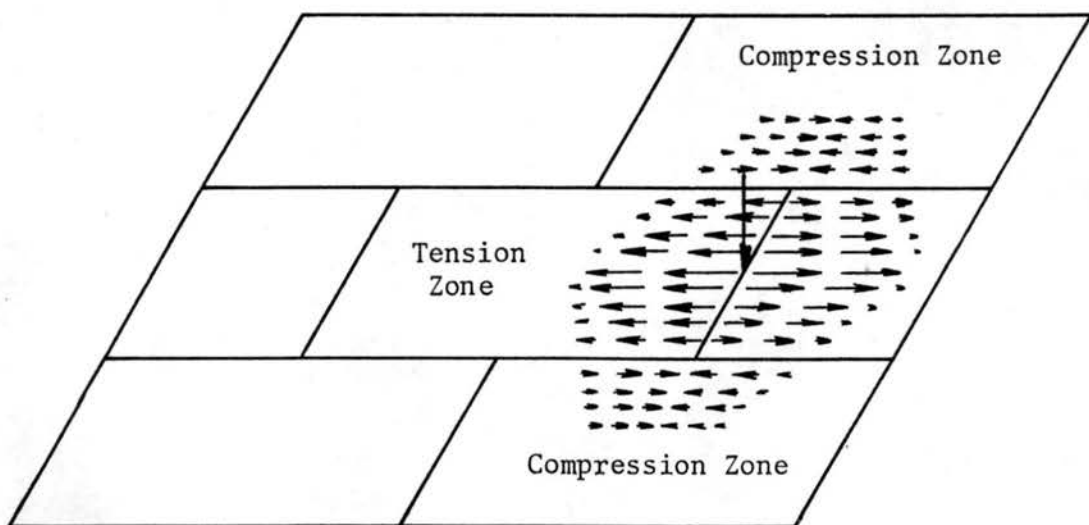


Fig. 5.4. Compression and tension regions of the plywood with a load applied at a plywood joint.

APPENDIX A

DESCRIPTION OF THE TESTING FRAME

A.1 Concrete Support Structure(a) Design

The T-beams and twelve by sixteen foot floors were supported upon a concrete frame. This concrete frame consisted of a rectangular beam configuration supported by six round columns, as shown in Figure A.1. The center line distances between the beams were twelve and sixteen feet.

The concrete frame was designed with the base of the columns assumed to be simply supported for a maximum concentrated load of fifty-five kips placed anywhere along the center line of the beams. The 55 kip load is the maximum capacity of the loading ram used with the frame. A center line loading was assumed because supporting sill plates will normally be placed approximately on the center line of each beam. Figure A.2 shows this testing configuration.

Strength design provisions of the 1971 American Concrete Institute Building Code, ACI No. 318-71 (2), were used in the design of the concrete frame. The load factor used in the flexural design was approximately the 1.7 value specified by the ACI Code for live loads. All the flexural reinforcement was No. 6, Grade 60 (60 ksi minimum yield) deformed bar. Number 6 bar was used because of its availability. Bundling of the reinforcement was required in some cases.

Figure A.3 shows the positive reinforcing steel pattern for the sixteen foot beam. Only an eight-foot section is shown because the

reinforcement is symmetrical about the center column. The stirrups provided to resist torsion and shear for the sixteen foot span and the longitudinal reinforcement placed within the stirrups are shown in Figures A.4a and b. The arrangement of the top reinforcing bars (negative reinforcement) is illustrated in Fig. A.5. The positive and negative reinforcement for the twelve foot spans were placed as shown in Figures A.6 and A.8. Stirrups and longitudinal reinforcement for the twelve foot span are shown in Figures A.7a and b. Minimum anchorage distances for the bars at the ends of the sixteen and twelve foot spans are shown in Figs. A.9a and A.9b respectively. Most anchorage lengths provided were approximately 6 to 8 inches longer than required because longer bars were not cut back to their design lengths. Details of the column and beam reinforcement for a corner column are shown in Fig. A.10. The stirrups in all columns were placed according to Figs. A.11a and b.

The maximum beam shearing stresses occur when a concentrated load is applied next to a column face. The 1971 ACI Code recommends that the calculated shearing stress be increased by seventy percent. This yields a load factor of 1.7, which is to compensate for low concrete strength and improper placement, and allowance for overloaded conditions. Due to the loading mechanism used only a 55 kip load or less could be applied. Therefore, to reduce the size of beam dimensions and obtain a reasonable stirrup spacing, a load factor for shearing stresses of 1.25 was used. The shear reinforcement consisted of closed stirrups fabricated from grade 60, No. 4 bar.

Concrete lifting inserts were imbedded in the support frame, to provide for fastening sill plates and equipment supports to the

frame. Fourteen standard coil inserts were placed on the inside of the platform about two inches from the bottom of the beams. These coil inserts have a safe working load of three kips and accept a 1/2 inch diameter bolt. They were used to support the bridges for the deflection dials. Ten more standard inserts were also placed along the top of the beams for use in attachment of the sill plates of each test specimen. One heavy lifting insert was placed in each corner column and two were placed at each center column. These heavy inserts have a tension load capacity of 8500 lbs, a shear load capacity of 11,500 lbs, and use a 1-inch diameter bolt. These inserts were also used to attach the floor and T-beams to the concrete base. All inserts imbedded in the top of the platform were approximately on the beam center lines.

(b) Construction

The monolithic concrete base was cast in one continuous pour on April 14, 1972 using 5 1/2 cubic yards of ready mix concrete specified to contain 6 1/2 sacks of cement per cubic yard or to provide a 28-day compressive strength of 4000 psi. This concrete was obtained from Poudre Readimix Company. Three 6 x 12 inch test cylinders were cast according to ASTM Standard C 31-66 (3) and cured under conditions similar to those for the support structure. These cylinders were tested at 29 days and indicated an average compressive strength of 4620 psi. Individual cylinder breaks were 4600, 4460, and 4810 psi.

A.2 Steel Frame

The steel frame surrounding the concrete supporting platform was designed for an upward load of 55 kips applied at any point

within the boundaries of the frame. The actuator, shown in Fig. A.12, was used only to apply a compressive force to the specimens in this testing program. The steel frame was tied to the structural floor to resist up-lift. These tie-downs consisted of two inch diameter bolts which screwed into 50-kip tensile capacity inserts previously cast in the structural floor. The connections of the frame were designed to allow rigid frame action to resist small lateral loads. As a consequence, the frame can support sizable downward loadings.

Analysis and design of the steel frame was done according to requirements in the Steel Construction Manual, seventh edition, published by the American Institute of Steel Construction (3). The structural sections selected using this manual are shown in Figs. A.13 and A.14. A36 steel with a minimum specified yield of 36 ksi was used for all members. Bolts were either A325 or A307, depending upon the strength needed.

Mobility of the actuator was obtained by suspending it from the crossing beam member using a trolley specifically designed to roll along the bottom flange of a wide-flange beam. This trolley had a capacity of 1 kip. An expanded view of this setup is shown in Fig. A.15. A similar type of rolling support was also used at either end of this W 14 x 78 beam which carried the movable actuator. This movable beam had one-half of a trolley setup at each end which rested on the outer half of the two horizontal beams in the rigid frame. The movable beam half trolleys had a combined load capacity of 4 kips. With this north-south and east-west mobility, any point supported by the concrete platform could be loaded.

The three-quarter inch jam bolt used to clamp the movable element into place can also be seen in the actuator trolley apparatus shown in Fig. A.15. This bolt extends through a bracket rigidly attached to the trolley frame. The point of this bolt can be extended down to bear upon the inner flange of the movable beam to lift the trolley and actuator so that the actuator bears tightly against the movable beam. This same procedure was used at the ends of the movable beam to raise it tightly against the outside beams. This procedure was necessary before loading to remove slack in the system to facilitate measurement of test specimen deflections with the LVDT contained in the loading ram.

Deflections of the steel framework due to applied loadings were also considered. Deflections of the concrete platform were considered to be negligible because the wood flooring system would crush before noticeable deflections of the base would occur. Because deflections of the steel frame are difficult to measure during a test, it was desirable to keep these deflections small. The total frame deflection consists principally of bending in the three W 14 x 78 beams. With a 55 kip load at midspan, the computed deflection of the movable beam is 0.57 inch. With a 55 kip load at midspan the beams in the rigid frame, the computed deflection is 0.71 inch. The total deflection of the two beams in combination due to a 55 kip load can be a maximum of approximately 0.90 inch for the most unfavorable load placement.

A.3 Hydraulic Loading System

The MTS Closed-Loop Structural Testing System, Model no. 908.75 consists of three components connected by hydraulic hoses and electric

cables. The power supply is an MTS Model No. 501.02 hydraulic pump. The control console is an MTS No. 850 unit as shown in Fig. A.16. The actuator used to apply the load and shown in Fig. A.12 is an MTS 204.71 unit.

The "Closed-Loop System" designation means that the system is self-controlling. A specific loading can be called for on the console and the ram then moves to apply this load to the test specimen. A load cell positioned between the ram of the actuator and the specimen measures the applied load and signals this quantity to the console. The ram of the actuator is moved so that the load called for on the control console and that detected by the load cell match within a specified limit. Two load cells were obtained with the system to allow adequate resolution of loads over a wide range. These two load cells have rated capacities of 2500 pounds and 50,000 pounds.

The ram of the actuator can be placed in either a stroke or load control mode. The same self-controlling systems exists for the stroke control mode except that an LVDT inside the actuator provides a signal to the console indicating how far the ram has extended. Care must be taken when using the system in the stroke control mode. The load cell, especially the 2500 pound capacity load cell, can be seriously damaged or destroyed if a stroke movement is requested which produces a large load significantly in excess of the load cell capacity. Limit controls exist within the control unit, but these may not be effective if the application of the load is very rapid.

The 2500 pound capacity load cell was used for all loading within the elastic range. When loading a floor to failure, the 50 kip capacity load cell was used.

The MTS console unit provided the connection points necessary to input the load and deflection signal into the X-Y plotters. After completion of a calibration procedure, the console and X-Y plotters were used to obtain continuous load versus deflection curves.

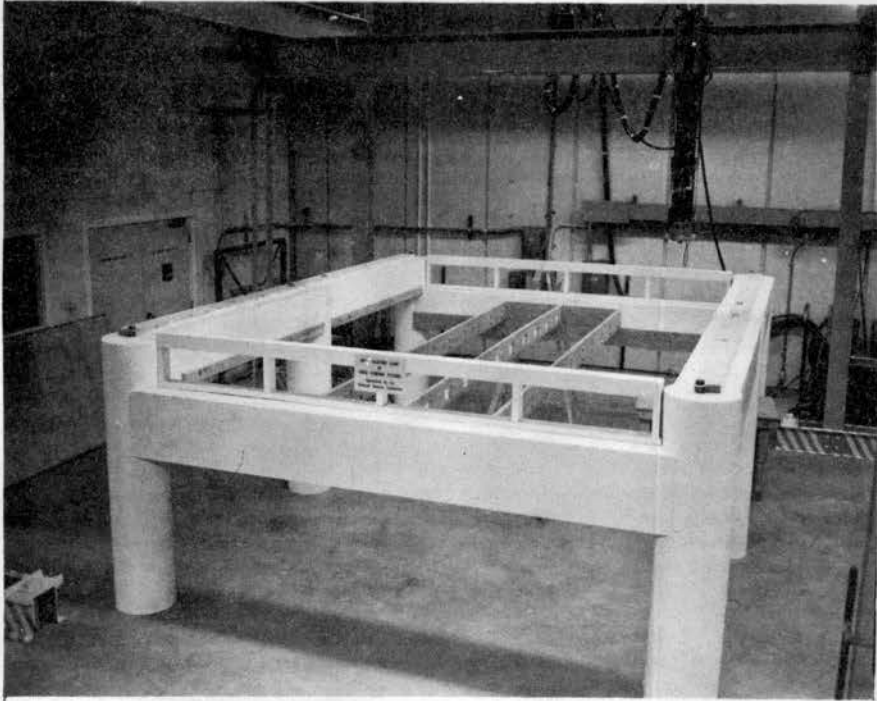


Fig. A.1. Concrete support structure with sill plates and deflection dial support.

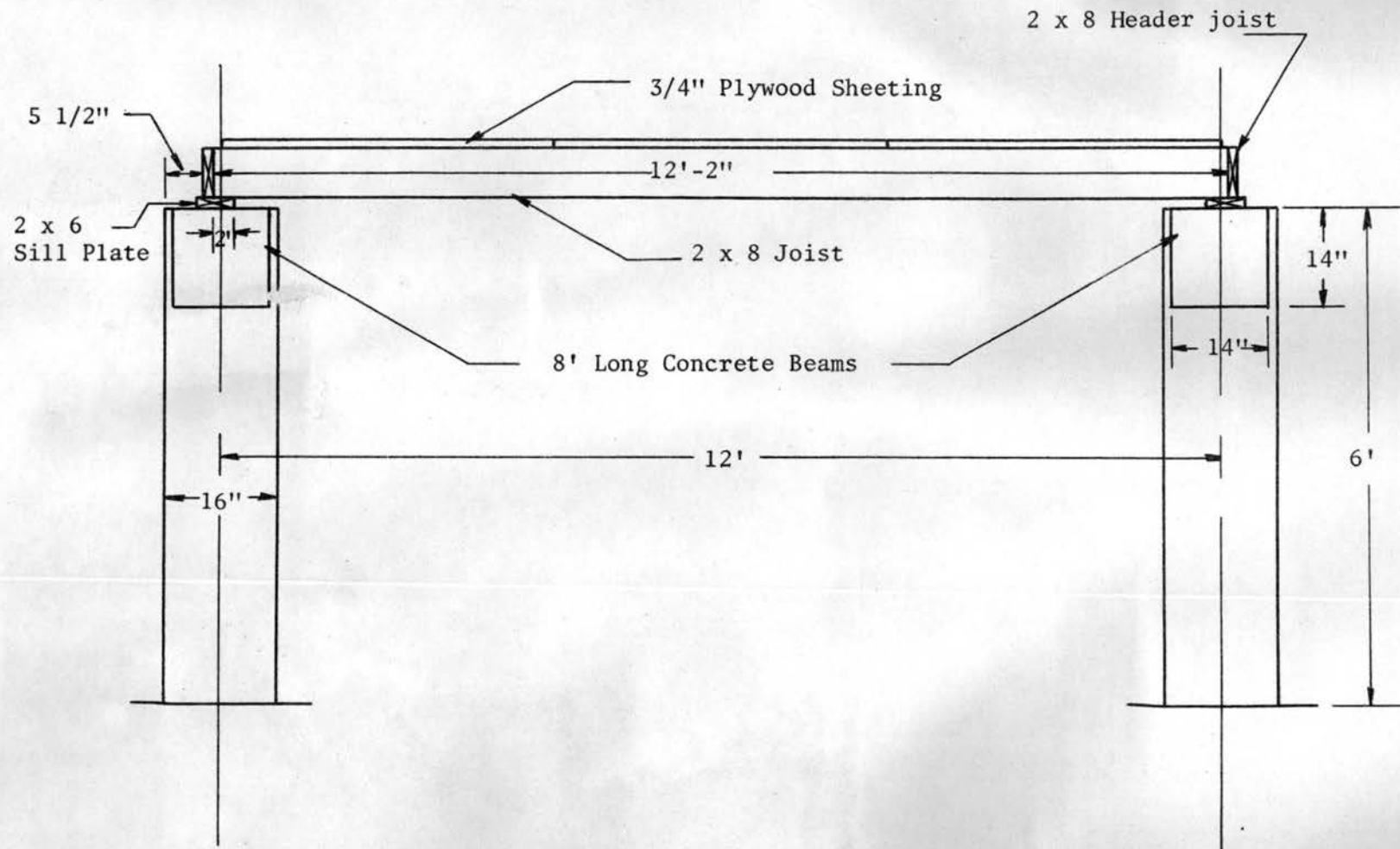


Fig. A.2. Specimen testing configuration.

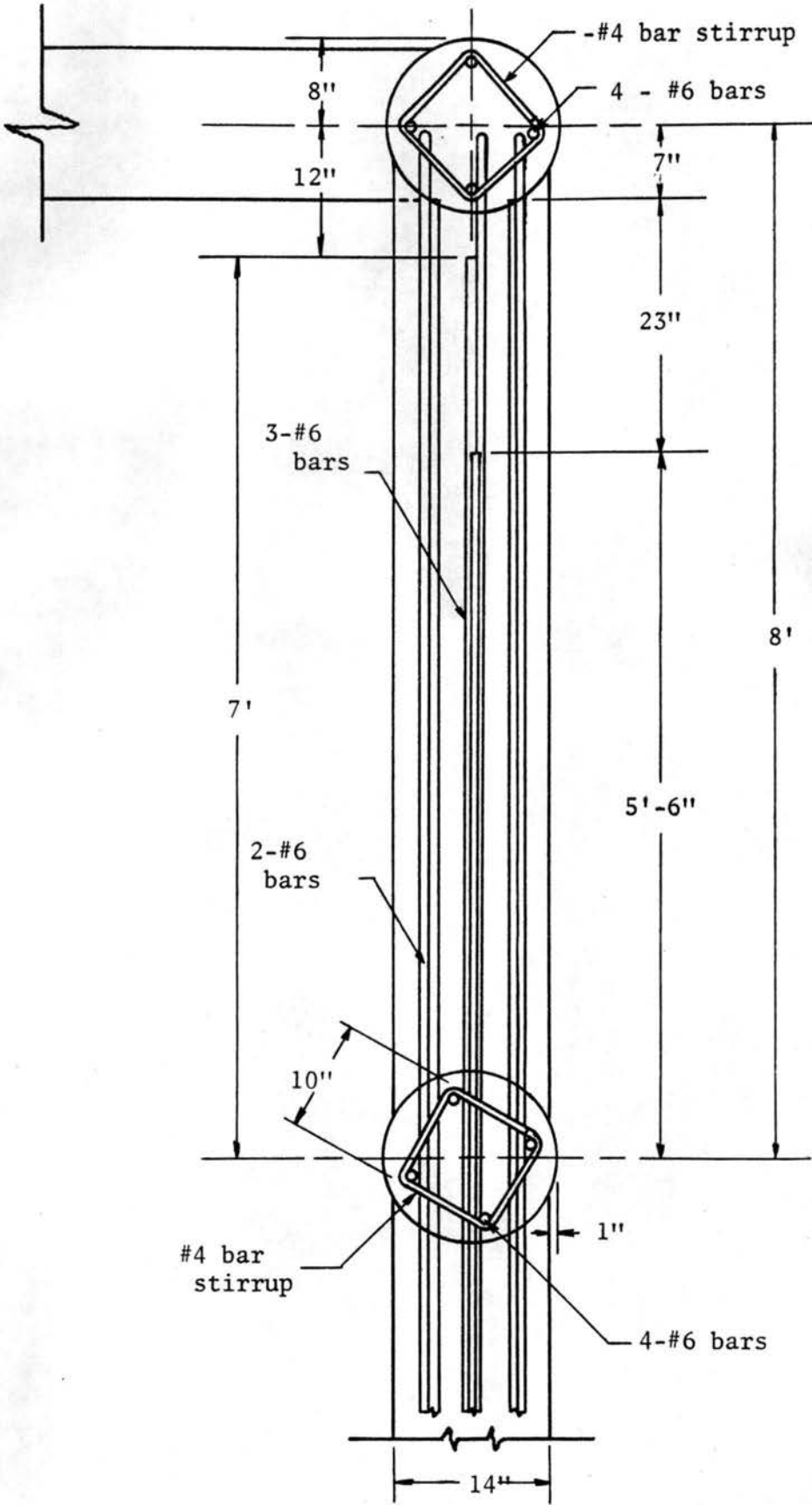
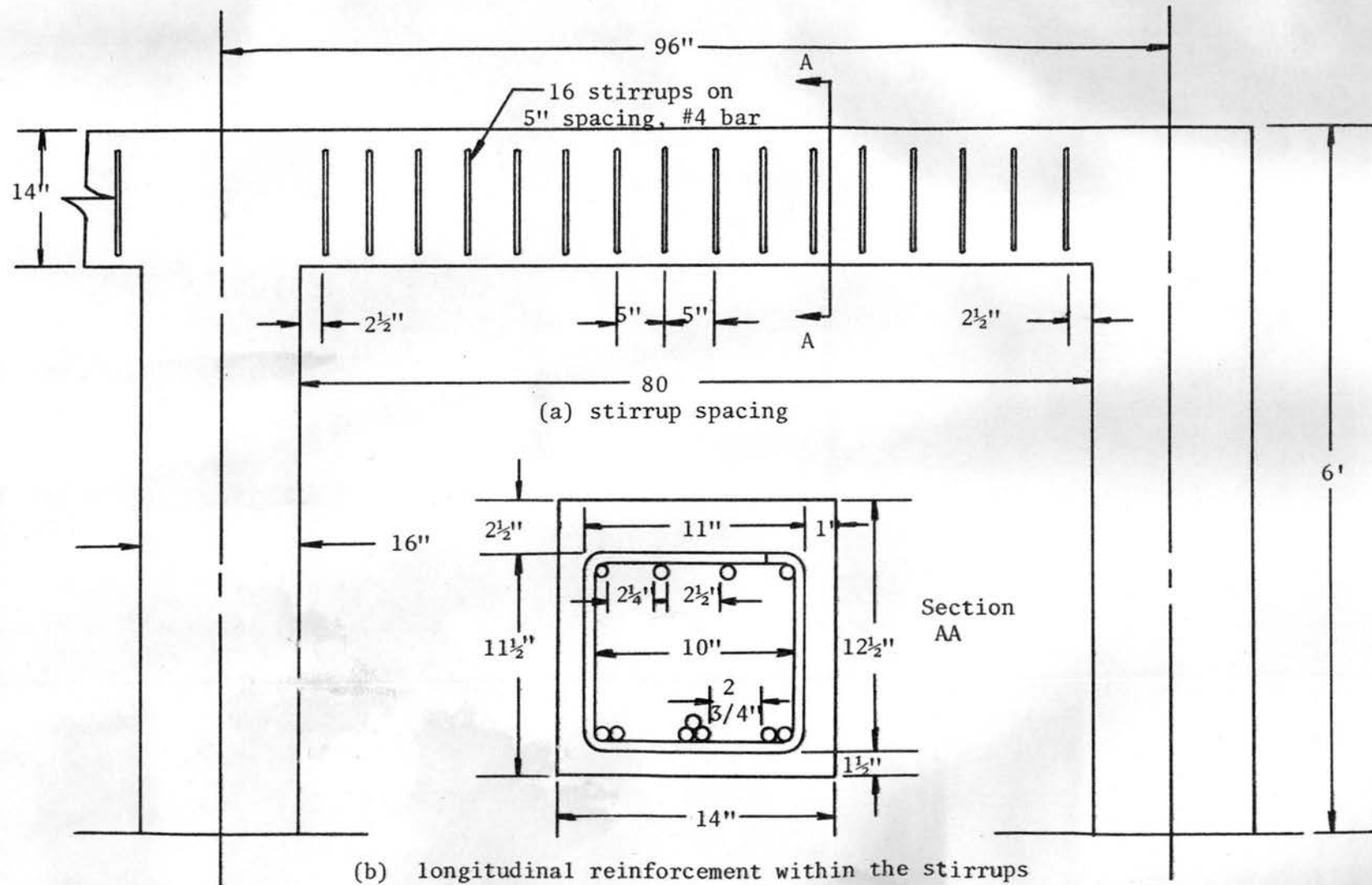


Fig. A.3. Positive reinforcement for the sixteen foot beam.



(b) longitudinal reinforcement within the stirrups

Fig. A.4. Stirrup reinforcement for the sixteen foot beams.

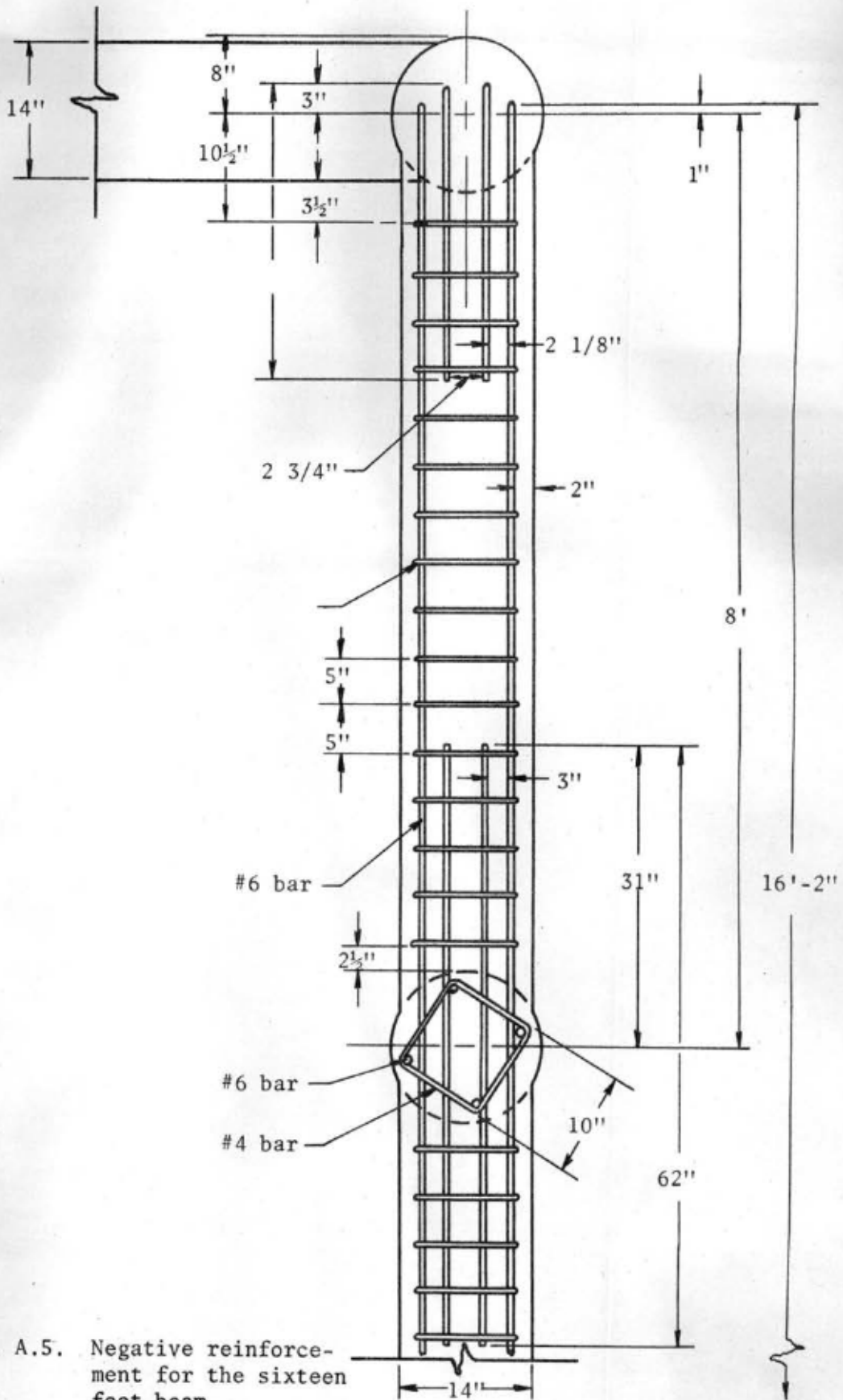


Fig. A.5. Negative reinforcement for the sixteen foot beam.

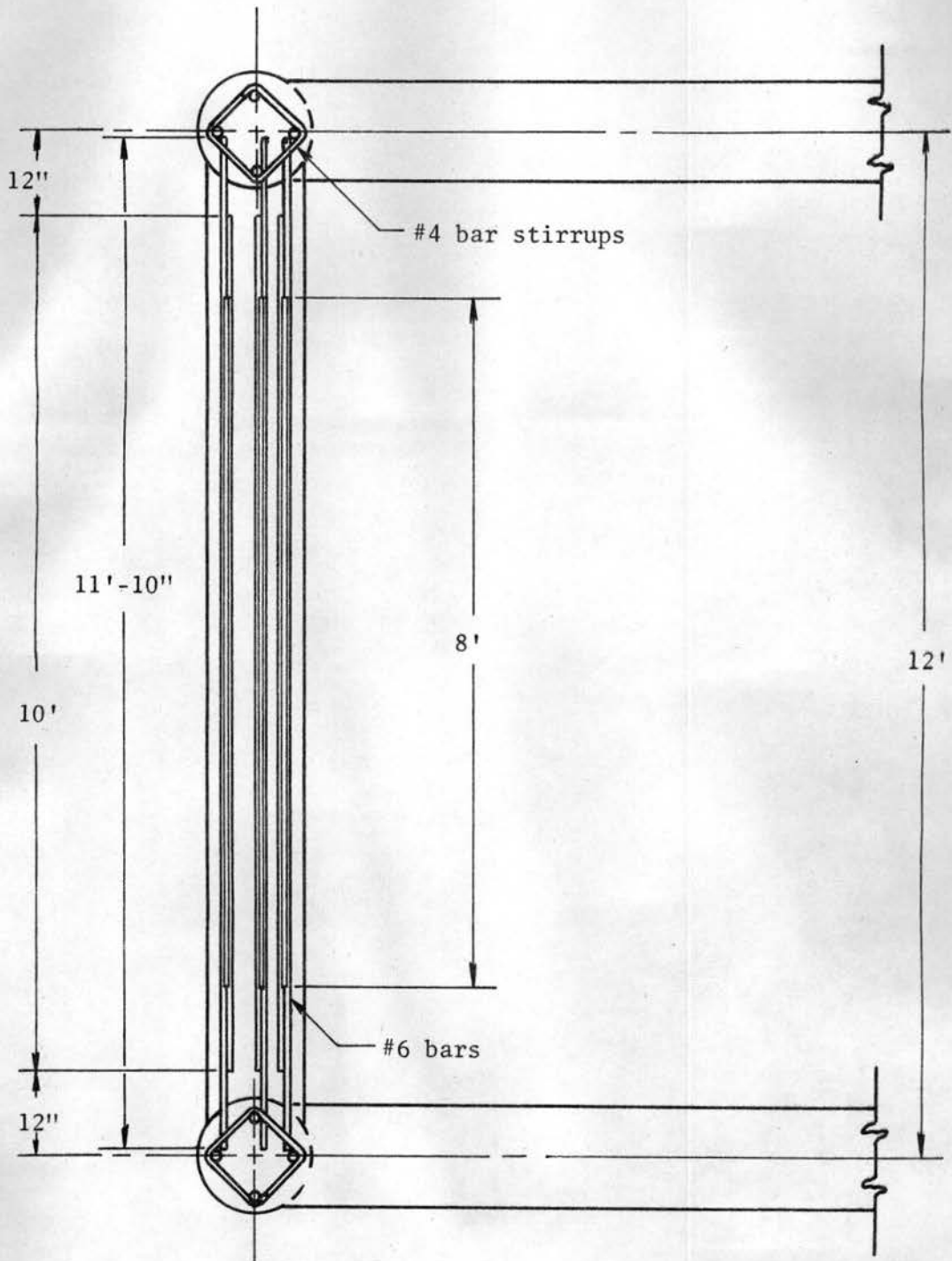


Fig. A.6. Positive reinforcement for the twelve foot span.

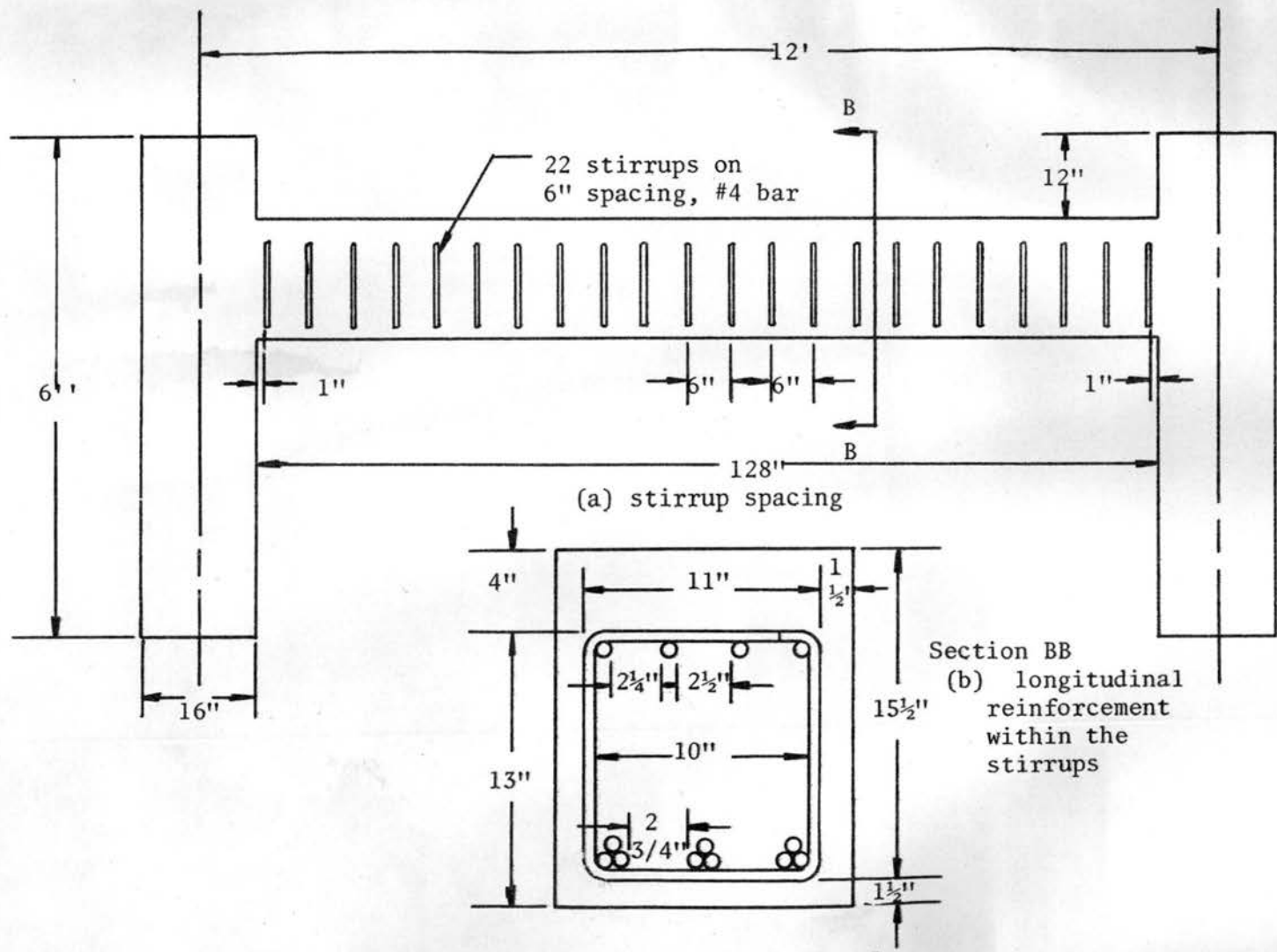


Fig. A.7. Stirrup reinforcement for the twelve foot span.

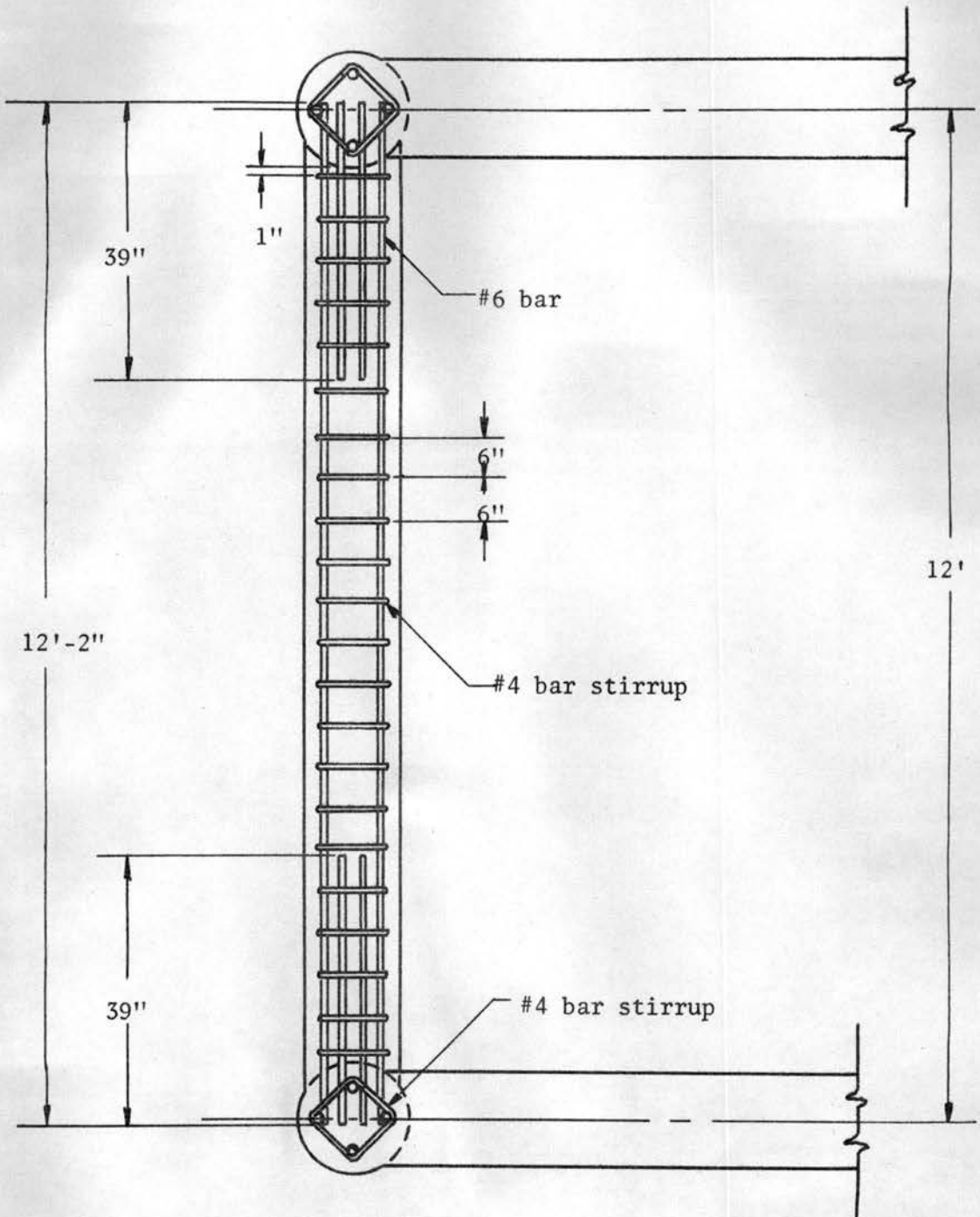


Fig. A.8. Negative reinforcement for the twelve foot span.

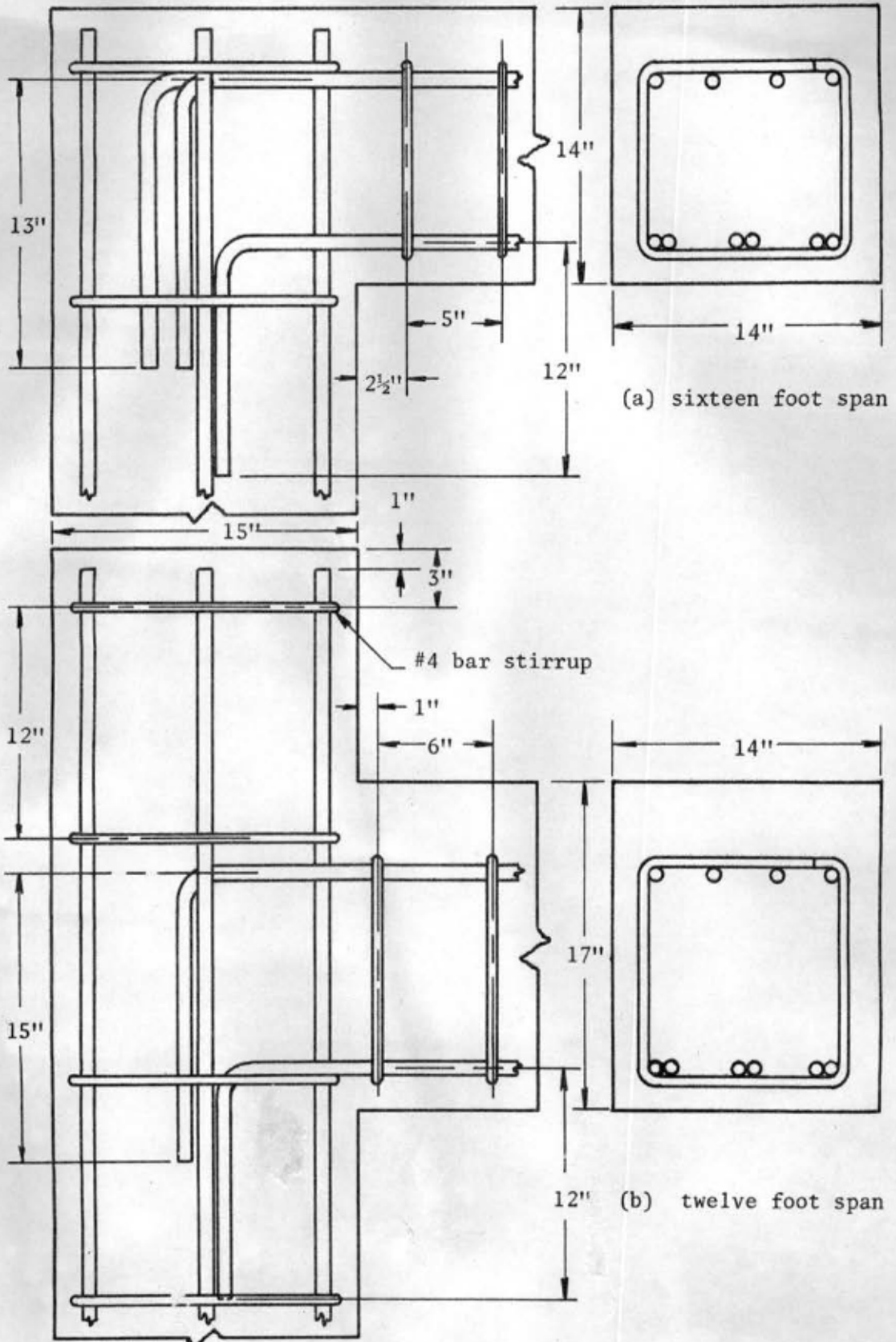


Fig. A.9. Anchorage reinforcement.

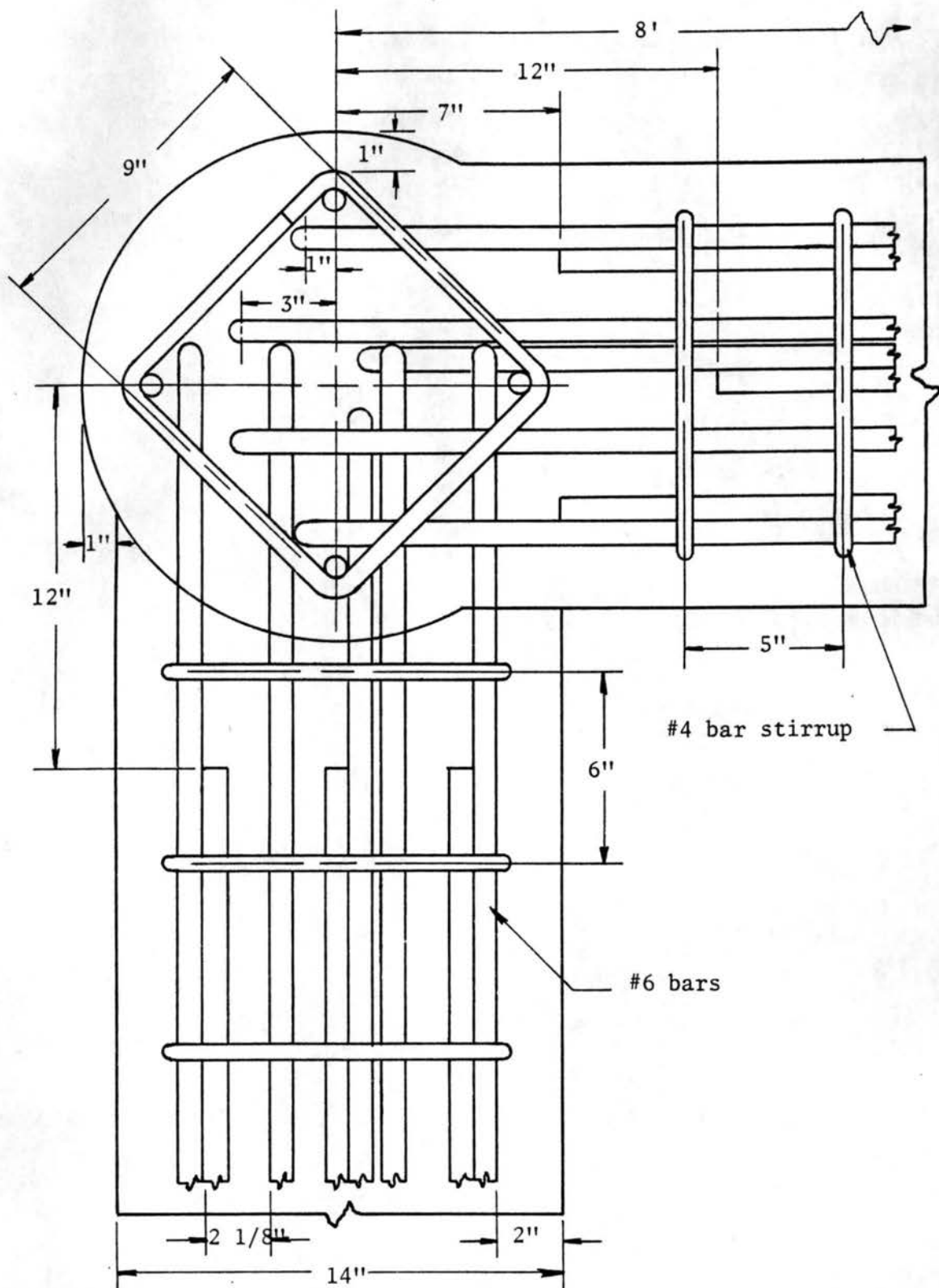


Fig. A.10. Meshing of reinforcement at a corner column

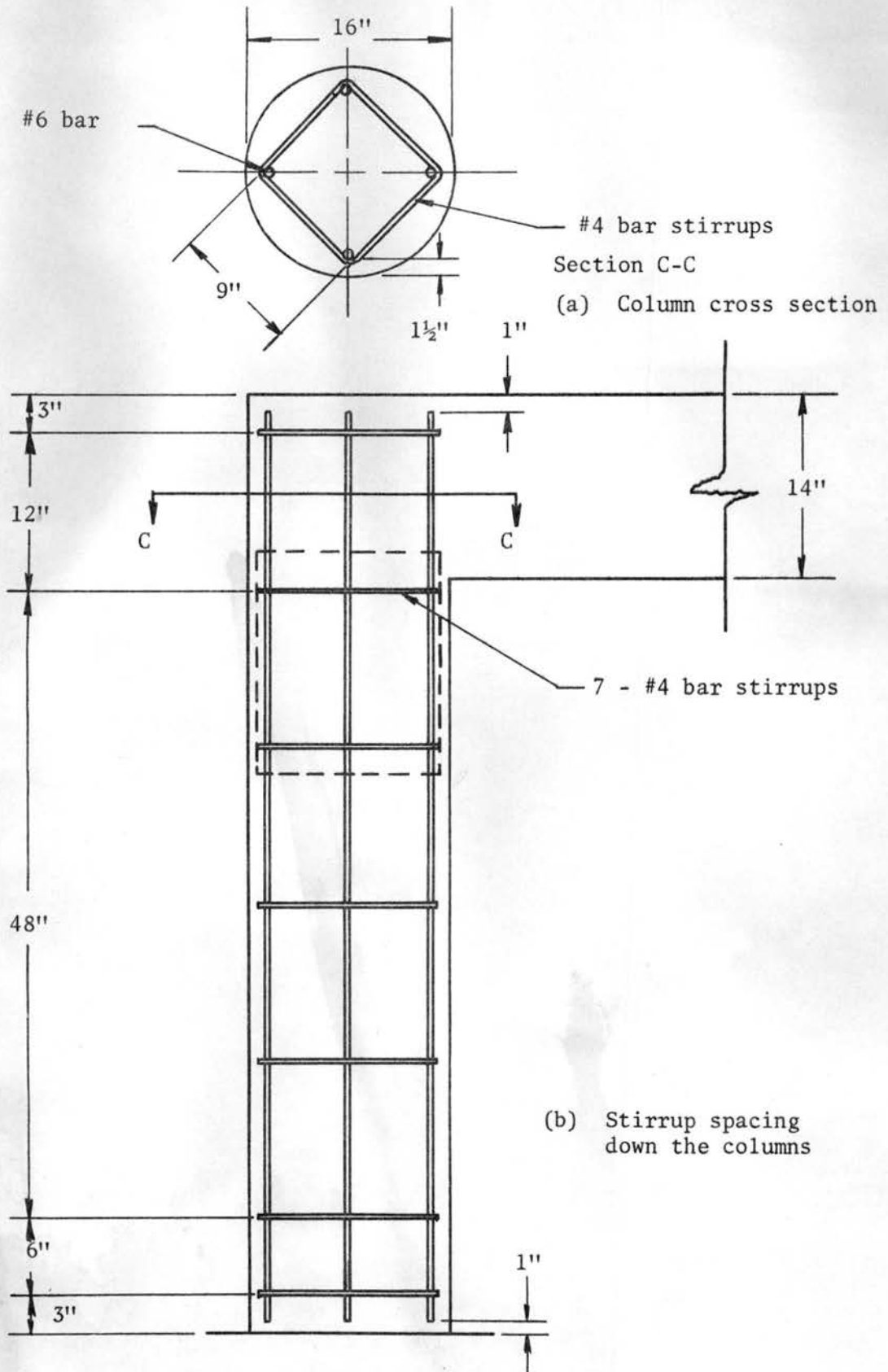


Fig. A.11. Reinforcement used in columns

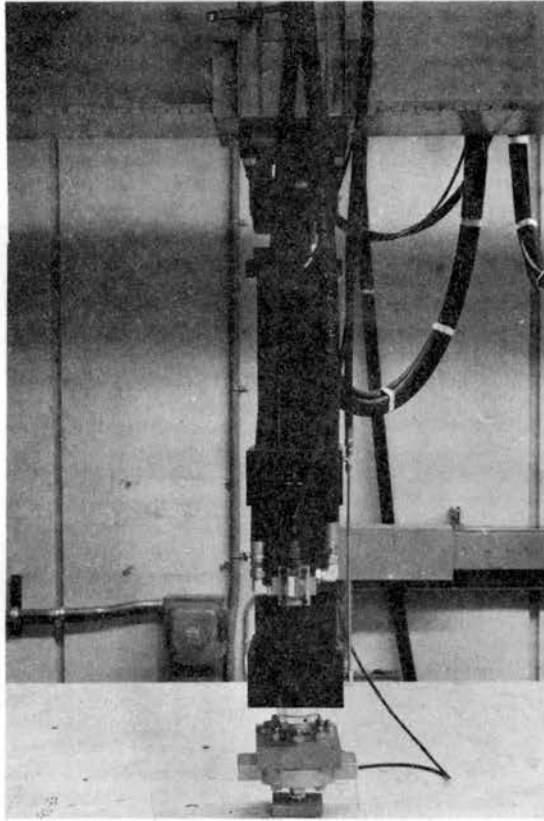


Fig. A.12. Actuator used in applying a concentrated load to a test specimen, with 50,000 pound load cell attached.

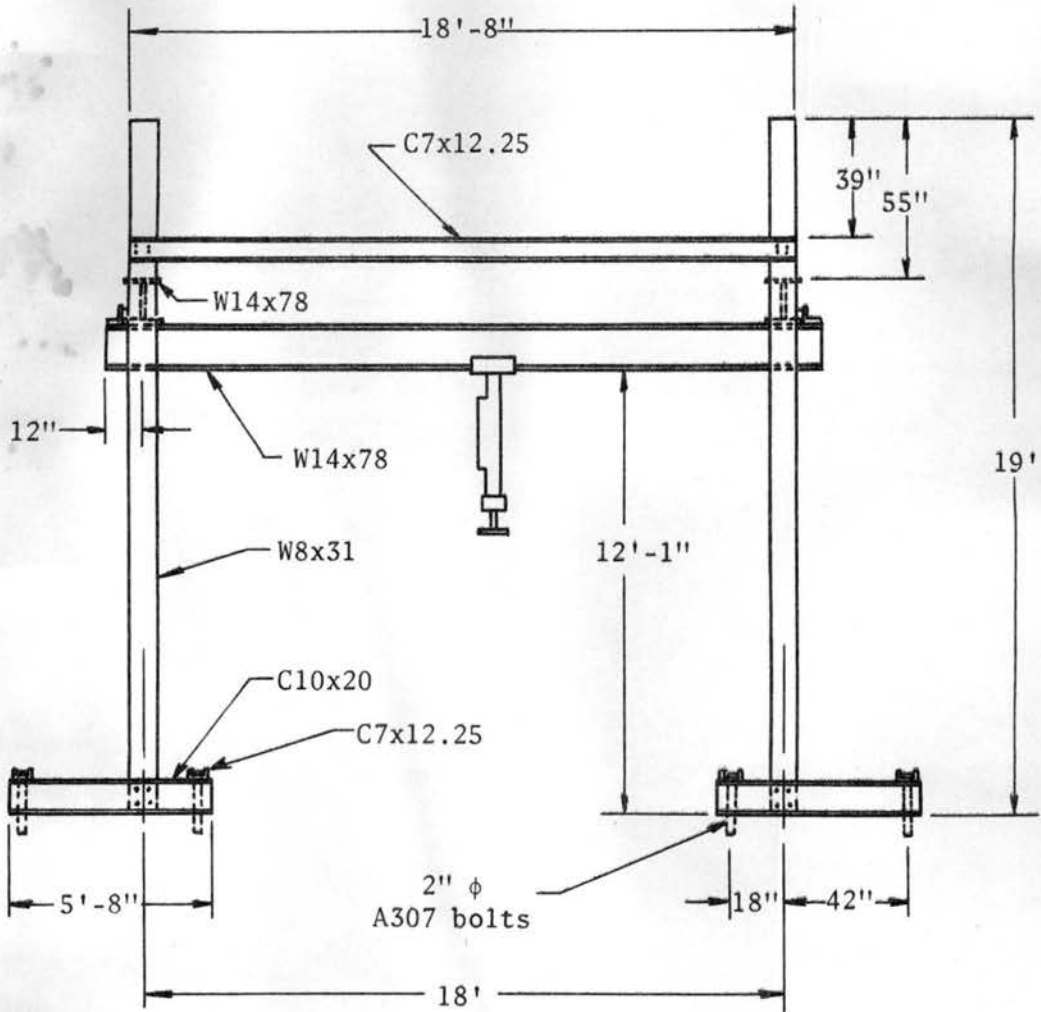


Fig. A.13. Front view of steel testing frame.

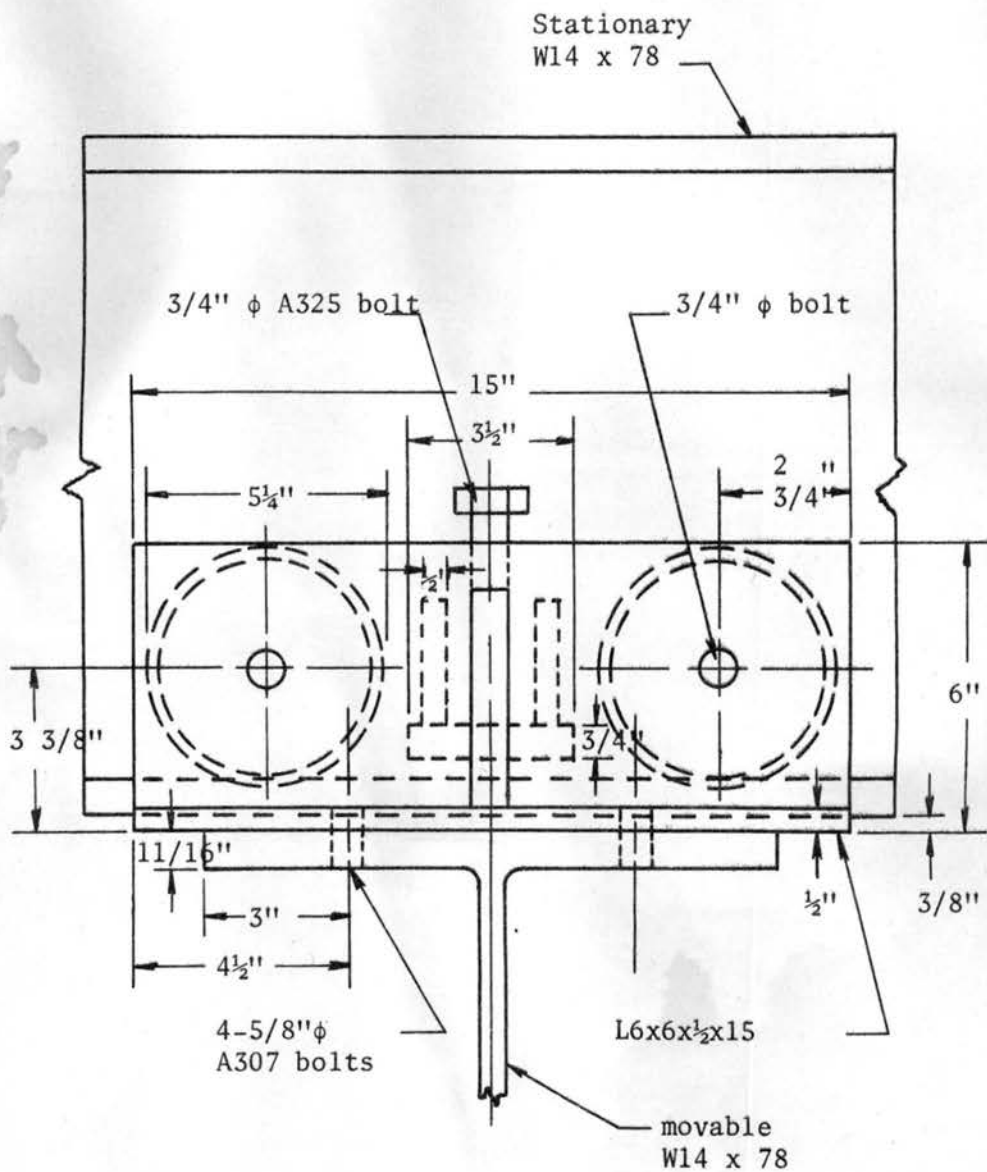


Fig. A.15. Trolley setup used to move the actuator and the movable beam.

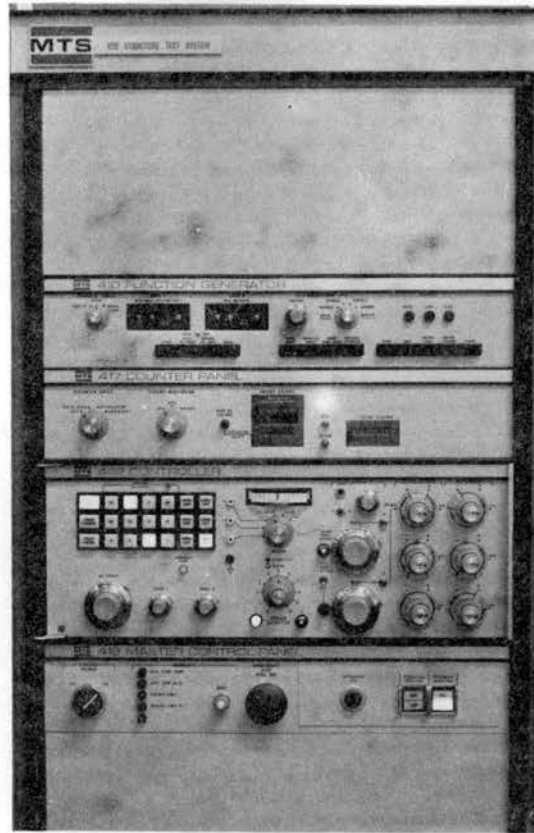


Fig. A.16. MTS Control console no. 850 used in applying a concentrated load to a test specimen.